A Thesis for the Degree of Doctor of Philosophy

Identification of the roles of EIIA^{Ntr} in amino sugar homeostasis and virulence regulation in *Salmonella enterica* serovar Typhimurium

Salmonella enterica serovar Typhimurium에서 EIIA^{Ntr}의 아미노당 항상성과 병원성에 대한 역할 규명

February, 2017

Woongjae Yoo

Department of Agriculture Biotechnology

College of Agriculture and Life Sciences

Seoul National University

Identification of the roles of EIIA^{Ntr} in amino sugar homeostasis and virulence regulation in *Salmonella enterica* serovar Typhimurium

Salmonella enterica serovar Typhimurium에서 EIIA^{Ntr}의 아미노당 항상성과 병원성에 대한 역할 규명

지도교수 유 상 렬

이 논문을 농학박사학위논문으로 제출함

2017 년 2 월

서울대학교 대학원
농생명공학부
유 웅 재

유웅재의 박사학위논문을 인준함
2017 년 2 월

위 원 장 _____ (인)
부위원장 _____ (인)
위 원 _____ (인)
위 원 _____ (인)
위 원 _____ (인)

Abstract

Yoo, Woongjae

Department of Agricultural Biotechnology

The Graduate School

Seoul National University

Salmonella enterica serovar Typhimurium is a rod-shaped, flagellated, facultative anaerobic, and Gram-negative bacterium. *Salmonella* Typhimurium is one of the major food-borne pathogens which causes a wide variety of diseases from gastroenteritis in millions of people worldwide to severe systemic infection in humans and animals. Various virulence factors and their regulation mechanisms have been identified in *Salmonella*, but the functions and mammalian targets of only a few have been known.

The term ‘phosphotransferase system (PTS)’ describes a system in which enzymes transfer phosphate moieties derived from phosphoenolpyruvate (PEP) from one enzyme to the other in a sequential order. In general, two different branches of the PTS exist; the

'sugar-PTS', responsible for the phosphorylation and uptake of sugars into the cell and the 'nitrogen-metabolic PTS' or 'PTS^{Ntr}', which fulfils exclusively regulatory functions.

Many *Proteobacteria* possess the paralogous nitrogen-metabolic phosphotransferase system (PTS^{Ntr}) which consists of enzyme I^{Ntr} (encoded by *ptsP*), NPr (encoded by *ptsO*), and enzyme IIA^{Ntr} (encoded by *ptsN*). Due to the location of *ptsO* and *ptsN* downstream of *rpoN* in the same operon, this system is postulated to be involved in nitrogen metabolism. Since a specific substrate transferred by PTS^{Ntr} is yet to be determined, this system is supposed to function mainly in a regulatory capacity.

In order to define the primary role of PTS^{Ntr} in *Salmonella* Typhimurium, ligand fishing was performed with EIIA^{Ntr} as a bait and revealed that D-glucosamine-6-phosphate synthase (GlmS) directly interacted with EIIA^{Ntr}. GlmS, which converts D-fructose-6-phosphate (Fru6P) into D-glucosamine-6-phosphate (GlcN6P), is a key enzyme producing amino sugars through glutamine hydrolysis. Amino sugar is an essential structural building block for bacterial peptidoglycan and lipopolysaccharide (LPS). I further verified that EIIA^{Ntr} interacted with

GlmS in a heterotrimeric formation and inhibited GlmS activity in a phosphorylation-state-dependent manner. $EIIA^{Ntr}$ was dephosphorylated in response to excessive nitrogen sources and was rapidly degraded by Lon protease upon amino sugar depletion. The regulation of GlmS activity by $EIIA^{Ntr}$ and the modulation of *glmS* translation by RapZ (RNase adaptor protein encoded immediately downstream of *ptsN*) suggest that the genes comprising the *rpoN* operon play a key role in maintaining amino sugar homeostasis in response to nitrogen availability and the amino sugar concentration in the bacterial cytoplasm.

In order to understand roles of nitrogen-metabolic PTS in *Salmonella* Typhimurium, whole transcriptome was also compared between the wild-type and a mutant strain lacking *ptsN* by RNA sequencing (RNA-Seq). Genome-wide transcriptomic analysis revealed that 3.5% of the whole annotated genes was up or down regulated by *ptsN* by three-fold or more. Genes differentially regulated by *ptsN* could be grouped into 5 categories based on their predicted functions including carbohydrate transport and metabolism, amino acid transport and metabolism, energy production and conversion, transcriptional regulation, and cell wall/membrane/envelope biogenesis. Among them,

the expression of genes involved in 1,2-propanediol (1,2-PDL) utilization and Ado-B_{12} synthesis was significantly decreased in the Δ*ptsN* mutant strain, and this phenomenon was complemented with the addition of glutathione (GSH) into the growth medium. Therefore the quantity of GSH was compared between wild-type and Δ*ptsN* mutant strain, and confirmed that GSH was about 3 folds lower in Δ*ptsN* mutant strain than wild-type.

Decreased expression level of genes involved in 1,2-PDL utilization and Ado-B_{12} synthesis in Δ*ptsN* mutant strain results in the lower production of propionate in the presence of 1,2-PDL compared to wild-type. Interestingly, the invasion ability of Δ*ptsN* mutant strain was about 5-fold higher than that of wild-type in the presence of 1,2-PDL. Concentration of 1,2-PDL can be high in the intestine because it can be produced by the fermentation of the common plant sugars L-rhamnose and L-fucose. L-fucose is also found in the glycoconjugates of intestinal cells, where it is involved in host-pathogen interaction. As previously reported, propionyl-CoA, the intermediate of 1,2-PDL metabolism, reduces the protein stability of HilD, a master regulator of *Salmonella* pathogenicity island-1 (SPI-1), leading to attenuation in *Salmonella*

virulence. Interestingly, $EIIA^{Ntr}$ protein level was increased by over 3 folds in the presence of 1,2-PDL. Based on these results, it is suggested that $EIIA^{Nt}$ can modulate *Salmonella* fitness and virulence via 1,2-PDL metabolism.

In conclusion, it was discovered that discovered the new roles of $EIIA^{Ntr}$, one of the components of nitrogen-metabolic PTS, in the regulation of amino sugar homeostasis and 1,2-PDL utilization pathway in *Salmonella enterica* serovar Typhimurium. GlmS is the only enzyme synthesizing amino sugar required for the peptidoglycan and LPS biosynthesis, and 1,2-PDL is a good carbon and energy source for *Salmonella* Typhimurium to compete with other intestinal microbiota. In this study, $EIIA^{Ntr}$ controlled GlmS enzyme activity and the expression of *cob-pdu* operon in response to environmental cues including amino sugar and 1,2-PDL, and the expression of $EIIA^{Ntr}$ was also regulated either post-translationally or translationally in response to the same environmental cues such as amino sugar and 1,2-PDL. It means that $EIIA^{Ntr}$ is a key player modulating *Salmonella* fitness and virulence through the interaction with its host environment, and I suggest the new possibility to reduce *Salmonella* disease by controlling the activity or the

expression of $EIIA^{Ntr}$.

Keywords: 1,2-propanediol utilization (*pdu*), Glucosamine-6-phosphate synthase (GlmS), Nitrogen-metabolic phosphotransferase system (PTS^{Ntr}), RNA-sequencing (RNA-seq), *Salmonella* pathogenicity island-1 (SPI-1), *Salmonella* pathogenicity island-4 (SPI-4), *Salmonella* Typhimurium

Student Number: 2011 - 21304

Contents

List of Figures

List of Tables

Chapter I.

General introduction

I-1. *Salmonella* enterica serovar Typhimurium

Salmonella is one of the most extensively studied bacterial pathogens in terms of its physiology, genetics, cell structure, and development. The bacterial genus *Salmonella* was named following the discovery of this pathogen by the United States Department of Agriculture (USDA) veterinary bacteriologist Dr. Daniel E. Salmon. This microorganism is a Gram-negative, motile, rod-shaped, and non-spore forming bacterium belonging to the *Enterobacteriaceae* family and is capable of infecting a wide range of animals resulting in several symptoms (salmonellosis, an infection with *Salmonella*) of disease including enteric fever, bacteremia, enterocolitis, and focal infection. The current classification of *Salmonella* is complex: based on the DNA-DNA hybridization the genus *Salmonella* is divided into two species: *Salmonella enterica* and *Salmonella bongori*. *S. enterica* can be subdivided into the six subspecies (*enterica*, *salamae*, *arizonae*, *diarizonae*, *houtenae*, and *indica*) based on the biochemical differences (Brenner *et al*, 2000) and more than 2,500 serovars (serotypes) using the Kauffman and White Scheme (Ezaki *et al*, 2000). *S. enterica* subspecies

enterica is mainly associated with infection of warm blooded animals, while the other subspecies and *S. bongori* rarely cause infection in these animals (Kingsley *et al*, 2003; Porwollik *et al*, 2004). It is generally accepted that there is a single species of *Salmonella* (*S. enterica*) and most investigators continue to designate "*S.* Typhimurium" rather than "*S. enterica* serovar Typhimurium" for a convenience. Thus, in this study, the *Salmonella s*erotypes are referred to by their "species" name.

According to host specificities and disease manifestation, there are two serotypes. Firstly, *S.* Typhi and *S.* Paratyphi are exclusively human pathogens causing typhoid fever. Typhoid fever is a protracted systemic illness including fever, abdominal pain, transient diarrhea, or constipation. The pathological hallmark is mononuclear cell infiltration and hypertrophy of the reticuloendothelial system including the intestinal Peyer's patches, mesenteric lymph nodes (MLNs), spleen, and bone marrow. Without treatment, mortality is 10-15%. On the other side of the spectrum, non-typhoidal *Salmonella* strains, such as *S.* Typhimurium and *S.* Enteritidis have broad host range including poultry, cattle, and pigs and usually cause self-limited gastroenteritis: abdominal pain, vomiting, and inflammatory diarrhea in humans. *S.* Typhimurium

also gives rise to the systemic disease in susceptible mouse strains similar to that of human *S*. Typhi infections (Alekshun, 2001). Therefore, murine typhoid is widely accepted as an animal model for human typhoid fever (Bumann, 2009; Flannagan *et al*, 2009).

Typhoid fevers are most common in the developing world; the highest incidence of typhoid is found in Southeast and Central Asia where it is endemic, and is a frequent disease in Africa, the Middle East. As of the year 2000, there were an estimated 22 million cases globally of typhoid fever each year, and roughly 10% of these cases were fatal. Estimates for numbers of non-typhoidal salmonellosis (NTS) cases worldwide vastly exceed those for enteric fevers. Every year, approximately 42,000 cases of NTS are reported in the United States (Centers for Disease Control and Prevention, 2015). Because many milder cases are not diagnosed or reported, the actual number of infections may be twenty-nine or more times greater. In Korea, the case of food poisoning of pathogenic bacteria has been increased and the scale of incidence was also increasing because of the increased group food service and deterioration of the public health infrastructures (KFDA reports).

Salmonella grows between 8°C and 45°C and pH 4-8. It is highly resistant towards dehydration in the environment and thus can survive in soil and water for a long period of time. Animals that are known to carry *Salmonella* include poultry swine, cattle, rodents, and pets. Human with mild and unrecognized cases are carriers as well. In the environment, *Salmonella* also exists in feces and contaminated food, which is the primary source of human infections, either directly or indirectly. Food sources that are known to spread *Salmonella* include: contaminated raw and undercooked eggs/egg products, raw milk/milk products, meat, poultry products, contaminated water, and raw fruits and vegetables (Kukanich, 2011; Sanchez-Vargas *et al*, 2011; Weber, 2009). Most people infected with *Salmonella* develop diarrhea, fever, and abdominal cramps 12 to 74 h after infection. The illness usually lasts 4 to 7 days and most persons recover without treatment. However, in some persons, the diarrhea may be so severe that the patient needs to be hospitalized.

Salmonella food poisoning treatment includes: Antibiotics in moderate to severe cases of *Salmonella* food poisoning, or when it occurs in a person who is at risk for complications, such as people with

weakened immune systems due to such conditions as HIV/AIDS, cancer, diabetes, taking steroid medications or undergoing chemotherapy, or avoiding solid food until symptoms subside. Drinking plenty of fluids to prevent dehydration: fluids include water on an oral rehydrating fluid. Hospitalization and rehydration with intravenous fluids would be required, if *Salmonella* food poisoning does not resolve quickly or lead to dehydration or other complications.

I-2. *Salmonella* pathogenesis and its virulence mechanisms

S. Typhimurium thrives in a variety of locations, including the gastrointestinal tract and the intracellular milieu of eukaryotic cells. About 10^5 to 10^6 bacteria are estimated to be required for the initial infection (Blaser *et al*, 1982), but the exact amount needed varies with the strain and the physiological state of the host (Buchwald *et al*, 1984; Chalker *et al*, 1988). During the early stages of infection, *S.* Typhimurium should survive the acid barrier of the stomach to reach small intestine. *S.* Typhimurium has an adaptive acid-tolerance response that might promote their survival in the low pH milieu of the stomach (Garcia *et al*, 1993).

After passage through the upper gastrointestinal tract, *Salmonella* traverse the intestinal mucous layer before encountering and evade being killed by digestive enzymes, bile salts, secretory IgA, antimicrobial peptides, and other immune defenses in order to gain access to the underlying epithelium (Michetti *et al*, 1992; Selsted *et al*, 1992). *S.* Typhimurium has the ability to invade the non-phagocytic

enterocytes of the intestinal epithelium, preferentially microfold (M) cell in the Peyer's patches by a morphologically distinct process termed bacterial-mediated active endocytosis (Francis *et al*, 1992; Jones *et al*, 1994). Shortly after bacteria adhere to the apical epithelial surface, profound cytoskeletal rearrangements occur in the host cell. Bacterial-mediated endocytosis requires coordinated synthesis of multiple bacterial proteins. Once the epithelial barrier has been breached, *S.* Typhimurium can across the intestinal epithelium and encounters another obstacle, the submucosal macrophage. *S.* Typhimurium enters intestinal macrophages by inducing macropinocytosis and subsequently activates virulence mechanisms that allow evasion of the microbicidal functions of the phagocyte allowing survival and replication in the intracellular environment (Alpuchearanda *et al*, 1994). Migration of infected phagocytes to other organs of the reticuloendothelial system facilitates dissemination of bacteria in the host.

After *Salmonella* has been taken up by macrophages, it does not enter into the cytoplasm but resides inside the phagosomal vacuole. In the phagosome, *Salmonella* has to be able to cope with environmental changes such as rapid decrease in pH and nutritional deprivation that are

restrictive for the growth of bacteria. In addition, phagosomes containing ingested particles usually enter the degradative pathway of the cells. After fusion with lysosomes to form a phagolysosome, engulfed *Salmonella* will encounter toxic substances such as hydrolytic enzymes (protease, lysozyme), small cationic proteins (defensins), and enzymes that produce reactive forms of oxygen to cause the oxidative burst, as well as reactive nitrogen intermediates (NO, NO^{2-}, NO^{3-}). Adapting to the nutrient limitation encountered within the phagosome requires induction of multiple biosynthetic genes necessary for *de novo* synthesis of essential metabolites, including aromatic amino acids and purines. Therefore, *Salmonella* activates various virulence mechanisms in order to survive and replicate (Bader *et al*, 2003; Miller *et al*, 1989; Ochman *et al*, 1996; Vazquez-Torres *et al*, 2000).

Studies performed by various groups have established that the function of a large number of virulence genes in required for the successful pathogenesis of *Salmonella* infections. Many of these virulence genes have defensive functions: protection of *Salmonella* against defense mechanisms of the innate and adaptive immune system of the infected host. However, recent studies revealed that *Salmonella*

has developed two complex virulence functions to actively interact with the host and to modify host cell functions (Groisman *et al*, 1997). Therefore, two interactions during infection: invasion into non-phagocytic cells and the intracellular survival within phagocytes had been hallmarks of *Salmonella* pathogenesis.

A specialized apparatus, named the type III secretion system (T3SS), is essential to *Salmonella* pathogenesis and the colonization of host tissues. The T3SS mediates the transfer of bacterial virulence proteins, known as effectors, from the bacterial cell into the host-cell cytoplasm. *Salmonella* encodes two distinct virulence-associated T3SSs within *Salmonella* pathogenicity islands-1 and -2 (SPI-1 and SPI-2) that function at different times during infection (Valdez *et al*, 2009). Whereas the SPI-1-encoded T3SS is active on contact with the host cell and translocates bacterial proteins across the plasma membrane (Schlumberger *et al*, 2006), the SPI-2 T3SS is expressed within the phagosome and translocates effectors across the vacuolar membrane. The SPI-1 system has been shown to be required for invasion of non-phagocytic cells, induction of intestinal inflammatory responses and diarrhea, as well as colonization of the intestine. The SPI-1 T3SS

apparatus is also required to kill the M cells that sample antigens and occlude access to gut-associated lymphoid tissue (Jones *et al*, 1994). The SPI-2 T3SS by contrast, confers an important role in bacterial survival in the macrophages and is required for establishment of systemic disease in the mouse infection model (Drecktrah *et al*, 2006; Hansen-Wester *et al*, 2001; Kuhle *et al*, 2004). The genetic locus SPI-2 comprises 40 genes, of which 25 have been shown to contribute to the intracellular phenotypes. Mutant deficient in the SPI-2 T3SS cannot replicate efficiently in tissue-culture cells and are highly attenuated in animal models of infection. Current hypotheses for the function of the SPI-2 T3SS propose the promotion of intracellular replication by altering host vesicular trafficking, so that useful metabolic molecules, such as amino acids and lipids, are routed to the SCV and the vesicular compartment membrane is expanded (Brumell *et al*, 2001; 2002; 2004; Figueira *et al*, 2012; Ramsden *et al*, 2007). Induction of SPI-2 genes depends on a two-component regulatory system, SsrA/SsrB, encoded within the SPI-2 region (Garmendia *et al*, 2003; Tomljenovic-Berube *et al*, 2010). Expression of SsrAB is also mediated by two-component regulatory systems, OmpR/EnvZ and PhoP/PhoQ, which sense osmotic stress and

cation limitation, respectively (Lee *et al*, 2000; Miao *et al*, 2002; Yoon *et al*, 2009). *Salmonella* has evolved these two elaborate virulence systems for different kinds of interactions with eukaryotic cells. However, the strategy by which *Salmonella* modifies the host cells to survive and cause symptoms is not yet fully understood. Despite this wealth of information, the known effector repertoire of the host-pathogen interactions is incomplete; therefore many reports place an emphasis on discovery of new effectors by using highly advanced technologies.

I-3. Objectives of this study

Salmonella is a leading cause of bacterial gastroenteritis and systemic infection. The increasing number of infection with *Salmonella* and the rapid growth in antimicrobial resistance have become a global problem. Thus, the development of efficient controlling methods and antimicrobial therapy to control *Salmonella* is crucial to address current issues in public health.

Identification of a role of $EIIA^{Ntr}$ in maintaining amino sugar homeostasis in *Salmonella* Typhimurium.

New binding partner of $EIIA^{Ntr}$ was discovered, and several experiments were performed to prove the role of $EIIA^{Ntr}$ in maintaining amino sugar homeostasis in *Salmonella* Typhimurium.

Genome-wide transcriptomic analysis for understanding the primary role of $EIIA^{Ntr}$ in *Salmonella* Typhimurium.

RNA sequencing and transcriptomic analysis were carried out to find out the effect $EIIA^{Ntr}$ on the gene expression pattern of

Salmonella enterica serovar Typhimurium.

Investigation of the role of EIIA^{Ntr} in *Salmonella* virulence.

The effect of EIIA^{Ntr} on *Salmonella* fitness and virulence during infection was assessed.

.

Chapter II.

Fine-tuning of amino sugar homeostasis by EIIA^{Ntr} in *Salmonella* Typhimurium

This chapter was published in *Sci. Rep.* **(2016) 6:** 33055.

II-1. Introduction

The phosphotransferase system (PTS) is a systematic bacterial device composed of a cascade of enzymes that transfer phosphate moieties derived from phosphoenolpyruvate (PEP) in sequential order. The canonical PTS that occurs in a wide range of bacteria is a sugar PTS called the phosphoenolpyruvate:carbohydrate PTS, which is comprised of enzyme I (EI), histidine phosphocarrier protein (HPr), and enzyme II complexes (EIIA, EIIB, EIIC, and sometimes EIID). The EIIA, EIIB, and EIIC proteins usually form substrate-specific transfer cascades with one membrane-spanning protein, EIIC in general, in contact with their extracellular substrates (Postma *et al*, 1993). In contrast, EI and HPr are universal cytoplasmic proteins, which take-up diverse carbohydrates, such as sugars and their derivatives. In addition to the uptake and concomitant phosphorylation of many carbohydrates, the PTS also conducts diverse regulatory functions, sensing available carbon sources (Görke *et al*, 2008; Lengeler *et al*, 2009; Escalante *et al*, 2012; Deutscher *et al*, 2014). The PTS accomplishes regulatory roles either by phosphorylating target proteins or by directly interacting with their

target proteins. Proteins containing a specific PTS-recognizable phosphorylation domain are phosphorylated by the components of the PTS phosphorylation cascade and their activities are modulated. The phosphorylatable target proteins include a variety of non-PTS transporters and transcription regulators (Deutscher *et al*, 2014). In the latter case, phosphorylated or unphosphorylated forms of the PTS proteins directly interact with target proteins, leading to activation or repression of their functions mainly involved in transport and transcription regulation (Lee *et al*, 2007; Choi *et al*, 2010). $EIIA^{Glc}$-mediated catabolite repression is a well-established regulatory mechanism by the PTS (Harwood *et al*, 1976; Feucht *et al*, 1980). Unphosphorylated $EIIA^{Glc}$ under glucose abundant conditions interacts with proteins necessary for the transport and metabolism of non-PTS carbohydrates, such as lactose, maltose, and glycerol, and inhibits their activities for PTS-catalyzed uptake of glucose as the preferred sugar. Interestingly, numerous *Proteobacteria* possess incomplete PTS cascades devoid of any known EIIB or EIIC proteins (Deutscher *et al*, 2014). Thus, an incomplete PTS lacking substrate-specific EIIB and EIIC proteins is supposed to conduct regulatory functions by interacting

with non-PTS substrates, instead of taking up sugar.

Extensive genome analysis revealed a paralog of the sugar PTS, called nitrogen PTS (PTS^{Ntr}) in many *Proteobacteria* (Powell *et al*, 1995). However, the repertoire is incomplete. In parallel with the sugar PTS, the PTS^{Ntr} possesses EI^{Ntr} (an EI paralog encoded by *ptsP*) and NPr (an HPr paralog encoded by *ptsO*), which catalyze phosphorylation of $EIIA^{Ntr}$ (an $EIIA^{Mtl}$ paralog encoded by *ptsN*) with a PEP-derived phosphoryl group but the PTS^{Ntr} is devoid of any known counterparts of the membrane-bound EIIB and EIIC enzymes, which transport extracellular substrates (Powell *et al*, 1995; Reizer *et al*, 1996; Peterkofsky *et al*, 2006). Accordingly, the PTS^{Ntr} has been speculated to conduct regulatory functions exclusively using $EIIA^{Ntr}$ as the output regulator protein rather than a component of transport machinery (Pflüger-Grau *et al*, 2010). An increasing number of data show that PTS^{Ntr} is associated with a plethora of cellular processes, including virulence (Choi *et al*, 2010; Higa *et al*, 2001), nitrogen metabolism (Powell *et al*, 1995; Lee *et al*, 2005), carbon metabolism (Jahn *et al*, 2013), K^+ homeostasis (Lee *et al*, 2007; Lüttmann *et al*, 2009; Reaves *et al*, 2011), and (p)ppGpp synthesis/hydrolysis (Karstens *et al*, 2014;

Ronneau *et al*, 2016).

The *ptsN* gene encoding $EIIA^{Ntr}$ is located downstream of *rpoN* in many *Proteobacteria* (Boël *et al*, 2003). An alternative σ^{54} sigma factor encoded by *rpoN* participates in the expression of diverse genes and operons exclusively associated with nitrogen utilization and metabolism (Reitzer *et al*, 2001). A genetic approach was employed on the *rpoN* operon containing *ptsN* to unravel the primary role of PTS^{Ntr} conserved in many bacteria during evolution and revealed that the ancestral *rpoN* operon composed of at least 11 genes has evolved to retain *rpoN*, *yhbH*, *ptsN*, *rapZ*, and *ptsO* in many *Gammaproteobacteria* (Pflüger-Grau *et al*, 2010; Comas *et al*, 2008), suggesting a conserved function for the remaining genes. Localization of the *ptsN* and *ptsO* PTS^{Ntr} genes in the *rpoN* operon suggests a role for PTS^{Ntr} associated with nitrogen metabolism. Due to the absence of a component responsible for uptake and concomitant phosphorylation of a specific substrate, it has been unclear what stimuli determine the phosphorylation status of the PTS^{Ntr} components. However, it was recently revealed that EI^{Ntr} senses nitrogen availability through the glutamine (Gln) and α-ketoglutarate (α-KG) ratio and accordingly

modulates the phosphorylation status of the $EIIA^{Ntr}$ output regulator in *E. coli* (Lee *et al*, 2013). Nitrogen is prerequisite for producing proteins, nucleic acids, and cell wall constituents. Therefore, it is critical for bacteria to sense availability of cellular nitrogen sources and allot them depending on the circumstances. The functional relevance of the genes comprising the *rpoN* operon to nitrogen utilization for cell wall construction has been frequently demonstrated. NPr encoded by *ptsO* decreases biosynthesis of lipid A in the lipopolysaccharides (LPS) layer by inhibiting LpxD activity and blocking the inflow of UDP-GlcNAc into cell wall constituents (Kim *et al*, 2011). RapZ encoded by *rapZ* negatively controls synthesis of the D-glucosamine-6-phosphate synthase (GlmS) by triggering decay of GlmZ, a small RNA facilitating *glmS* translation (Göpel *et al*, 2013). GlmS is a key enzyme in the LPS and peptidoglycan biosynthetic pathways. The association between σ^{54}, a transcription factor encoded by *rpoN*, and bacterial exterior constitution has been observed in many bacteria (Fisher *et al*, 2005; Francke *et al*, 2011). Co-clustering of PTS^{Ntr} genes with *rpoN* and convergent negative roles of the *rpoN* operon genes during synthesis of cell envelope constituents have led to exploring a concordant role for $EIIA^{Ntr}$ in cell

envelope formation in response to nitrogen abundance. In this study, I discovered direct protein-protein interaction between $EIIA^{Ntr}$ and GlmS and suggest a novel role for *ptsN* regulating amino sugar biosynthesis, which is contextually associated with adjacent genes.

II-2. Materials and Methods

Bacterial strains, plasmids, and culture conditions. *Salmonella* was genetically manipulated using the phage λ Red recombination system (Datsenko & Wanner, 2000) and phage P22-mediated transduction (Chan *et al*, 1972) with *Salmonella enterica* serovar Typhimurium SL1344 as the parent strain. The phage λ-derived Red recombination system was used to delete genes in-frame or to fuse genes/proteins with peptide tags (Datsenko & Wanner, 2000). The Km^R cassette from pKD13 was amplified using the ptsN-del-F and ptsN-del-R and glmS-del-F and glmS-del-R primers, respectively, to construct the SR7001 (Δ*ptsN*) and SR7002 (Δ*glmS*) strains, and the resulting PCR products were introduced into the SL1344 strain containing the pKD46 plasmid. Recombinant bacteria containing the Km^R cassette in place of the target genes were detected using kanamycin resistance and diagnostic PCR. The Km^R cassette was further removed using the pCP20 plasmid (Datsenko & Wanner, 2000). GlcNAc (0.2%) was added to the medium during Δ*glmS* selection to complement the lethality of Δ*glmS*. *lon* was deleted and $EIIA^{Ntr}$ was tagged with the FLAG peptide at the C-terminus

using a phage λ-mediated recombination system (Datsenko & Wanner, 2000; Ellermeier *et al*, 2002). The strain carrying a *lacZ* fusion to *ssaG* was constructed as described above. The Km^R cassette that was PCR-amplified from the pKD3 plasmid using the ssaG-lacZ-F and ssaG-lacZ-R primers was introduced downstream of *ssaG* and then replaced with the pCE70 *lacZY* gene via the FRT site. All bacterial strains and plasmids used in this study are listed in Table II-1 and II-2. The primers used to construct the bacterial strains are listed in Table II-3. Bacteria were grown aerobically at 37°C in LB or M9 minimal medium supplemented with nutrients as described. Antibiotics were used at the following concentrations: ampicillin, 50 μg/ml; chloramphenicol, 25 μg/ml; and kanamycin, 50 μg/ml.

Plasmid construction. DNA containing the *Salmonella ptsN* gene was amplified by PCR using the ptsN-comple-F and ptsN-comple-R primers to construct pWJ04 producing $EIIA^{Ntr}$ under its putative intrinsic promoter, and the PCR products were introduced between the pACYC184 HindIII and SphI sites. The *ptsN* gene was PCR amplified using the ptsN-F and ptsN-R primers to construct pWJ06 expressing

$EIIA^{Ntr}$ from the *lac* promoter. The purified DNA fragments were inserted between the EcoRI and BamHI sites of the pUHE21-2*lacI*^{q} vector (Soncini *et al*, 1995). The *ptsN* gene was amplified using the ptsN-His-F and ptsN-His-R primers to construct pWJ07 producing $EIIA^{Ntr}$ tagged with six histidines at its C-terminus, and the PCR products were introduced between the EcoRI and BamHI sites of the pUHE21-2*lacI*^{q} vector. The pWJ10 plasmid expressing GlmS from the *lac* promoter was constructed by introducing PCR fragments containing *glmS* between the BamHI and HindIII sites of the pUHE21-2*lacI*^{q} vector. The glmS-F and glmS-R primers used to construct pWJ10. The pKT25-*ptsN* and pUT18C-*glmS* plasmids were constructed for the bacterial two-hybrid analysis. The *ptsN* and *glmS* genes were amplified using the ptsN-BTH-F and ptsN-BTH-R, and glmS-BTH-F and glmS-BTH-R primers, respectively. The purified PCR products were inserted between the BamHI and EcoRI sites of the pKT25 plasmid vector or between the BamHI and SacI sites of the pUT18C plasmid vector (Karimova *et al*, 2001). The pWJ11, pWJ12, pWJ13, and pWJ14 plasmids were constructed to extract and purify EI^{Ntr}, NPr, $EIIA^{Glc}$, and GlmS proteins, respectively. The pET28a vector was used to purify soluble proteins containing a His_6-tag at their N-termini.

Plasmids expressing $EIIA^{Ntr}$ with H73A and K75D substitutions were constructed using a QuickChange II site-directed mutagenesis kit (Stratagene, La Jolla, CA, USA) with the ptsN-H73A-F and ptsN-H73A-R primers for $EIIA^{Ntr}$ (H73A) and the ptsN-K75D-F and ptsN-K75D-R primers for $EIIA^{Ntr}$ (K75D). Plasmids expressing $EIIA^{Ntr}$ or its derivatives were introduced into a Δ*ptsN* mutant strain with P*ssaG-lacZ* to verify the regulatory activity of $EIIA^{Ntr}$ on *ssaG* (Choi *et al*, 2010), and all plasmids tested complemented the Δ*ptsN* mutant. The pWJ15, pWJ16, and pWJ17 plasmids were constructed for the pull-down assay. The pETDuet-1 vector was used to express His_6-GlmS and $EIIA^{Ntr}$. The *glmS* and *ptsN* genes were amplified using the Duet-glmS-His-F and Duet-glmS-His-R and Duet-ptsN-F and Duet-ptsN-R primers, respectively. The purified PCR products of the *glmS* and *ptsN* genes were inserted between the NcoI and HindIII, and NdeI and KpnI sites of the pETDuet-1 vector, respectively. The primers used to construct the plasmids in this study are listed in **Table II-3**.

Ligand fishing to search for $EIIA^{Ntr}$-His_6 protein targets. *Salmonella* Typhimurium SL1344 cells were grown overnight in 300 ml

LB broth at 37°C with shaking and were harvested and resuspended in 10 ml lysis buffer [20 mM Tris-HCl (pH 8.0) and 300 mM NaCl]. The cells were disrupted by sonication on ice and then pelleted by centrifugation at 15,000 *g* for 1 h at 4°C. The supernatant was mixed with 1 mg $EIIA^{Ntr}$-His_6 or not and was further incubated with 300 μl Ni-NTA resin for 1 h at 4°C. The incubated mixture was loaded onto a Poly-Prep chromatography column (8 × 40 mm) (Bio-Rad, Hercules, CA, USA), washed with 5 ml washing buffer [20 mM Tris-HCl (pH 8.0), 300 mM NaCl, and 5 mM imidazole], and the proteins bound to the resin were eluted with elution buffer [20 mM Tris-HCl (pH 8.0), 300 mM NaCl, and 250 mM imidazole]. Aliquots of the eluted protein samples were analyzed by SDS-PAGE and stained with Coomassie Brilliant Blue G. The protein that was specifically bound to $EIIA^{Ntr}$-His_6 was excised from the gel and subjected to in-gel digestion with trypsin and LC-MS/MS analysis as described previously (Jeong *et al*, 2004).

Bacterial two-hybrid system for studying protein-protein interactions. To analyze protein-protein interactions between the phosphorylated/dephosphorylated forms of $EIIA^{Ntr}$ and GlmS under *in*

vivo conditions, the BACTH (Bacterial Adenylate Cyclase Two-Hybrid) system based on reconstitution of adenylate cyclase (CyaA) activity through heterodimerization of the hybrid proteins was used with the *E. coli* BTH101 reporter strain, which lacks an endogenous functional *cyaA* gene. The proteins to be tested were fused to the T25- and T18-fragments of the CyaA protein from *Bordetella pertussis*. The T25- and T18-domains are unable to interact with each other without a fusion partner. However, when fused to proteins that interact with each other, the T25- and T18- domains assemble into a functional CyaA protein that synthesizes cAMP. cAMP synthesis is monitored by the expression of cAMP-CRP-dependent genes, such as *lacZ* encoding β-galactosidase. Therefore, β-galactosidase activities reflect the strength of the interactions between the proteins fused to the CyaA domains. The pKT25 and pUT18C plasmids were used to construct the T25-CyaA and T18-CyaA fusions, respectively, to the N-termini of $EIIA^{Ntr}$/$EIIA^{Ntr}$ (H73A) and GlmS as potential interaction partners. The *E. coli* BTH101 reporter strain was co-transformed with two recombinant plasmids (e.g., pKT25-*ptsN* and pUT18C-*glmS* or pKT25-*ptsN* (H73A) and pUT18C-*glmS*) and plated on LB agar medium supplemented with kanamycin, 50 μg/ml;

ampicillin, 50 μg/ml; 5-bromo-4-chloro-3-indolyl-β-D-galactoside, 40 μg/ml; and IPTG, 0.5 mM (final concentration). The plates were incubated at 30°C for 24 h or more. Blue colonies were selected and streaked on the same agar plate or inoculated into LB broth containing IPTG to validate the interactions between the tested proteins. For the latter case, the β-galactosidase activities were determined to compare interaction strength between pairs of hybrid proteins. A detailed description of the procedure can be found in Miller (1972) and Karimova *et al.* (1998).

β-Galactosidase assay. The β-galactosidase assay was carried out in triplicate, and activity was determined as described previously (Miller, 1972).

Immunoprecipitation of EIIA^{Ntr} using His$_6$-Glms *in vivo*. *E. coli* BL21 (DE3) cells, which produce GlmS tagged with His$_6$ at its N-terminus (His$_6$-GlmS) and EIIA^{Ntr} on pETDuet-*glmS*·*ptsN*, were grown in 200 ml LB, and protein expression was induced by adding 1 mM IPTG at OD_{600} of 2.0 for 6 h. The cell suspension was disrupted by sonication,

centrifuged, and the supernatant was mixed with 1 ml Ni-NTA metal-affinity resin. After the mixture was loaded onto a Poly-Prep chromatography column, the column was washed four times with 2 ml washing buffer [20 mM Tris-HCl (pH 8.0), 300 mM NaCl, and 20 mM imidazole]. The proteins bound to the column were eluted with 500 μl of elution buffer [20 mM Tris-HCl (pH 8.0), 300 mM NaCl, and 50–200 mM imidazole]. Aliquots from the total cell extract (T), the supernatant after the cell extract was centrifuged (S), column eluate (F), wash from washing (W), and the eluted fractions (E) were separated on 12% SDS-PAGE, and the gels were analyzed after staining with Coomassie Brilliant Blue G.

***In vitro* phosphorylation assay.** To measure of $EIIA^{Ntr}$ PDMS, $EIIA^{Ntr}$-His_6 (K75D) (2 μg) was incubated with His_6-EI^{Ntr} (1 μg) and His_6-NPr (1 μg) in the presence or absence of PEP (1 mM) in a total volume of 20 μl containing 0.1 M Tris-HCl (pH 7.5), 2 mM $MgCl_2$, 1 mM EDTA, 10 mM KCl, and 0.5 mM dithiothreitol (Lee *et al*, 2013b). After a 20 min incubation at 37°C, the reaction was stopped by adding 5 μl 4× SDS-Sample Buffer (L1100-001; GeneDEPOT, Barker, TX, USA) [250 mM

Tris-HCl (pH 6.8), 40% glycerol, 8% SDS, and 8% β-mercaptoethanol], and the aliquots were analyzed by 15% SDS-PAGE. The proteins were stained with Coomassie Brilliant Blue G. To examine the effect of various metabolites on PTS^{Ntr} phosphotransferase activity, $EIIA^{Ntr}$-His_6 (K75D) (3 μg) was incubated with PEP (1 mM), His_6-EI^{Ntr} (0.3 μg), and His_6-NPr (0.3 μg) in the presence of 5 mM Gln, α-KG, and GlcN6P. After a 5 min incubation at 37°C, the reactions were stopped and processed as described above.

Purification of His_6-tagged proteins. For purification of soluble His_6-tagged proteins (His_6-EI^{Ntr}, His_6-NPr, His_6-$EIIA^{Glc}$, and His_6-GlmS: all tagged at their N-termini; $EIIA^{Ntr}$-His_6, $EIIA^{Ntr}$-His_6 (H73A), and $EIIA^{Ntr}$-His_6 (K75D): all tagged at their C-termini), *E. coli* BL21 (DE3) or *S.* Typhimurium SL1344 Δ*glmS* strains harboring plasmids expressing His_6-tagged proteins were grown overnight in LB medium, and protein expression was induced by adding 1 mM IPTG. The His_6-tagged proteins were purified using nickel-nitrilotriacetic acid (Ni-NTA) resin (Qiagen) according to the manufacturer's instructions, and bound proteins were eluted with elution buffer [20 mM Tris-HCl (pH 8.0), 300 mM NaCl, and

250 mM imidazole] (Fig. II-1). The eluted proteins were concentrated using a VivaSpin 20 instrument (3,000-molecular-weight cutoff [MWCO] polyethersulfone; Sartorius, Göttingen, Germany), and the elution buffer was replaced with storage buffer [20 mM Tris-HCl (pH 8.0), 300 mM NaCl, and 50% glycerol] using a PD MidiTrap G-25 column (GE Healthcare, Buckinghamshire, United Kingdom). Protein concentration was determined using the Bradford assay (Bio-Rad) with BSA as the standard. To remove the His_6-tag from the purified proteins, the Thrombin Cleavage Capture Kit (69022-3; Novagen, Gibbstown, NJ, USA) was used according to the manufacturer's instructions. Cleavage of the His_6-tag from the purified proteins was confirmed by SDS-PAGE stained with Coomassie Brilliant Blue G and Western blot analysis using anti-His_6 antibody (sc-8036; Santa Cruz Biotechnology).

In vitro **protein-protein interactions between phosphorylated/unphosphorylated $EIIA^{Ntr}$ and GlmS.** To compare the binding affinities of $EIIA^{Ntr}$ to GlmS depending on phosphorylation status, $EIIA^{Ntr}$-His_6 (K75D) (100 μg) was incubated with His_6-EI^{Ntr} (10 μg) and His_6-NPr (10 μg) in the presence or absence of PEP (2 mM) in a total

volume of 100 µl, as described above. PEP-dependent phosphorylation of $EIIA^{Ntr}$-His_6 (K75D) was verified by 15% SDS-PAGE analysis, and the remainder (95 µl of each) that was not used in $EIIA^{Ntr}$-His_6 (K75D) PDMS was mixed with Ni-NTA resin (50 µl) in 1 ml binding buffer [20 mM Tris-HCl (pH 8.0), and 300 mM NaCl] and incubated at 4°C for 30 min. Purified GlmS (100 µg) was cleaved by thrombin to detach the His_6-tag from His_6-GlmS and was added to each reaction and incubate for 30 min at 4°C under the same conditions. To dissociate the bound proteins, elution buffer [20 mM Tris-HCl (pH 8.0), 300 mM NaCl, and 250 mM imidazole] was passed through the Ni-NTA resin several times. The eluent was subsequently analyzed by SDS-PAGE, followed by Coomassie Brilliant Blue staining.

Size exclusion chromatography with multi-angle light scattering. SEC-MALS experiments were performed using a fast protein liquid chromatography system (GE Healthcare) connected to a Wyatt MiniDAWN TREOS MALS instrument and a Wyatt Optilab rEX differential refractometer. A Superdex 200 10/300 GL (GE Healthcare) gel-filtration column pre-equilibrated with equilibrium buffer [20 mM

Tris-HCl (pH 8.0) and 300 mM NaCl] was normalized using ovalbumin protein. Proteins (2 mg) were injected at a flow rate of 0.5 ml/min. Data were analyzed using the Zimm model for static light-scattering data fitting and graphed using EASI graph with a UV peak in ASTRA V software (Wyatt Technology Corp., Goleta, CA, USA).

Glucosamine-6-phosphate synthase activity assay. The following stock solutions were prepared before the GlmS activity assay: 0.5 M Tris-HCl (pH 7.5), 0.5 M KCl, 10 mM EDTA (pH 7.5), 60 mM Fru6P, and 50 mM L-Gln. A pre-warmed solution containing 6 mM Fru6P, 10 mM L-Gln in 50 mM Tris-HCl (pH 7.5), 50 mM KCl, and 1 mM EDTA was mixed with GlmS (0–16 pmol) and incubated at 37°C for 30 min. GlmS activity was inactivated by heating at 80°C for 20 min, and the GlcN6P product was measured by HPLC. To determine the effects of $EIIA^{Ntr}$ on GlmS, different amounts of $EIIA^{Ntr}$-His_6 (K75D) (0–16 pmol) were added to the reaction, and the levels of GlcN6P produced were compared. Reaction mixtures without GlmS or Fru6P were used as negative controls. A detailed description of the procedure can be found in Li *et al.* (2007).

RNA isolation and quantitative real-time RT-PCR. *Salmonella* strains were grown in LB or W-salts medium. W-salts medium was supplemented with 20 mM alanine and 0.26 mM histidine. Different carbon sources were added separately when required: 0.2% GlcNAc, 0.2% glucose or 0.2% glycerol. Total RNAs were isolated at the mid-log phase using the RNeasy mini kit (Qiagen, Valencia, CA, USA). After DNase treatment of the isolated total RNAs, cDNA was synthesized with the RNA to cDNA EcoDry^{TM} Premix and random hexamers (Clontech, Palo Alto, CA, USA). The synthesized cDNA was mixed with 2× iQ SYBR Green Supermix (Bio-Rad), and real-time PCR was performed using the CFX 3.1 (Bio-Rad). mRNA expression levels of target genes were normalized relative to that of the *gyrB* (DNA gyrase subunit B). All qRT-PCR primer sets used in this study are listed in **Table II-4**.

SDS-PAGE and Western blotting analysis. Protein samples (purified or interaction complexes) or whole-cell fractions (cell extract after sonication or cell pellets) were dissolved in Laemmli sample buffer

and boiled for 5 min. The protein samples were loaded onto 12% or 15% SDS-PAGE, the proteins were separated based on molecular weight, and transferred to a polyvinylidene difluoride membrane. The membrane was blocked with 5% nonfat dry milk in 1× Tris-buffered saline-Tween 20 (TBS-T) buffer and probed with anti-FLAG antibody (3:2,000 dilution, F1804; Sigma, St. Louis, MO, USA), anti-His_6 antibody (3:2,000 dilution, sc-8036; Santa Cruz Biotechnology, Santa Cruz, CA, USA), or anti-DnaK antibody (1:10,000 dilution, ADI-SPA-880; Enzo Life Science, Farmingdale, NY, USA) as primary antibodies. Anti-mouse IgG conjugated with peroxidase (3:5,000 dilution, sc-2005; Santa Cruz Biotechnology) was used as the secondary antibody in all Western blots. The chemiluminescent signals were developed with a West-Zol plus Western blot detection system (Intron Biotechnology, Seoul, South Korea).

Analysis of protein stability. Protein stability was determined as described previously (Biran *et al*, 2000). *Salmonella* strains producing the $EIIA^{Ntr}$-FLAG protein from the chromosome were grown in LB medium with or without 0.2% GlcNAc for 3 h, and 0.2 mg/ml chloramphenicol

was added to block *de novo* protein synthesis. Aliquots of the cultures were taken at the indicated time points after adding chloramphenicol and were subjected to Western blotting, as described above.

Table II-1. Bacterial strains used in this study.

Strains	Description	References or source
***Salmonella enterica* serovar Typhimurium**		
SL1344	Wild type, Sm^R	(Robin & Lee, 2000)
SR7001	Δ*ptsN*	This study
SR7002	Δ*glmS*	This study
SR7003	Δ*glmS* Δ*ptsN*	This study
SR7011	P*ssaG-lacZ*	This study
SR7012	P*ssaG-lacZ*, Δ*ptsN*	This study
SR7021	$EIIA^{Ntr}$-FLAG	This study
SR7022	$EIIA^{Ntr}$-FLAG, Δ*glmS*	This study
SR7023	$EIIA^{Ntr}$-FLAG, Δ*glmS* Δ*lon*	This study
SR7024	$EIIA^{Ntr}$-FLAG, Δ*glmS* Δ*clpXP*	This study
Escherichia coli		
BTH101	F^- *cyaA-99 araD139 galE15 galK16 rpsL1 hsdR* ^{2} µ*rA1* µ*rB1*	(Karimova *et al*, 2000)
DH5α	*gyrA96 recA1 relA1 endA1 thi-1 hsdR17 glnV44 deoR Δ(lacZYA-argF)U169* [Φ80d Δ(*lacZ*)*M15*]	(Woodcock *et al*, 1989)
BL21 (DE3)	F^- *ompT* $hsdS_B$ (r_B^- m_B^-) *gal dcm* (DE3)	(Studier & Moffattf, 1986)

Table II-2. Plasmids used in this study.

Plasmids	Description	References or source
pKD46	Ap^R P_{BAD}-*gam-beta-exo oriR101 repA101*^{ts}	(Datsenko & Wanner, 2000)
pKD13	Ap^R FRT Km^R FRT PS1 PS4 *oriR6Kγ*	(Datsenko & Wanner, 2000)
pCP20	Ap^R Cm^R *cI*857 λP_R*flp oripSC101*^{ts}	(Datsenko & Wanner, 2000)
pCE70	Km^R FRT *tnpR lacZY*$^+$ *oriR6Kγ*	(Merighi *et al*, 2005)
pACYC184	Tet^R Cm^R p15A *ori*	(Chang & Cohen, 1978)
pUHE21-2*lacI*^{q}	rep_{pMB1} Ap^R *lacI*^{q}	(Soncini *et al*, 1995)
pKT25	ori p15A, *Plac*::*cyaA* 1–224, MCS, *neo*	(Karimova *et al*, 2001)
pUT18C	ColEI-ori, *Plac*::*cyaA* 225–399, MCS, *bla*	(Karimova *et al*, 2001)
pKT25-zip	ori p15A, *Plac*::*cyaA* 1–224ΦGCN4-zip, *neo*	(Karimova *et al*, 2001)
pUT18C-zip	ColEI-ori, *Plac*::*cyaA* 225–399ΦGCN4-zip, *bla*	(Karimova *et al*, 2001)
pET28a	Expression vector with a hexahistidine tag, Kan^r	Novagen
pETDuet-1	Co-expression vector with a hexahistidine tag, Amp^r	Novagen
pWJ01	pKT25-*ptsN*	This study
pWJ02	pKT25-*ptsN* (H73A)	This study
pWJ03	pUT18C-*glmS*	This study
pWJ04	pACYC184-*ptsN*	This study
pWJ05	pACYC184-*ptsN* (H73A)	This study
pWJ06	pUHE21-2*lacI*^{q}-*ptsN*	This study
pWJ07	pUHE21-2*lacI*^{q}-*ptsN*-His_6	This study
pWJ08	pUHE21-2*lacI*^{q}-*ptsN*-His_6 (H73A)	This study
pWJ09	pUHE21-2*lacI*^{q}-*ptsN*-His_6 (K75D)	This study
pWJ10	pUHE21-2*lacI*^{q}-*glmS*	This study
pWJ11	pET28a-*ptsP*	This study
pWJ12	pET28a-*ptsO*	This study
pWJ13	pET28a-*crr*	This study
pWJ14	pET28a-*glmS*	This study
pWJ15	pETDuet-*glmS*	This study
pWJ16	pETDuet-*ptsN*	This study
pWJ17	pETDuet-*glmS*·*ptsN*	This study

Table II-3. Primers used to construct the bacterial strains and plasmids.

Primers	Sequence (5' to 3')
ptsN-del-F	CTG GCC ATC AAC CTG ACA GGA CAG GTT CTT AGG TGA AAT TTG TAG GCT GGA GCT GCT TCG
ptsN-del-R	CGT TTC GCC ACC AGC GAC AGC GTG TGC AGA TGC GTT TTA ATT CCG GGG CTC CGT CGA CC
glmS-del-F	TTG CGC TCG AAG GCG CGC TGA AGC TGA AAG AGA TCT CTT ATG TAG GCT GGA GCT GCT TCG
glmS-del-R	CG TCT GTC GAC GGC CTT CTG CCT GGT ACT ACA TTT GTA CAT TCC GGG GAT CCG TCG ACC
lon-del-F	ATC TGA TTA CCT GGC GGA CAC TAA ACT AAG AGA GAG CTC TTG TAG GCT GGA GCT GCT TCG
lon-del-R	GCG CAC GCA CCA CGG TCA GCG CCG CCT GAA TGG ATT CCT GAT TCC GGG GAT CCG TCG ACC
clpXP-del-F	AGT ACA GCA GAT TTT TTC AAT TTT TAT CCA GGA GAC GGA ATG TAG GCT GGA GCT GCT TCG
clpXP-del-R	ACT GCT TGG TCA GCG CAT TTT TCG GCT CTT TCA GGA TTT GAT TCC GGG GAT CCG TCG ACC
ptsN-FLAG-F	TCA AAT CAT TAC TGA CAC CGA AGG TGA GCA GAA TGA GGC A GGC AGC GGC GAC TAC AAA GAC GAT GAC GAC AAG TAA TGT AGG CTG GAG CTG CTT CG
ptsN-FLAG-R	GTT TCT CCT CAC AAC GAC AGA AAT AAA TGC CAT TGA GTT GAT TCC GGG GAT CCG TCG ACC
ssaG-lacZ-F	ATA TTT ATT AAT TAC GAA AGT TCA CTG ATC GTG TAG GCT GGA GCT GCT TC
ssaG-lacZ-R	AAT AAA ATT TTC GCG GCT TTT AGC GGC TCA ATG GGA ATT AGC CAT GGT CC
ptsN-comple-F	AAA AAG CTT ACG CAC ATC TCG GAT GCG AC
ptsN-comple-R	AAA GCA TGC CCG CTG ACG ATC ATC AGT AC
ptsN-F	CAG GTT CTG AAT TCA AAT TAT GA
ptsN-R	GTA CCA GGA TCC GTT TCT C
ptsN-His-F	AAA GGA TCC ATG ATA AAT AAC GAT ACG AC
ptsN-His-R	AAA AAG CTT TCA GTG GTG GTG GTG GTG GTG GCC GCT GCC TGC CTC ATT CTG CTC ACC TT
ptsN-BTH-F	AAA GGA TCC TAT GAT AAA TAA CGA TAC GA
ptsN-BTH-R	AAA GAA TTC ACA ACG ACA GAA ATA AAT GC
ptsN-H73A-F	GTA ATG GTA TCG CCA TCC CGG CGG GGA AAC TGG AAG AAG ATA C
ptsN-H73A-R	GTA TCT TCT TCC AGT TTC CCC GCC GGG ATG GCG ATA CCA TTA C
ptsN-K75D-F	GCC ATC CCG CAC GGG GAT CTG GAA GAA GAT ACC T
ptsN-K75D-R	AGG TAT CTT CTT CCA GAT CCC CGT GCG GGA TGG C
glmS-F	AAA GGA TCC ATG TGT GGA ATT GTT GGC GCA AAA AGC TTG CTC TTC AGC CAC CAT AGA G
glmS-R	AAA AAG CTT GCT CTT CAG CCA CCA TAG AG
glmS-BTH-F	AAA GGA TCC TAT GTG TGG AAT TGT TGG C
glmS-BTH-R	AAA GAG CTC CTT CTG CCT GGT ACT ACA TT

Table II-3. Primers used to construct the bacterial strains and plasmids.

Primers	Sequence (5' to 3')
ptsP-His-F	AAA CAT ATG CTC ACT CGC CTG CGC
ptsP-His-R	AAA GAG CTC TGT TGT CTG CGC CGT GAA TC
ptsO-His-F	AAA CAT ATG ACC GTA AAG CAA ACT GTT G
ptsO-His-R	AAA GAG CTC GAC TGT CAT CAA ATA CCG GG
crr-His-F	AAA CAT ATG GGT TTG TTC GAT AAA CTA AA
crr-His-R	AAA GAG CTC CAC TGC GGC AAG AAT TAC TT
glmS-His-F	AAA CCA TGG CTA TGT GTG GAA TTG TTG GCG
glmS-His-R	AAA CTC GAG CTC TAC GGT AAC CGA TTT CGC
Duet-glmS-His-F	AAA CCA TGG CTA TGT GTG GAA TTG TTG GC
Duet-glmS-His-R	AAA AAG CTT CTT CTG CCT GGT ACT ACA TT
Duet-ptsN-F	AAA CAT ATG ATA AAT AAC GAT ACG AC
Duet-ptsN-R	AAA GGT ACC ACA ACG ACA GAA ATA AAT GC

Table II-4. qRT-PCR primers.

Primers	Sequences (5' to 3')
qRT-glmS-F1	CTG AAA CCG ACA CCG AAG TG
qRT-glmS-R1	CAG AAC AGC CTC ACG CAG AGT
qRT-glmU-F1	GCG CGG ACA TGA AAC GTT
qRT-glmU-R1	CTG TTC GGC CTG GTA AAT ACG
qRT-glmM-F1	GCC TCG TTT ACC GGA CCT ATG
qRT-glmM-R1	AGG CAG TTT CGT ACC GTC GAT
qRT-ptsN-F1	AGC GGC GTT CAT TGT CAG A
qRT-ptsN-R1	GGA GGT AAA CTG AGC TGT TTT GC
qRT-rapZ-F1	GAT GAA TAA TCT GCC TGG TGC TT
qRT-rapZ-R1	TGT AGC GGC GAA TCA AGG TA
qRT-gyrB-F1	ATA ACG CCA CGC AGA AAA TGA
qRT-gyrB-R1	TGG CTG ATA CAC CAG CTC TTT G

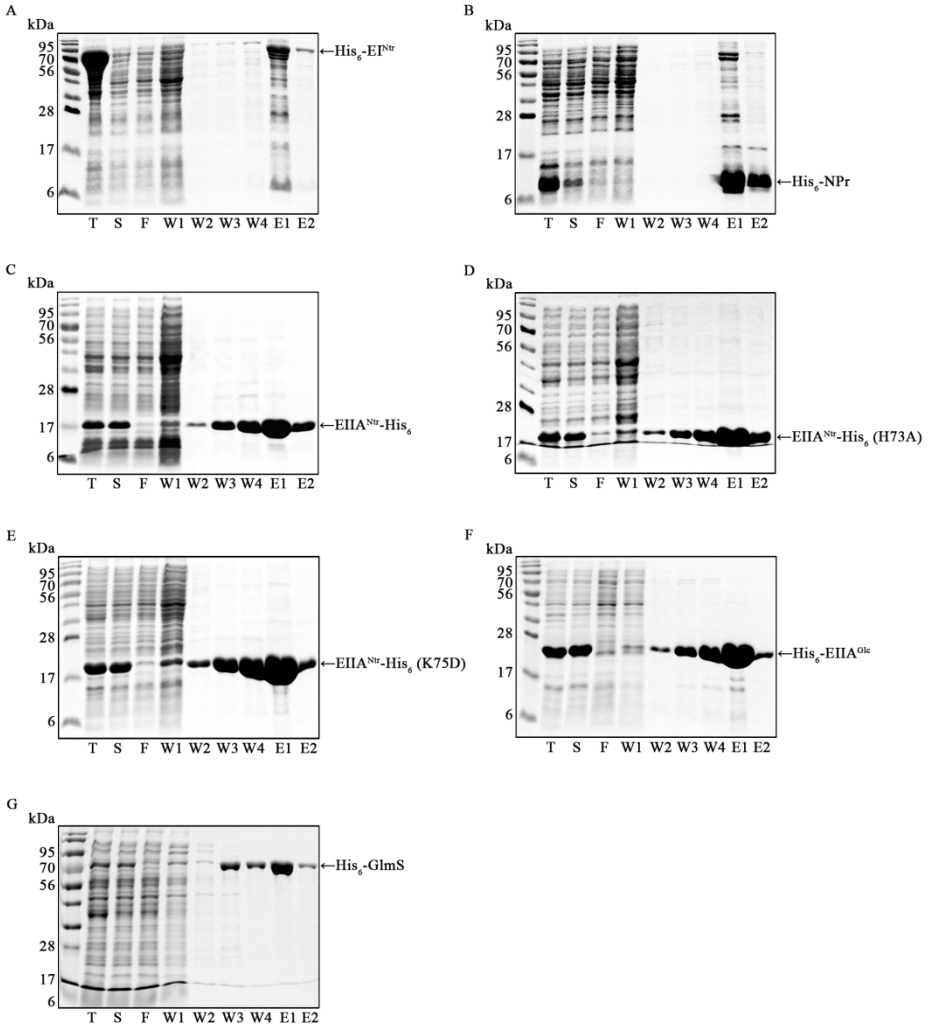

Figure II-1. Over-expressed proteins were purified using affinity chromatography. SDS-PAGE analyses to examine the purity of isolated proteins. Bacterial transformants over-producing His_6-tagged proteins after adding IPTG were lysed, and the lysates were subjected to Ni-NTA affinity purification. Aliquots from total cell extracts (T),

supernatant after centrifugation of the cell extracts (S), column flow-through (F), washes from four washing steps, and the two eluted fractions were separated on 12% SDS-PAGE, and the gels were analyzed after Coomassie Brilliant Blue G staining. Figures of **(A)** to **(G)** denote purification of His_6-EI^{Ntr}, His_6-NPr, $EIIA^{Ntr}$-His_6, $EIIA^{Ntr}$-His_6 (H73A), $EIIA^{Ntr}$-His_6 (K75D), His_6-$EIIA^{Glc}$, and His_6-GlmS, respectively. Molecular masses of the standards are presented in kDa on the left.

II-3. Results

Specific interaction between Enzyme IIA^{Ntr} and glucosamine-6-phosphate synthase in *Salmonella* Typhimurium. Although the general sugar PTS components exert regulatory functions by either phosphorylating or interacting with target proteins, PTS^{Ntr} EIIA^{Ntr} seems to have a bias toward interaction-mediated regulation. Many studies have demonstrate direct interactions between unphosphorylated EIIA^{Ntr} and diverse proteins involved in K^+ transport (Lee *et al*, 2007; Lüttmann *et al*, 2009), virulence regulation (Choi *et al*, 2010), and the ppGpp-mediated stringent response (Karstens *et al*, 2014; Ronneau *et al*, 2016). A common theme of these EIIA^{Ntr} interactions is that unphosphorylated EIIA^{Ntr} prevails during the protein-protein interaction. To search for target proteins interacting with EIIA^{Ntr}, EIIA^{Ntr} tagged with His_6 at its C-terminus (EIIA^{Ntr}-His_6) was isolated in its unphosphorylated form and used as bait in a ligand-fishing strategy with *Escherichia coli* as a representative *Gammaproteobacteria* (Lee *et al*, 2007; Kim *et al*, 2011). Here, to archive more diversity in binding partners, *Salmonella enterica* serovar Typhimurium, a member of

Enterobacteriaceae with high genetic similarity to *E. coli*, was chosen. $EIIA^{Ntr}$-His_6 was incubated with a crude protein extract of *Salmonella* Typhimurium SL1344, and the proteins bound to $EIIA^{Ntr}$-His_6 were pulled down with a metal-affinity resin. The sodium dodecyl sulfate-polyacrylamide gel electrophoresis (SDS-PAGE) analysis of isolated protein complexes from ligand-fishing experiments revealed a protein band of approximately 70 kDa that specifically co-precipitated with $EIIA^{Ntr}$-His_6 (Fig. II-2A). Liquid chromatography-tandem mass spectroscopy (LC-MS/MS) peptide mapping identified this protein as GlmS. Other proteins predicted together with GlmS in the LC-MS/MS analysis are listed in Table II-5. The specific interaction between $EIIA^{Ntr}$ and GlmS was further validated *in vivo*. His_6-GlmS and $EIIA^{Ntr}$ were produced simultaneously under the *lac* promoter of the pETDuet plasmid in *E. coli,* and the crude protein extract was passed through a Ni-NTA resin column. $EIIA^{Ntr}$ was pulled down together with His_6-GlmS (Fig. II-2B). These results indicate direct interactions between $EIIA^{Ntr}$ and GlmS *in vitro* and *in vivo*.

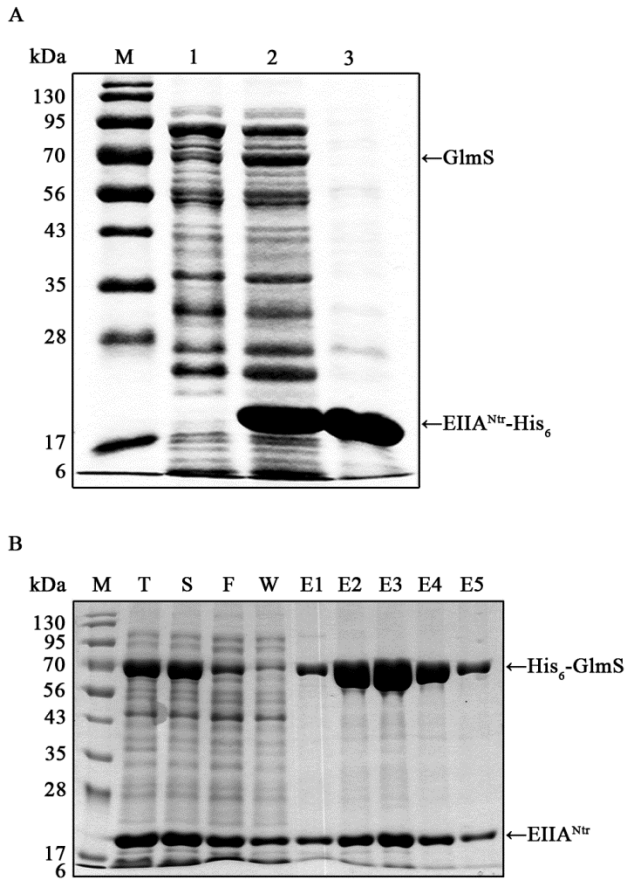

Figure II-2. EIIA^{Ntr} specifically binds to glucosamine-6-phosphate synthase (GlmS). (A) Ligand-fishing using EIIA^{Ntr}-His$_6$ as a bait. Total cell extract from *S.* Typhimurium SL1344 culture was incubated with EIIA^{Ntr}-His$_6$ or not. The proteins eluted from Ni-NTA resin (lane 1, whole cell extract only; lane 2, whole cell extract mixed with EIIA^{Ntr}-His$_6$) and purified EIIA^{Ntr}-His$_6$ (lane 3) were analyzed by SDS-PAGE. The protein band indicated by the arrow in lane 2 was identified as GlmS by LC-MS/MS analysis. Size markers (M) in kDa are aligned at

left. **(B)** Co-purification of $EIIA^{Ntr}$ and GlmS *in vivo*. *E. coli* BL21 (DE3) harboring pETDuet-*glmS·ptsN* was genetically manipulated to produce $EIIA^{Ntr}$ and His_6-tagged GlmS simultaneously by isopropyl β-D-1-thiogalactoside (IPTG) addition. $EIIA^{Ntr}$ bound to His_6-GlmS was co-purified using Ni-NTA metal-affinity resin. Proteins analyzed in SDS-PAGE are aliquots from total cell extracts (T), supernatant after centrifuging the cell extracts (S), column flow-through (F), wash (W), and the five elution fractions (E1–E5). Molecular masses of standards are presented in kDa on the left.

Table II-5. Proteins identified in the ligand fishing-associated LC-MS/MS.

Gene	Locus_tag	Function
tlpA	SL1344_P1_0059	Alpha-helical coiled coil protein
yjbF	SL1344_4159	Hypothetical lipoprotein
polA	SL1344_3947	Reversed DNA polymerase I
kdpB	SL1344_0687	Reversed K^+-transporting ATPase B chain
tufB	SL1344_4085	Elongation factor Tu
groEL	SL1344_4267	60 kDa chaperonin
	SL1344_3498	Hypothetical dehydratase
glmS	SL1344_3828	Glutamine--fructose-6-phosphate aminotransferase

Phosphorylation status of EIIA^{Ntr} influences its binding affinity with GlmS. An intimate association between PTS^{Ntr} and nitrogen metabolism has been proposed undoubtedly through genetic localization of *ptsN* and *ptsO* in the *rpoN* operon and multiple experimental results. The intracellular Gln: α-KG ratio indicates the balance between nitrogen and carbon sources and controls the regulatory circuit assigned to assimilate extracellular ammonia into Gln (Ninfa & Atkinson, 2000) and the phosphorylation status of PTS^{Ntr}. The EI^{Ntr} GAF domain senses the abundance of nitrogen through a high Gln/α-KG ratio, dampens autophosphorylation of EI^{Ntr}, and dephosphorylates EIIA^{Ntr} (Lee *et al*, 2013). Other *ptsO* mutants unable to phosphorylate EIIA^{Ntr} reduce the expression of genes required for nitrogen assimilation and glutamine synthetase, suggesting a negative role for unphosphorylated EIIA^{Ntr} during nitrogen incorporation into Gln (Merrick & Coppard, 1989; Merrick *et al*, 1995). It is plausible that EIIA^{Ntr} responding to nitrogen availability orchestrates the rate of nitrogen acquisition and its utilization in other cellular components. However, it remains unresolved which molecule interacts with phosphorylated or unphosphorylated EIIA^{Ntr} in the nitrogen metabolic

and utilization pathways. The finding of an interaction between $EIIA^{Ntr}$ and GlmS may provide a clue to define the role of PTS^{Ntr} in nitrogen metabolism, as GlmS (D-glucosamine-6-phosphate synthase, EC 2.6.1.16) consumes Gln to produce equimolar D-glucosamine-6-phosphate (GlcN6P), lowering intracellular nitrogen resources.

As demonstrated in other $EIIA^{Ntr}$ binding partners, I assumed that the unphosphorylated status of $EIIA^{Ntr}$ was preferred during complex formation with GlmS. Unphosphorylated $EIIA^{Ntr}$ under high Gln concentrations was likely to bind GlmS and stimulate its GlcN6P production with Gln consumption. However, to my surprise, the binding affinity of $EIIA^{Ntr}$ to GlmS was enhanced by phosphorylation. For this observation, *Salmonella* $EIIA^{Ntr}$-His_6 was modified to $EIIA^{Ntr}$-His_6 (K75D) (Fig. II-3A) to exhibit a phosphorylation-dependent mobility shift (PDMS) on SDS-PAGE without changing its functional properties (Fig. II-4A and B), as established in *E. coli* (Lee *et al*, 2013b). *Salmonella* $EIIA^{Ntr}$-His_6 (K75D) showed an upshift in mobility after PEP-derived phosphorylation (Fig. II-3B) and was downshifted by adding Gln, indicating its unphosphorylated status due to excess nitrogen (Fig. II-3C), as expected. When phosphorylated or

unphosphorylated $EIIA^{Ntr}$-His_6 (K75D) was incubated with GlmS, phosphorylated $EIIA^{Ntr}$ recruited more GlmS than did the unphosphorylated form in a concentration-dependent manner (Fig. II-5B) but $EIIA^{Glc}$ used as a control did not interact (Fig. II-6A). The possibility of non-specific interaction of GlmS with anti-His_6 antibody or Ni-NTA resin was ruled out as detailed in Fig. II-7A and B.

The differential binding affinity of $EIIA^{Ntr}$ to GlmS due to its phosphorylation status was further verified *in vivo* using a bacterial two-hybrid system (Karimova *et al*, 1998). $EIIA^{Ntr}$ and GlmS fused to two different sub-domains of *Bordetella pertussis* adenylate cyclase bound each other and elevated cAMP levels. In accordance with the *in vitro* observations, $EIIA^{Ntr}$ (H73A), a derivative with a mutation at the phosphorylation site (Lee *et al*, 2005), caused lower cAMP levels than that of intact $EIIA^{Ntr}$ (Fig. II-5A and 6B). This result was confirmed by the different color intensities between bacterial cultures containing 5-bromo-4-chloro-3-indolyl-β-D-galactoside (X-gal) (Fig. II-6B).

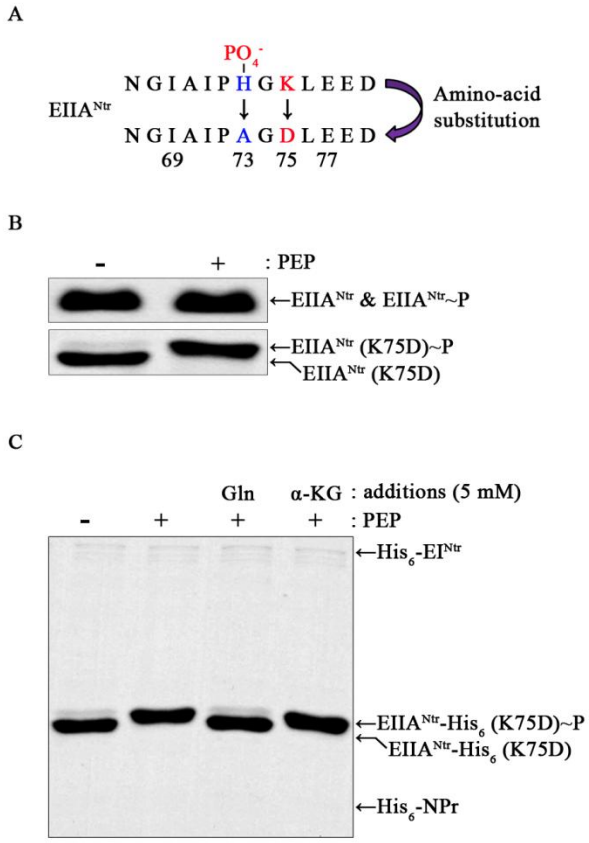

Figure II-3. EIIA^{Ntr} phosphorylation status is influenced by nitrogen abundance. (A) EIIA^{Ntr} modification strategy. The number of SDS molecules bound to a protein is affected by the charge of the amino acids around the phosphorylation site, which can change the mobility of the protein on SDS-PAGE (Lee *et al*, 2013a; 2013b). A histidine (73) amino acid of EIIA^{Ntr} was changed to alanine (73) to construct the unphosphorylated form of EIIA^{Ntr} (H73A), and lysine (75) was

substituted for aspartic acid (75) to provide negative charge effects on $EIIA^{Ntr}$. **(B)** Phosphorylation-dependent upshift of $EIIA^{Ntr}$. The intact form of $EIIA^{Ntr}$ and its $EIIA^{Ntr}$ (K75D) mutant derivative were incubated with or without 1 mM PEP under phosphorylating conditions and then analyzed by SDS-PAGE. $EIIA^{Ntr}$ (K75D) showed excellent phosphorylation-dependent mobility shift (PDMS), whereas the intact form of $EIIA^{Ntr}$ showed comparable mobility independent of its phosphorylation. **(C)** Differential phosphorylation status of $EIIA^{Ntr}$ between metabolites. The phosphorylation-dependent mobility shift of $EIIA^{Ntr}$-His_6 (K75D) was assessed using different metabolites. $EIIA^{Ntr}$-His_6 (K75D) was incubated with PEP, His_6-EI^{Ntr}, and His_6-NPr in the presence of glutamine (Gln) or α-ketoglutarate (α-KG). $EIIA^{Ntr}$-His_6 phosphorylation levels (K75D) were compared by SDS-PAGE.

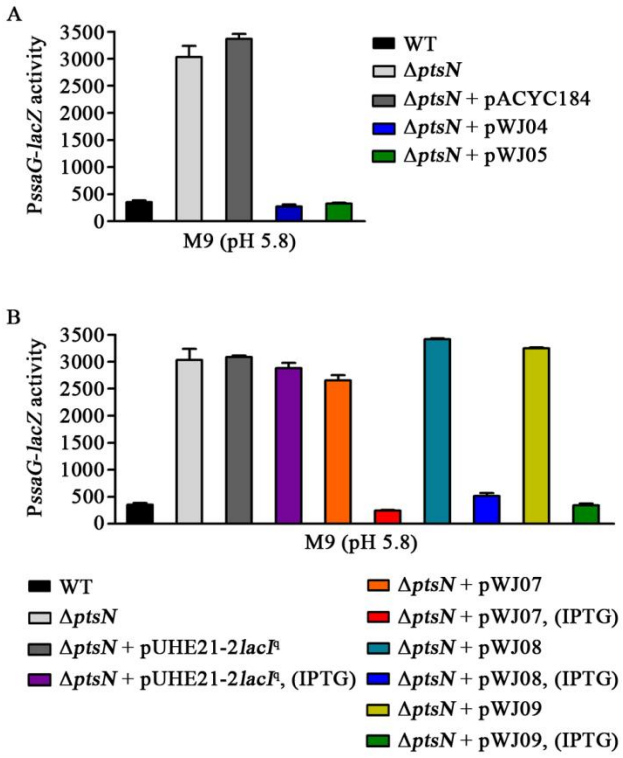

Figure II-4. Modification of EIIA^{Ntr} and its derivatives did not impair its regulatory role in *Salmonella* virulence gene expression. **(A)** Evaluation of the regulatory activities of EIIA^{Ntr} and its derivative EIIA^{Ntr} (H73A) for controlling *ssaG* expression. Intrinsic EIIA^{Ntr} negatively regulates *ssaG*, a component gene of *Salmonella* pathogenicity island 2 (SPI-2) (Choi *et al*, 2010). The pWJ04 and pWJ05 plasmids with pACYC184 as a backbone were introduced into a Δ*ptsN* mutant strain with P*ssaG-lacZ* to produce EIIA^{Ntr} and its derivative EIIA^{Ntr} (H73A), respectively, in the *trans* configuration.

Salmonella strains were cultivated in M9 minimal medium (pH 5.8) for 8 h, and *ssaG* expression was compared in triplicate using β-galactosidase assay. **(B)** Evaluation of the regulatory activities of His_6-tagged $EIIA^{Ntr}$ and its derivatives for controlling *ssaG* expression. The pWJ07, pWJ08, and pWJ09 plasmids using pUHE21-2*lacI*^{q} as a backbone were introduced into the Δ*ptsN* mutant strain harboring P*ssaG-lacZ*, and the β-galactosidase assay was performed in triplicate as described above in the presence or absence of IPTG (0.1 mM). pWJ07, pWJ08, and pWJ09 were designed to express $EIIA^{Ntr}$-His_6, $EIIA^{Ntr}$-His_6 (H73A), and $EIIA^{Ntr}$-His_6 (K75D), respectively, in the Δ*ptsN* mutant upon induction with IPTG (0.1 mM). This experiment was performed in triplicate.

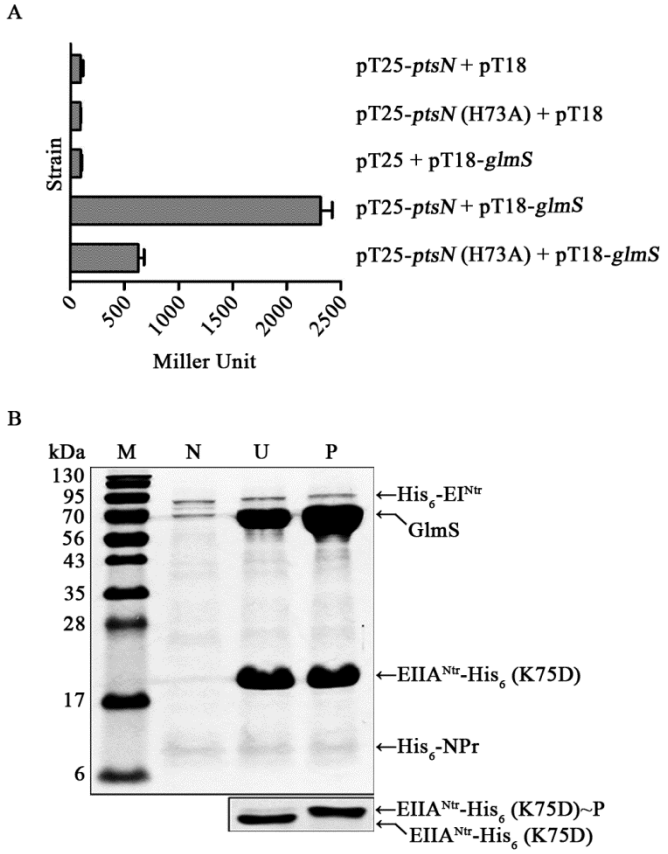

Figure II-5. Phosphorylation status of EIIA^{Ntr} influences the binding affinity between EIIA^{Ntr} and GlmS. (A) Increased binding affinities of EIIA^{Ntr}-His$_6$ (K75D) to GlmS after phosphorylation. Phosphorylated and unphosphorylated forms of EIIA^{Ntr}-His$_6$ (K75D) were incubated with equivalent amounts of GlmS, and the levels of GlmS bound to phosphorylated (P) or unphosphorylated (U) EIIA^{Ntr}-His$_6$ (K75D) were compared (top). PEP-dependent phosphorylation of EIIA^{Ntr}-His$_6$ (K75D) was verified in parallel (bottom inlet). Line (N) does not contain either

the $EIIA^{Ntr}$-His_6 (K75D) or the GlmS protein as a control. This experiment was performed in triplicate. **(B)** Differential interaction between $EIIA^{Ntr}$ and GlmS depending on $EIIA^{Ntr}$ phosphorylation status *in vivo*. Protein-protein interactions between $EIIA^{Ntr}$ and GlmS were verified using a bacterial two-hybrid system. Plasmid pKT25 containing *ptsN* or *ptsN* (H73A) and plasmid pUT18 harboring *glmS* were introduced into a reporter strain respectively or in combination. The reporter strains were cultivated in LB broth supplemented with IPTG, and β-galactosidase activity was determined to examine the strength of the protein-protein interactions.

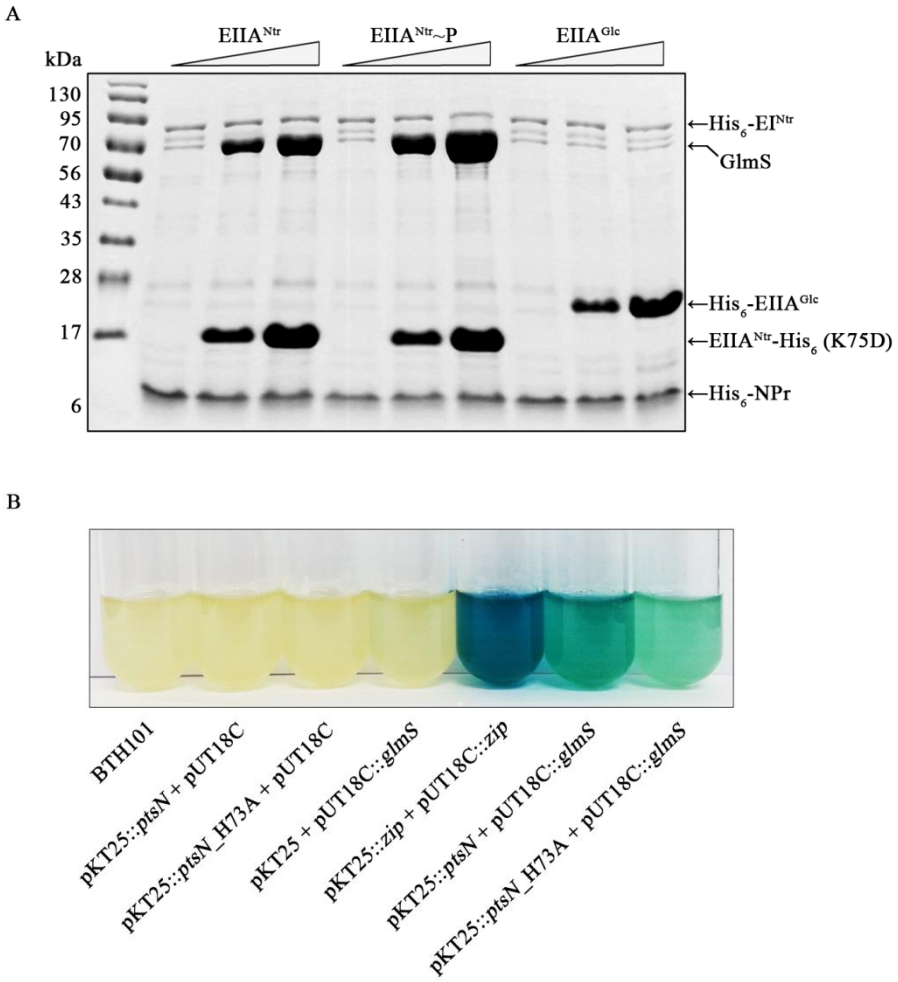

Figure II-6. EIIA^{Ntr} binds to GlmS directly in a phosphorylation-status-dependent manner. (A) Phosphorylation and concentration-dependent interactions between EIIA^{Ntr} and GlmS. GlmS (100 μg) was incubated with various amounts (0, 25, and 100 μg) of EIIA^{Ntr}-His$_6$ (K75D) or His$_6$-EIIA^{Glc} and subjected to a pull-down assay using Ni-NTA metal affinity resin. **(B)** Increase in the interactions between

EIIA^{Ntr} and GlmS by its phosphorylation *in vivo*. The pKT25 plasmid containing *ptsN* or *ptsN* (H73A) and the pUT18 plasmid harboring *glmS* were co-transformed into a reporter *E. coli* strain. All strains were grown in LB medium containing X-gal, and colorimetric X-gal degradation was compared.

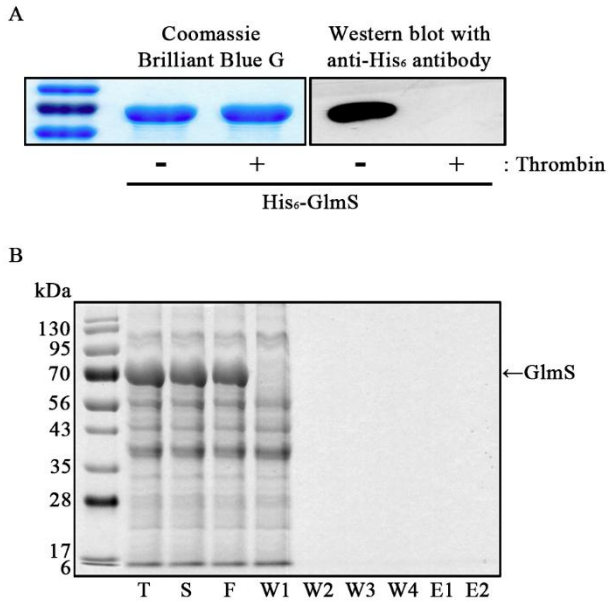

Figure II-7. GlmS does not bind to anti-His_6 antibody and Ni-NTA resin non-specifically. (A) Purified His_6-GlmS proteins were incubated at 37 °C for 6 h in the presence or absence of thrombin protease to detach His_6-tag from GlmS. Samples treated with thrombin or not were separated on 12% SDS-PAGE gel. The protein gel was stained with Coomassie Brilliant Blue G, or further analyzed by western blot using anti-His_6 antibody. **(B)** Bacteria containing pWJ10 (pUHE21-2*lacI*^{q}::*glmS*) over-produced GlmS protein upon IPTG addition and their lysates were incubated with Ni-NTA affinity resin to examine non-specific binding of GlmS to the resin. Aliquots from total cell extracts (T), supernatant after centrifugation of the cell extracts (S), column

flow-through (F), washes from four washing steps (W), and the two eluted fractions (E) were separated on 12% SDS-PAGE, and the gels were analyzed after Coomassie Brilliant Blue G staining. Molecular masses of the standards are presented in kDa on the left.

EIIA^{Ntr} inhibits GlmS activity. EIIA^{Ntr} unlike others that bind to TrkA (Lee *et al*, 2007), KdpD (Lüttmann *et al*, 2009), and E1 of pyruvate dehydrogenase (Pflüger-Grau *et al*, 2011), and SsrB (Choi *et al*, 2010) prefers the phosphorylation state to interact with GlmS. To decipher the link between PTS^{Ntr} and nitrogen or amino acid metabolism, the influence of EIIA^{Ntr} binding to GlmS on GlmS activity was elucidated. EIIA^{Ntr} has positive and negative effects on the roles of partner proteins (Lüttmann *et al*, 2009; Pflüger-Grau *et al*, 2011). GlmS converts D-fructose-6-phosphate (Fru6P) into GlcN6P by hydrolyzing Gln to glutamate (Glu). To determine the influence of the EIIA^{Ntr} interaction with GlmS on GlcN6P production, the optimal enzymatic reaction condition was set up using Gln, Fru6P, and GlmS at several concentrations to measure GlcN6P production by high performance liquid chromatography (HPLC) at different incubation times (Fig. II-8A and B). Based on the devised GlmS assay conditions, GlmS was incubated with the phospho- or dephospho-forms of EIIA^{Ntr}-His$_6$ (K75D), and GlcN6P production was compared. Adding EIIA^{Ntr}-His$_6$ (K75D) decreased GlcN6P production, and its phosphorylation caused a more drastic reduction in GlcN6P production (Fig. II-9A), indicating a

negative role of $EIIA^{Ntr}$ in GlmS activity. GlmS exerts negative feedback regulation in response to GlcN6P. Excessive GlcN6P production stimulates degradation of *glmS* mRNA (Göpel *et al*, 2013; Collins *et al*, 2007). To define the negative effect of $EIIA^{Ntr}$ on amino sugar production in detail, the levels of mRNAs relevant to amino sugar metabolism were evaluated in the presence or absence of $EIIA^{Ntr}$. Quantitative reveres transcription-polymerase chain reaction (qRT-PCR) revealed that the mRNA levels of *glmS*, *glmM*, and *glmU* required to convert Fru6P to uridinediphospho-*N*-acetylglucosamine (UDP-GlcNAc), a main amino sugar substrate for cell wall structure, were not affected by $EIIA^{Ntr}$ (Fig. II-9B), indicating that $EIIA^{Ntr}$ modulates GlmS activity by protein-protein interaction and not by transcriptional regulation.

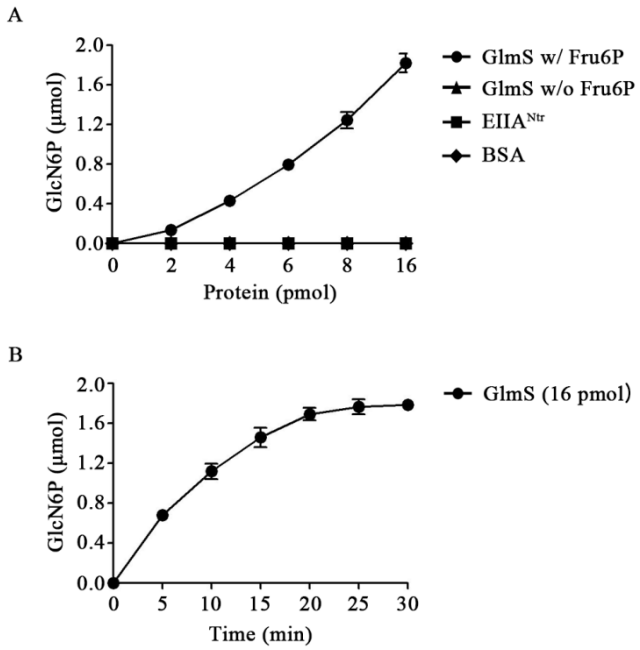

Figure II-8. Optimal conditions to assay GlmS activity was designed by measuring GlcN6P using HPLC. (A) GlmS reaction conditions using different GlmS concentrations. Gln (10 mM) was mixed with GlmS (0–16 pmol) in the presence or absence of Fru6P (6 mM) and incubated at 37°C for 30 min. GlcN6P production increased in proportion to the quantity of enzyme added. $EIIA^{Ntr}$-His_6 (K75D) and BSA were used as negative controls. This experiment was performed in triplicate. **(B)** GlmS reaction conditions using different reaction times. GlcN6P production was measured every 5 min after adding 16 pmol GlmS to the reaction mixture containing Gln and Fru6P to optimize

incubation time. Maximal GlcN6P production was observed at 30 min. This experiment was performed in triplicate.

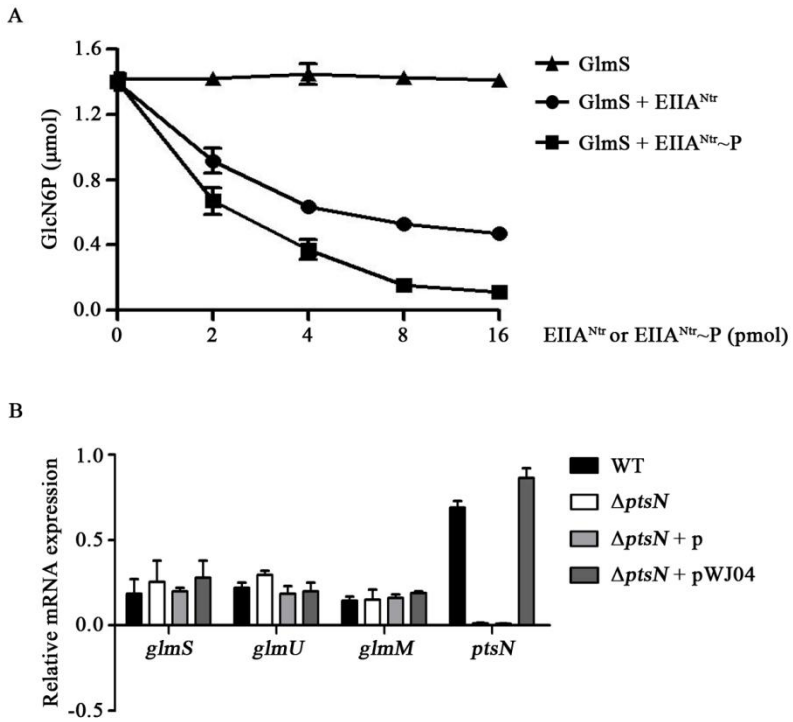

Figure II-9. EIIA^{Ntr} inhibits GlmS-mediated GlcN6P production. (A) Negative roles of EIIA^{Ntr} in GlcN6P production. GlmS was incubated with different amounts of phosphorylated or unphosphorylated EIIA^{Ntr}-His_6 (K75D) (0–16 pmol) and GlcN6P production was measured by HPLC. The results are plotted in triplicate. **(B)** No effect of EIIA^{Ntr} on the expression of genes involved in amino sugar metabolism. Wild-type and Δ*ptsN* mutant strains were transformed with pWJ04 containing *ptsN* and its presumable promoter, and qRT-PCR was conducted to compare mRNA levels of *glmS, glmU, glmM*, and *ptsN*. All mRNA levels were

normalized using *gyrB,* and the relative expression ratios were averaged from three independent measurements. This experiment was performed in triplicate.

EIIA^{Ntr} affects the GlmS-mediated bacterial growth rate. Inhibiting GlmS activity through the interaction with EIIA^{Ntr} was further confirmed *in vivo*. GlmS is a key enzyme in the production of amino sugars, which are essential precursors for bacterial cell wall peptidoglycans and LPS in the outer membrane of Gram-negative bacteria. Therefore, bacteria deprived of functional GlmS suffer from attenuated growth due to a lack of building blocks for constructing the cell wall when exogenous amino sugars are depleted (Sarvas, 1971; Plumbridge *et al*, 1993). To examine whether growth of *Salmonella* is attenuated by the interaction between EIIA^{Ntr} and GlmS, a balanced-lethal system was established in which the absence of chromosomal *glmS* was partially complemented by controlled expression of *glmS* on the pWJ10 plasmid containing the *lac* promoter (Fig. II-10). A Δ*glmS* mutant strain with a severe growth defect due to the lack of cell envelope components (Kim *et al*, 2013) was supplemented with approximately 50% growth of wild-type *Salmonella* using pWJ10 in the presence of 10 μM IPTG (Fig. II-11A). The additional deletion of the *ptsN* gene in this strain restored growth to a level similar in wild-type cells, suggesting that GlmS relieved the inhibition by EIIA^{Ntr}.

Accordingly, introducing plasmids producing intact $EIIA^{Ntr}$ or its derivative, $EIIA^{Ntr}$ (H73A), re-repressed the growth of the Δ*glmS* Δ*ptsN* strain containing pWJ10. As expected, $EIIA^{Ntr}$ (H73A), which is incapable of phosphorylation in response to stimuli (Lee *et al*, 2005), showed less of an inhibitory effect than the intact form probably due to diminished binding affinity to GlmS (Fig. II-11B). Examination of viable cell number under the same condition showed the consistent result with that of bacterial growth rate analysis described above (Fig. II-12).

These results verify that $EIIA^{Ntr}$-mediated GlmS inhibition might lead to a growth defect attributable to the impaired integrity of the cell wall and further imply a role for $EIIA^{Ntr}$ controlling the production rate of amino sugars depending on nitrogen accessibility.

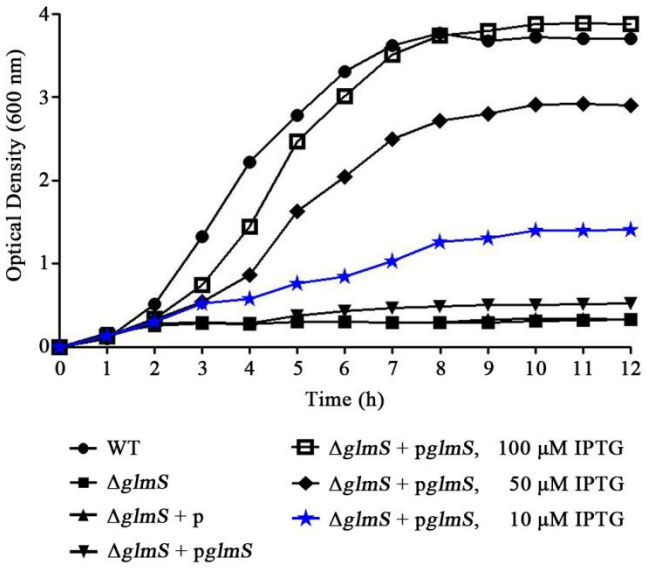

Figure II-10. Lethality due to the absence of GlmS was modulated by GlmS production in the *trans* configuration. *Salmonella* was cultured at 37°C in LB medium for 12 h to compare growth rate between strains. The growth defect of the Δ*glmS* mutant strain was resolved by transforming the mutant strain with p*glmS* (pWJ10: pUHE21-2*lacI*^{q} harboring *glmS* under a *lac* promoter) and culturing in different IPTG concentrations (10–100 μM. The 10 μM IPTG concentration showed partial growth complementation and was chosen for further study. This experiment was performed in triplicate.

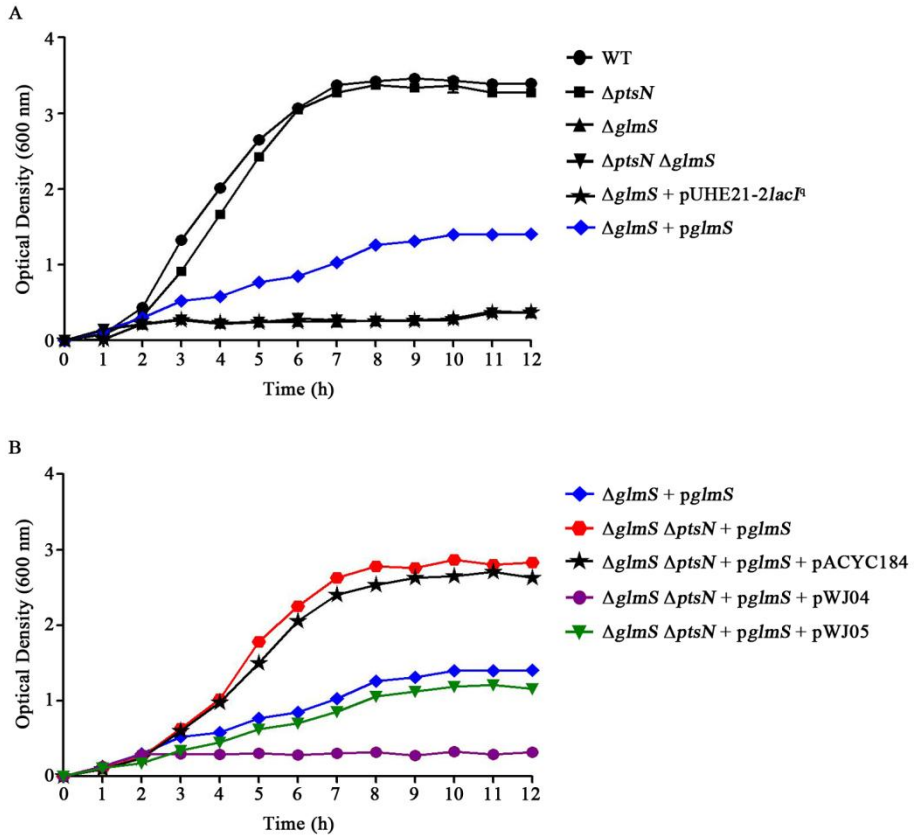

Figure II-11. *Salmonella* growth is influenced by the interaction between EIIA^{Ntr} and GlmS. (A) The absence of *glmS* is lethal to bacteria. Effects of GlmS and EIIA^{Ntr} on bacterial growth were assessed individually or in combination. Introducing p*glmS* (pWJ10, pUHE21-2*lacI*^{q}::*glmS*) to provid GlmS as *trans* partially restored the growth defect in mutants lacking GlmS. GlmS production level was titrated using 10 μM IPTG (Fig. II-10). **(B)** Modulation of growth rate by the interaction between EIIA^{Ntr} and GlmS. Using the Δ*glmS* mutant

complemented with p*glmS* as a parent strain, the effect of the $EIIA^{Ntr}$ interaction with GlmS on bacterial growth was evaluated by deleting the chromosomal *ptsN* gene and introducing pWJ04 and pWJ05, which provided $EIIA^{Ntr}$ and $EIIA^{Ntr}$ (H73A), respectively. All growth measurements in A and B were performed in triplicate, and the average observed values at 600 nm are plotted.

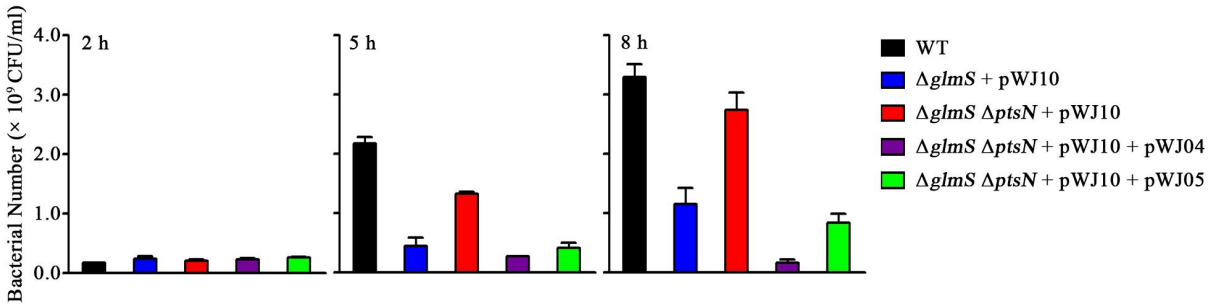

Figure II-12. Viability of *Salmonella* is influenced by the interaction between GlmS and EIIA^{Ntr}. To compare the bacterial viability among *Salmonella* strains wild-type, Δ*glmS*, and Δ*glmS* Δ*ptsN* strains containing pWJ10 (pUHE21-2*lacI*^{q}::*glmS*), pWJ04 (pACYC184::*ptsN*), or pWJ05 (pACYC184::*ptsN*_H73A), culture aliquots were collected at 2, 5, and 8 h time points and then serially diluted in PBS. Dilutions of the suspension were plated on LB agar medium to enumerate the CFU. This experiment was performed in triplicate.

EIIA^{Ntr} and GlmS interact to form a heterotrimeric complex.

A cascade of enzymes, including GlmS, GlmM, and GlmU are required for *bona fide* amino sugar synthesis. GlmS, which is responsible for the first and rate-limiting step in the hexosamine pathway, converts Fru6P into GlcN6P. GlcN6P is subsequently modified to glucosamine-1-phosphate (GlcN1P) by GlmM and further converted to UDP-GlcNAc by GlmU (Mengin-Lecreulx & Van Heijenoort, 1993; 1994; 1996). However, in the presence of abundant exogenous *N*-acetylglucosamine (GlcNAc) transported via NagE and ManXYZ, the GlmS-catalyzed reaction is bypassed, whereas GlmM and GlmU are consistently required for its conversion into UDP-GlcNAc (Durand *et al*, 2008). Hence, the activity of GlmS is selectively shut down in response to amino sugar availability.

As *glmS* and *glmU* constitute the *glmUS* operon and their transcripts are strictly coupled (Plumbridge, 1995), there should be a regulatory mechanism differentiating synthesis and activity of GlmS from those of GlmU after transcription. For example, translation of *glmS* mRNA is separately controlled by the GlmY/GlmZ/RapZ system, which responds to the cellular concentration of GlcN6P (Göpel *et al*, 2013), as

described in detail below. In addition, GlmS changes its structure from an active dimer to an inactive hexamer as cellular concentration increases, leading to accumulation of GlcN6P as the product (Mouilleron *et al*, 2012). To refine the interaction between $EIIA^{Ntr}$ and GlmS in greater detail, I determined the stoichiometric mass-action model in the $EIIA^{Ntr}$ and GlmS complex. I first assumed the architectural contribution of $EIIA^{Ntr}$ toward converting the GlmS structure into the inactive hexameric form: $EIIA^{Ntr}$ binding likely helps GlmS molecules conglomerate in an inactive form without repulsion or stabilizes the inactive polymeric structure and preventing return to the active dimer form. To examine this possibility, $EIIA^{Ntr}$ and GlmS in solution were subjected to size exclusion chromatography with multi-angle light scattering (SEC-MALS) in combination or individually (Fig. II-13A). GlmS peaked at about 128 kDa, which is equivalent to the mass of the dimeric form of GlmS, and $EIIA^{Ntr}$ was maintained as a monomer, showing a peak of around 20 kDa in solution. During SEC, the MALS detected a large molecule of approximately 148 kDa in the solution containing GlmS and $EIIA^{Ntr}$, suggesting two molecules of GlmS obstructed by a molecule of $EIIA^{Ntr}$. The peaks were further dissected by

SDS-PAGE to define the protein composition (Fig. II-13B).

These results suggest that $EIIA^{Ntr}$ inhibits GlmS by binding to its active dimeric form but is less likely to contribute to conversion of GlmS into the inactive hexameric form.

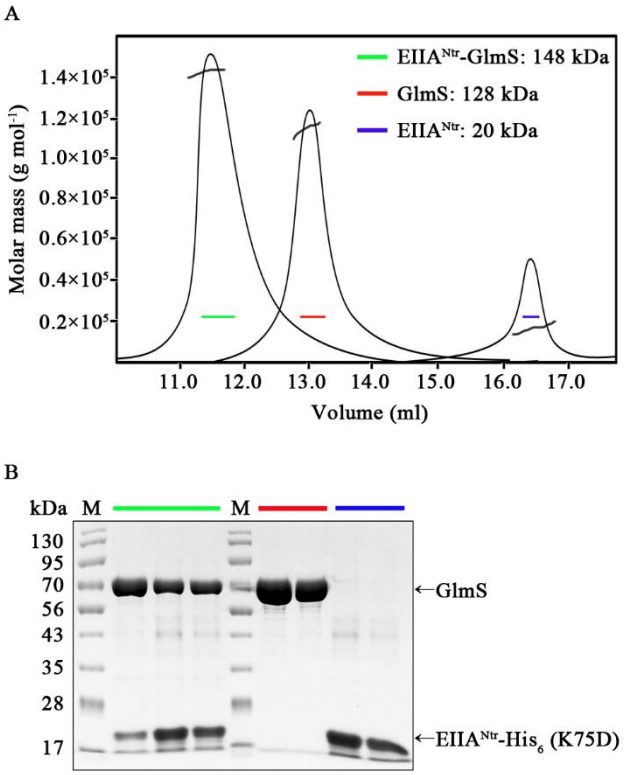

Figure II-13. Trimeric complex is formed between EIIA^{Ntr} and GlmS. (A) Stoichiometric analysis of the EIIA^{Ntr} and GlmS complex. A solution of the EIIA^{Ntr} and GlmS complex was analyzed by SEC-MALS. The molecular mass of GlmS alone in solution was 128 kDa, indicating the active dimer, and that of EIIA^{Ntr} was 20 kDa, indicating the monomeric form. A macromolecule with a peak of 148 kDa appeared in the solution composed of EIIA^{Ntr} and GlmS, and the size was accordant with a EIIA^{Ntr}-GlmS$_2$ heterotrimer composed of two GlmS molecules

(128 kDa) and one $EIIA^{Ntr}$ (20 kDa). **(B)** Identifying the eluted fractions by SDS-PAGE. The SEC-LALS eluted fractions from the 148, 128, and 20 kDa proteins, which were presumably the $EIIA^{Ntr}$-$GlmS_2$ complex, GlmS dimer, and the $EIIA^{Ntr}$ monomer, respectively, were analyzed by SDS-PAGE and Coomassie Blue staining. Green, red, and blue lines indicate the 148, 128, and 20 kDa fractions, respectively.

EIIA^{Ntr} stability is modulated by Lon in response to amino sugar availability. Maintaining GlcN6P homeostasis has been ascribed to the GlmY/GlmZ/RapZ system (Göpel *et al*, 2013). RapZ inhibits GlmS expression by accelerating the decay of the small RNA GlmZ, which facilitates *glmS* translation. However, bacteria sensing an amino sugar deficiency exploit GlmY to antagonize GlmZ degradation by RapZ. Co-localization of *ptsN* and *rapZ* in the *rpoN* operon reinforces the concordant role of these two genes in GlmS-mediated regulation of cell envelope integrity. I suspected that amino sugar was the signal triggering coordinated negative regulation of EIIA^{Ntr} and RapZ on GlmS. However, *ptsN* and *rapZ* mRNA levels were not affected by amino sugar availability, whereas *glmS* transcription was negatively feedback regulated by ample amino sugars, as reported previously (Kalamorz *et al*, 2007; Göpel *et al*, 2013) (Fig. II-14 and 15). Instead, intriguingly, the level of the EIIA^{Ntr} protein decreased when GlcN6P production stopped due to the lack of GlmS and when no exogenous GlcNAc, a metabolite substitute for GlcN6P (Kalamorz *et al*, 2007; Kawada-Matsuo *et al*, 2012; Göpel *et al*, 2013) was supplied (Fig. II-16A). In contrast, adding GlcNAc increased the levels of EIIA^{Ntr} regardless of the presence of

GlmS and vice versa (Fig. II-16A). These results indicate that intracellular amino sugar availability controls $EIIA^{Ntr}$ at the protein level.

To further explore modulation of intracellular $EIIA^{Ntr}$ concentration depending on amino sugar availability, the rate of $EIIA^{Ntr}$ proteolysis was compared between amino sugar-abundant and -depleted conditions. To prevent *de novo* protein synthesis, chloramphenicol was added to the culture 3 h post-inoculation when amino sugar availability influenced bacterial growth rate (Fig. II-17) (Weisberger, 1967; Göpel *et al*, 2013). The Δ*glmS* mutant strain depleted of amino sugars rapidly degraded $EIIA^{Ntr}$-FLAG but retained $EIIA^{Ntr}$-FLAG at high levels for at least 2 h when provided with excessive GlcNAc, indicating regulation of the $EIIA^{Ntr}$ proteolysis rate by amino sugar availability (Fig. II-16B). Lon and Clp proteases in *E. coli* and other bacteria are responsible for 70–80% of energy-dependent protein degradation (Maurizi, 1992). I observed that deleting *lon* quenched the programmed proteolysis of $EIIA^{Ntr}$-FLAG upon amino sugar depletion in the Δ*glmS* mutant strain (Fig. II-16C). In this experiment, DnaK levels were measured in parallel to verify equivalent total protein amounts between lanes, and a similar test using RpoB, which was used as an additional control instead of

DnaK, was also conducted (Fig. II-18).

These results indicate that Lon accelerates $EIIA^{Ntr}$ degradation when *Salmonella* lacks amino sugar metabolites.

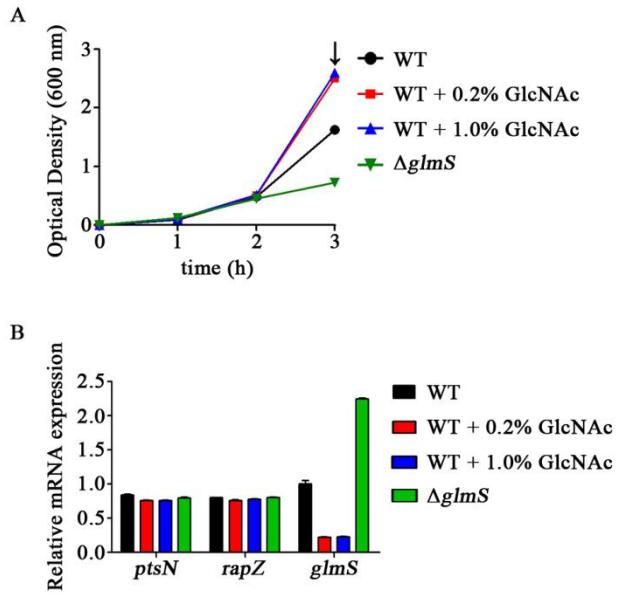

Figure II-14. *ptsN* and *rapZ* mRNA expression was not influenced by the abundance of amino sugars. (A) Estimate of growth time when amino sugar availability may influence bacterial growth. Wild-type and Δ*glmS* mutant strains were cultured in LB medium supplemented with GlcNAc (0.2 or 1.0%) or not. *Salmonella* cells began to show different growth rates after 3 h, depending on the presence of GlmS or availability of GlcNAc, suggesting that intracellular amino sugars were depleted at around 3 h and that growth was attenuated unless GlmS synthesized GlcN6P or exogenous GlcNAc was provided. This experiment was performed in triplicate. **(B)** Effect of amino sugar abundance on *ptsN*,

rapZ, and *glmS* mRNA levels. Total RNAs were isolated from wild-type and Δ*glmS* mutant strains in the presence or absence of GlcNAc at 3 h under the conditions described above and subjected to qRT-PCR. *ptsN* and *rapZ* were expressed equivalently between the conditions, whereas *glmS* expression was significantly influenced by the availability of amino sugar. Gene expression was normalized based on *gyrB* expression. qRT-PCR was performed in triplicate.

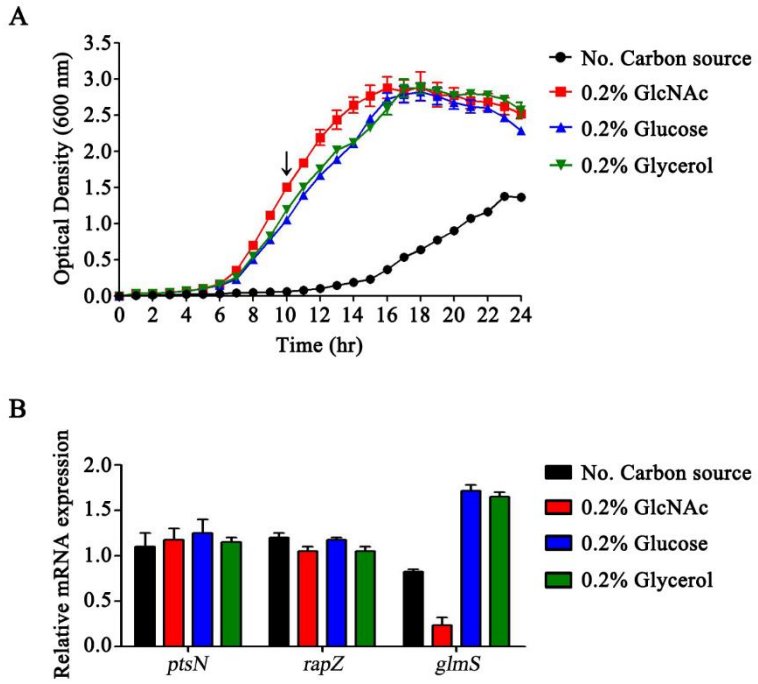

Figure II-15. *ptsN* and *rapZ* mRNA expression was independent of carbon source. (A) *Salmonella* Typhimurium growth curves with different carbon sources. Wild-type *Salmonella* was cultured in minimal medium (W-salts) containing either GlcNAc, glucose, or glycerol, respectively. Bacterial growth was depicted, and total RNAs were isolated 10 h post-inoculation. This experiment was performed in triplicate. **(B)** Comparison of *ptsN*, *rapZ*, and *glmS* expression levels in response to the different carbon sources. mRNA levels were compared between the different carbon sources using qRT-PCR. *gyrB* expression

was used to normalize gene expression between tested conditions. Relative mRNA expression normalized using *gyrB* mRNA was averaged. This experiment was performed in triplicate.

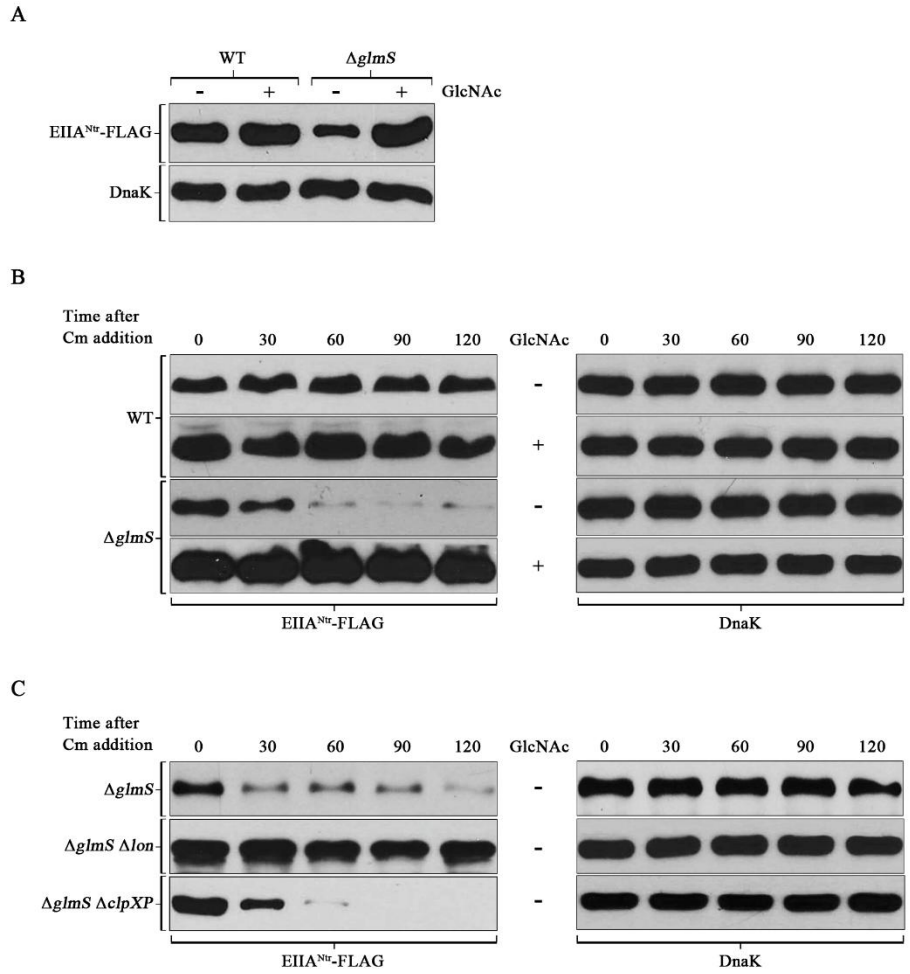

Figure II-16. EIIA^{Ntr} degradation is controlled by Lon protease in response to amino sugar availability. (A) Comparison of EIIA^{Ntr}-FLAG protein levels between wild-type and Δ*glmS* mutant strains. The wild-type and Δ*glmS* mutant strain protein samples were isolated in the presence or absence of GlcNAc 3 h post inoculation as described above and equivalent amounts of total proteins were subjected to Western blot

analysis to compare the $EIIA^{Ntr}$-FLAG levels between conditions. DnaK levels were measured in parallel to verify equivalent total protein between lanes. **(B)** Effect of amino sugar availability on stability of $EIIA^{Ntr}$-FLAG. Chloramphenicol was added to the cultures of the wild-type and Δ*glmS* mutant strains at 3 h as described above, and total protein harvested every 30 min was used to assess the $EIIA^{Ntr}$ and DnaK decay rates. Equivalent amounts of total protein were loaded in each lane for SDS-PAGE. **(C)** Comparison of the stability of $EIIA^{Ntr}$-FLAG in the absence of Lon or ClpXP protease in the Δ*glmS* mutant strain. The Δ*glmS*, Δ*glmS* Δ*lon*, and Δ*glmS* Δ*clpXP Salmonella* strains were cultured under conditions identical to those used above, and the stability of $EIIA^{Ntr}$-FLAG and DnaK was assessed in each strain using Western blotting every 30 min after adding chloramphenicol.

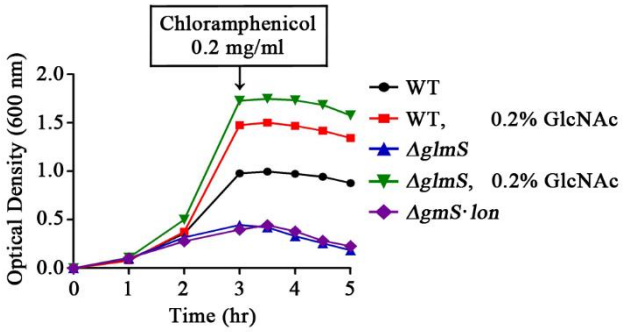

Figure II-17. *Salmonella* growth rate is affected by amino sugar availability. *Salmonella* strains growth curves used in Fig. II-16. Wild-type, Δ*glmS*, and Δ*glmS* Δ*lon* strains were cultured in the presence or absence of GlcNAc (0.2%), and chloramphenicol (0.2 mg/ml) was added to the culture 3 h after inoculation to quench further protein synthesis. The availability of amino sugar began to affect bacterial growth rate at around 3 h, which was chosen to determine the $EIIA^{Ntr}$-FLAG levels under each condition. This experiment was performed in triplicate.

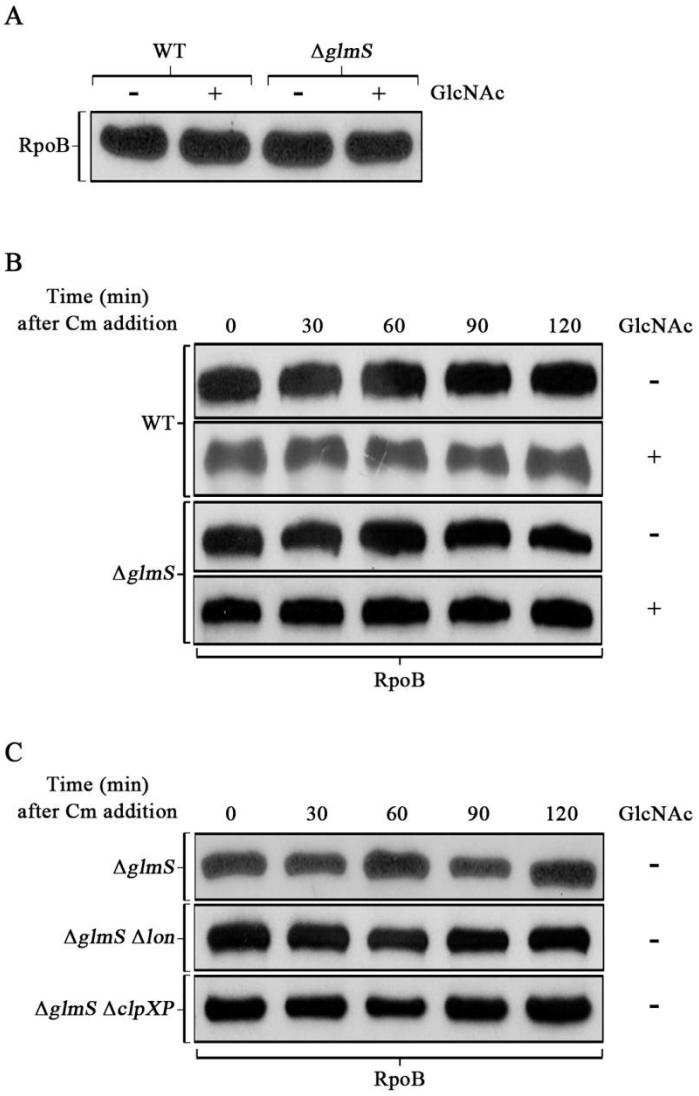

Figure II-18. The stability of RpoB was not changed by Lon protease. The identical protein samples used in Fig. II-16 were applied in western blot analysis using anti-RpoB antibody. The RpoB levels were comparable between lanes regardless of the presence of Lon and ClpXP.

II-4. Discussion

Nitrogen is crucially essential to every living organism, including bacteria; it is assimilated into amino acids and further into proteins, which constitute cellular components that conduct diverse biological activities. Nitrogen is also used in amino sugar compounds, the structural residues of bacterial cell walls. The nitrogen moiety of Gln is integrated into Fru6P by GlmS, producing GlcN6P. GlcN6P is further converted to UDP-GlcNAc by a cascade of cytoplasmic enzymes, such as GlmM and GlmU. UDP-GlcNAc is an essential structural building block for peptidoglycans and LPS in bacterial cell walls. Therefore, the balance between synthesis and decomposition of amino sugars is directly influenced by the availability of carbon and nitrogen.

Cells under excessive nitrogen convert α-KG to Glu and further to Gln (Doucette *et al*, 2011). Gln is utilized as a nitrogen source under nitrogen-limiting conditions (Magasanik, 1993). Hence, the Gln: α-KG ratio is generally used to predict the cellular balance between nitrogen and carbon abundance: high Gln/α-KG values under nitrogen-rich conditions vs. low Gln/α-KG values under nitrogen-depleted conditions.

Bacteria must promptly recognize detrimental changes, such as nutrient deprivation, and adjust metabolic processes for their adaptation. For example, it has been recently revealed that *Caulobacter crescentus* triggers the phosphorylation of EI^{Ntr}, the first enzyme of PTS^{Ntr} in response to low glutamine concentrations and subsequently phosphorylates $EIIA^{Ntr}$, which in turn inhibits the hydrolase activity of SpoT by directly binding to SpoT. Modulation of SpoT activity by PTS^{Ntr} influences the cellular accumulation of (p)ppGpp, an alarmone controlling bacterial cell cycle progression and growth (Ronneau *et al*, 2016).

A similar role of PTS^{Ntr} sensing the nitrogen availability and modulating cellular metabolism was disclosed in this study. GlmS is the rate-limiting enzyme that consumes a molecule of Gln to synthesize an equivalent amount of the amino sugar GlcN6P. Thus, GlmS activity is tightly controlled in response to the availability of cellular nitrogen and amino sugars. Based on my results, I propose a regulatory circuit wherein $EIIA^{Ntr}$ fine tunes GlmS activity by assessing the abundance of nitrogen and amino sugars (Fig. II-19). In the presence of sufficient nitrogen, dephosphorylated $EIIA^{Ntr}$ does not significantly compromise

GlmS activity, which, in turn, provides abundant amino sugars for constructing cell walls. When cells suffer from depleted nitrogen, phosphorylated $EIIA^{Ntr}$ tightly binds to GlmS and inhibits the enzyme from consuming Gln to produce GlcN6P, which slows down LPS and peptidoglycan synthesis. Not only nitrogen availability but also amino sugar abundance modulates the influence of $EIIA^{Ntr}$ on GlmS activity. Bacteria supplemented with abundant amino sugars, such as GlcNAc, delay the decay of $EIIA^{Ntr}$ and subsequently decelerate *bona fide* amino sugar synthesis via GlmS. However, when the supply of exogenous amino sugars is suspended and the GlcN6P remnants are exhausted, Lon accelerates $EIIA^{Ntr}$ proteolysis and relieves GlmS to supplement the lack of cellular amino sugars.

GlmS is a pivotal enzyme for maintaining cell wall integrity and employs multiple latch devices for regulation. GlmS maintains its own structural equilibrium between the active dimeric conformation and the inactive hexameric state by shifting toward the inactive hexameric form when its concentration increases and the GlcN6P product accumulates (Mouilleron *et al*, 2012). In addition to the conformational dynamics of GlmS, its translation is also controlled by the coordinated

action between two regulatory GlmY and GlmZ small RNAs and the RapZ RNase adaptor protein. Following dissociation of the *glmS* monocistronic transcript from the *glmUS* cotranscript by RNaseE-mediated processing, GlmZ base-pairs with *glmS* mRNA and the aid of Hfq activate translation of *glmS* mRNA (Görke & Vogel, 2008). GlmZ turnover is determined by binding with RapZ, which recruits RNase E to the complex to facilitate GlmZ degradation. However, under low cellular GlcN6P concentrations, GlmY, with a secondary structure similar to GlmZ, increases and sequesters RapZ from GlmZ as a decoy, liberating GlmZ from activating GlmS synthesis and subsequent GlcN6P production (Göpel *et al*, 2013). The results in my study established that GlmS is not only controlled at the post-transcriptional level by GlmY/GlmZ/RapZ but is also coordinated at the post-translational level by $EIIA^{Ntr}$ and Lon. PTS^{Ntr} senses accessibility of nitrogen and controls the phosphorylation status of $EIIA^{Ntr}$. Phosphorylated or unphosphorylated $EIIA^{Ntr}$ hampers catalytic GlmS activity by binding to the active duplex form with different affinities. However, GlmS is released from inhibition by Lon-mediated degradation of $EIIA^{Ntr}$ upon depletion of cellular amino sugars.

Because of the incomplete architecture of PTS^{Ntr} lacking the phosphate recipient coupled with $EIIA^{Ntr}$, $EIIA^{Ntr}$ has been speculated to serve as a substantive regulator, and its pleiotropic regulation has been observed in diverse cellular processes, including nitrogen metabolism, potassium homeostasis, and interactions with host cells (Lee *et al*, 2005; Lüttmann *et al*, 2009; Choi *et al*, 2010). However, the pleiotropic regulatory effects of PTS^{Ntr} may not be completely attributable to the direct interactions between PTS^{Ntr} components and cellular targets; rather, many of the regulatory outputs might be secondarily caused by a few unmediated processes operated by $EIIA^{Ntr}$. Potassium homeostasis is controlled by direct binding of $EIIA^{Ntr}$ to TrkA and KdpD, which would explain such a mechanistic link (Lee *et al*, 2007; Lüttmann *et al*, 2009). The cellular K^+ concentration managed by $EIIA^{Ntr}$ could be a manifold signal leading to activation or inhibition of enzymes, transcriptional regulation, and pH homeostasis (Pflüger-Grau & Görke, 2010).

Similarly, additional direct targets of $EIIA^{Ntr}$ may yet to be identified, and GlmS is one of them. Direct regulation of GlmS by $EIIA^{Ntr}$ discloses a sophisticated regulatory circuit balancing metabolite

fluxes among carbon, nitrogen, and amino sugars. The possibility of a metabolic link between carbon and nitrogen has been undoubtedly raised. The sugar PTS and nitrogen PTS cross-talk by phosphorylating counterpart components (Powell *et al*, 1995; Rabus *et al*, 1999). α-KG has been identified as a key molecule balancing carbon and nitrogen assimilation and controlling $EIIA^{Ntr}$ regulatory activity. A challenge for bacteria living in fluctuating nutritional conditions is to notice the accessibility of essential nutrients, such as carbon and nitrogen, and determine the flux rates from nutrients to energy production and building biomass. Doucette *et al.* (2011) observed that a sudden increase in nitrogen availability leads to immediate glucose uptake and discovered that α-KG, which accumulates under nitrogen-depleted conditions, inhibits autophosphorylation of enzyme I (EI) of the sugar PTS and blocks entry of glucose, which synchronizes carbon uptake with nitrogen availability. α-KG which is accumulated in nitrogen-limiting conditions and, in turn, binds to the NifA GAF domain, which is a transcriptional activator for the nitrogen fixation (*nif*) gene, and triggers nitrogen uptake into cells (Little & Dixon, 2003). Cells fortified with nitrogen convert α-KG to Glu and further to Gln and subsequently

resume glucose uptake by releasing the sugar PTS EI from α-KG inhibition. Intriguingly, the GAF domain responding to α-KG is also possessed by EI^{Ntr} of PTS^{Ntr} and a nitrogen deficiency is directly delivered to $EIIA^{Ntr}$ (Lee *et al*, 2013), which dampens GlmS activity, thereby shutting down inflow of nitrogen into amino sugars. Thus, one could speculate that α-KG serves as an interface signal integrating cellular physiological status and coordinating carbon and nitrogen assimilation; physiological status is further transformed to $EIIA^{Ntr}$ across the PTS^{Ntr} phosphorelay system, which accommodates amino sugar biosynthesis on demand.

It was observed that the unphosphorylated form of $EIIA^{Ntr}$ is exclusively dominant during rapid growth of *Pseudomonas putida*, a member of *Gammaproteobacteria*, and suggested that $EIIA^{Ntr}$ phosphorylation status might be influenced by cellular physiological status representing the availability of carbon and nitrogen (Pflüger & Lorenzo, 2007). However, it is unknown how phosphorylation of $EIIA^{Ntr}$ alters bacterial fitness during environmental adaptation. My results suggest that $EIIA^{Ntr}$, which is phosphorylated under nitrogen-limiting conditions, compromises *bona fide* amino sugar biosynthesis by

inhibiting GlmS and decelerating production of peptidoglycans and LPS. *Gammaproteobacteria* with the *rpoN* operon comprising the PTS^{Ntr} genes and *rapZ* have presumably evolved the *rpoN* operon to control amino sugar homeostasis in accordance with nitrogen availability.

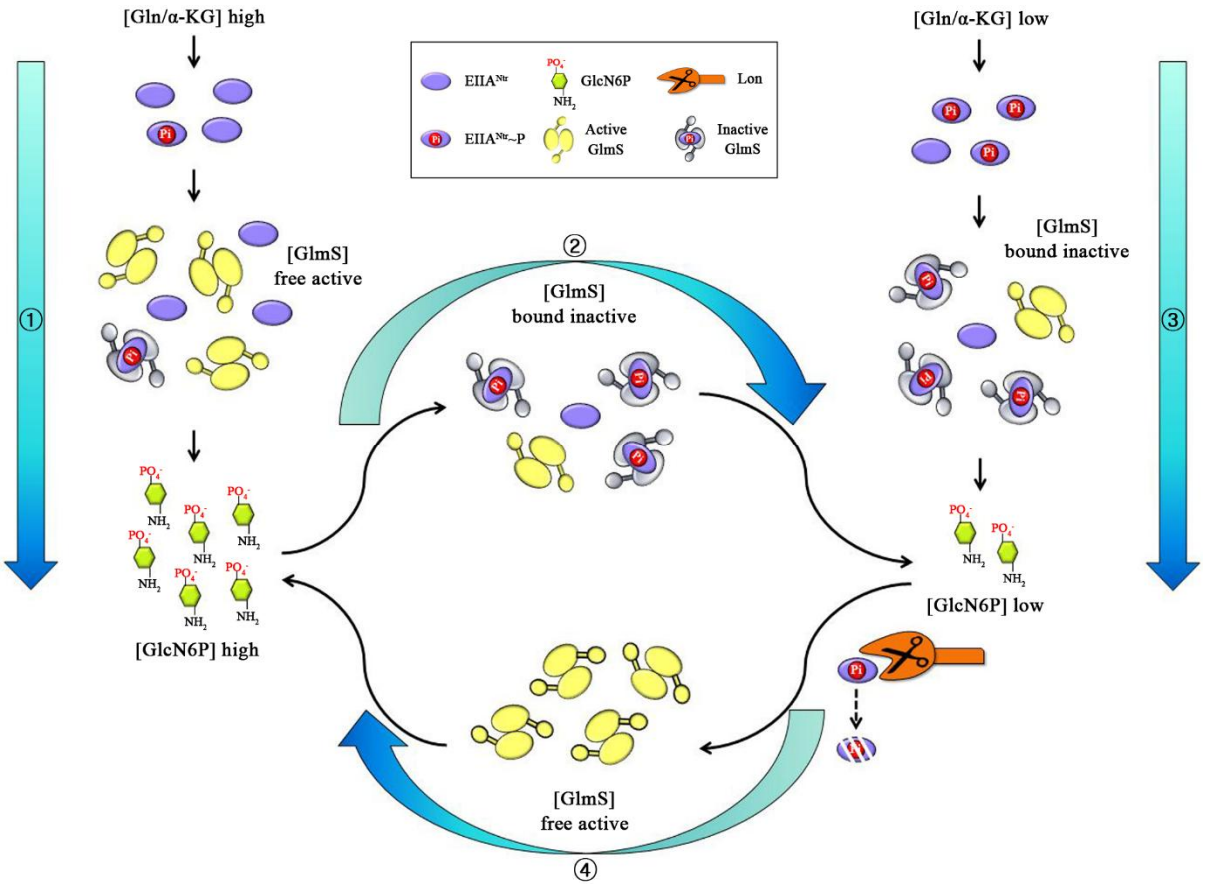
[Gln/α-KG] high
[Gln/α-KG] low
EIIA^Ntr
GlcN6P
Lon
EIIA^Ntr~P
Active GlmS
Inactive GlmS
[GlmS] free active
[GlmS] bound inactive
[GlmS] bound inactive
[GlmS] free active
[GlcN6P] high
[GlcN6P] low
①
②
③
④

Figure II-19. Proposed regulatory model for the control of GlmS activity by $EIIA^{Ntr}$ in response to nitrogen and amino sugar availability. At high cellular glutamine (Gln) concentrations, $EIIA^{Ntr}$ tends to be unphosphorylated and liberates the active form of GlmS that supplies GlcN6P and accelerates synthesis of the bacterial cell envelope (①). When GlcN6P is present in excess (②) or when Gln availability is restricted (③), phosphorylated $EIIA^{Ntr}$ binds GlmS with increased affinity and inhibits its activity. The depletion of pre-existing GlcN6P leads to $EIIA^{Ntr}$ degradation by Lon protease, freeing the active form of GlmS to supplement the lack of GlcN6P and maintain amino sugar homeostasis (④).

Chapter III.

Transcriptomic analysis of *Salmonella enterica* serovar Typhimurium lacking *ptsN*

III-1. Introduction

Most *Proteobacteria* possess the regulatory nitrogen-metabolic phosphotransferase system (PTS^{Ntr}), which operates in parallel to the phosphoenolpyruvate (PEP)-dependent carbohydrate PTS (Powell *et al*, 1995; Peterkofsky *et al*, 2006; Pflüger-Grau & Görke, 2010). PTS^{Ntr} is composed of the proteins EI^{Ntr} (encoded by *ptsP*) and NPr (encoded by *ptsO*) and the final phosphate acceptor $EIIA^{Ntr}$ (encoded by *ptsN*). In this system, three proteins form a phosphorylation chain working in the sequential order EI^{Ntr}→NPr→$EIIA^{Ntr}$ (Rabus *et al*, 1999; Zimmer *et al*, 2008) (Fig. III-1). $EIIA^{Ntr}$ has been known to play various regulatory roles relevant to potassium (K^+) transport (Lee *et al*, 2007; Lüttmann *et al*, 2009), phosphate (Lüttmann *et al*, 2012) homeostasis, σ factor selectivity (Lee *et al*, 2010), fluxes through carbohydrate pathways and central metabolism (Chavarría *et al*, 2012; Jahn *et al*, 2013), stringent response (Karstens *et al*, 2014; Ronneau *et al*, 2016), and virulence (Higa & Edelstein, 2001; Choi *et al*, 2010). For instance, $EIIA^{Ntr}$ maintains the intracellular K^+ homeostasis through binding to the low-affinity K^+ transporter TrkA and the sensor histidine kinase KdpD of

high-affinity K^+ transporting system in *Escherichia coli* (Lee *et al*, 2007; Lüttmann *et al*, 2009), which results in K^+-mediated global gene regulation in association with both σ^D- and σ^S-dependent promoters (Lee *et al*, 2010). Dephosphorylated-$EIIA^{Ntr}$ is also required for full adaptation to phosphate limitation condition by direct interaction with sensor kinase PhoR of two-component system involved in inorganic phosphate homeostasis (Lüttmann *et al*, 2012), and controlling the connection between C metabolism and many other cellular functions by binding to pyruvate dehydrogenase (PDH) which generates acetyl-CoA from pyruvate (Pflüger-Grau *et al*, 2011). It has been recently revealed that $EIIA^{Ntr}$ inhibits the hydrolase activity of SpoT by direct interaction in *Caulobacter crescentus* (Ronneau *et al*, 2016), which influences the cellular accumulation of (p)ppGpp, an alarmone controlling bacterial cell cycle progression, growth and virulence, for its adaptation to the environmental changes. In addition, $EIIA^{Ntr}$ has been also known to be associated with virulence in *Legionella pneumophila* (Higa & Edelstein, 2001) and *Salmonella enterica* (Choi *et al*, 2010).

To better understand roles of $EIIA^{Ntr}$, I compared whole transcriptome between the wild-type and a mutant strain lacking *ptsN* by

RNA-seq. Genes involved in vitamin B_{12} synthesis and 1,2-propanediol (1,2-PDL) utilization were significantly down-regulated in the Δ*ptsN* mutant strain, while SPI-1 and SPI-4 were up-regulated. It has been reported that *Salmonella* can acquire carbon sources from 1,2-propanediol (1,2-PDL), an abundant fermentation product derived from plant sugars, L-rhamnose and L-fucose. 1,2-PDL is degraded into propionaldehyde by Ado-B_{12}-dependent 1,2-propanediol dehydratase and further processed to 1-propanol and propionate through the intermediate propionyl-Coenzyme A (propionyl-CoA) with the coordinated action of *pdu* operon products (Havemann *et al*, 2002; Sampson & Bobik, 2008) (Fig. III-2). Propionyl-CoA further degrades into pyruvate and succinate via the 2-methylcitric acid cycle (MCC) (Hammelman *et al*, 1996; orswill & Escalante-Semerena, 1997) (Fig. III-2). Besides being a metabolic intermediate for energy production, propionyl-CoA also exerts a role as a regulatory signal compromising the stability of HilD, the transcriptional regulator of *Salmonella* pathogenicity island-1 (SPI-1), and finally affects *Salmonella* invasion into intestinal epithelial cells (Hung *et al*, 2013).

Therefore I suggest that $EIIA^{Ntr}$ is able to control *Salmonella*

invasion via balancing propionyl-CoA in response to environmental carbon metabolites.

III-2. Materials and Methods

Bacterial strains, media, and culture conditions. All bacterial strains were derived from *Salmonella* Typhimurium SL1344 as the parent and are listed in Table III-1. Luria-Bertani (LB) medium containing 1% Bacto-tryptone, 0.5% yeast extract and 1% NaCl, pH 7.5 was used as the complex culture medium for the routine growth of bacteria. All *Salmonella* Typhimurium strains were grown aerobically at 37°C with antibiotics supplementation at the following concentrations: ampicillin, 50 μg/ml; kanamycin, 50 μg/ml.

Construction of strains and plasmids. The *ptsN* deletion mutant strain was constructed using the lambda red recombination method for in-frame gene deletion (Datsenko & Wanner, 2000). For the construction of Δ*ptsN* mutant strain, SR7001, the Km^R cassette from pKD13 was amplified using primers ptsN-del-F and ptsN-del-R. The resulting PCR products were integrated into the *ptsN* region in the SL1344 wild-type strain containing the plasmid pKD46, followed by selection for Δ*ptsN*::kan transformants. The Km^R cassette was removed

using the plasmid pCP20 (Datsenko & Wanner, 2000). The sequences of primers used in constructing *Salmonella* strains and plasmids are listed in Table III-2.

RNA isolation and sequencing. *Salmonella* strains were grown in LB medium to the log phase with the OD_{600} of 1.2-1.4 under aerobic condition at 37°C (Fig. III-3). RNAprotect bacterial reagent (Qiagen, Hilden, Germany) was treated to appropriate volume of each collected sample before total RNA extraction. Total RNA was isolated by using RNeasy mini kit (Qiagen) according to the manufacturer's instructions and residual DNA was removed with Ambion Turbo DNA-*free*™ (ThermoFisher Scientific, Braunschweig, Germany). The quantity and quality of total RNA were examined by using Agilent 2100 Bioanalyzers (Agilent Technologies, CA, USA) and the RNA integrity value (RIN) was determined. Only RNAs with a RNA integrity number (RIN)>9 were used in further experiments. Extracted total RNA was stored at -80°C until use. All RNA-seq and alignment process were performed by Chunlab, Inc. (Seoul, Korea). Five micrograms of total RNA from each sample was used as starting material. If needed, the

concentrating process of RNA was processed to get high amount of RNA. The RNA was subjected to a substractive hybridization/bead capture procedure based rRNA-removal technology by using Ribo-Zero kit (Epicentre Biotechnologies, WI, USA). The mRNA was fragmented ultrasonically and the fragmented mRNA was converted into a RNA-seq library using the mRNA-seq library construction kit v.2 (Illumina, CA, USA) according to the manufacturer's instructions. RNA 2×100 bp paired-end sequencing was performed using the Illumina GAII (Illumina), according to the manufacturer's protocol (Fig. III-4). The mapped results were visualized by the CLRNAseq program (Chunlab).

Heat-map generation. Heat map was drawn to analyze the global response pattern. To quantify gene expression from RNA-seq data, reads per kilobase per million mapped reads (RPKM) was analyzed. It was visualized that the $\log_2$RPKM values of relative gene expression of *Salmonella enterica* serovar Typhimurium SL1344 wild-type and the Δ*ptsN* mutant strain. Heat map and hierarchical clusters were then generated by using Gitools v2.2.2..

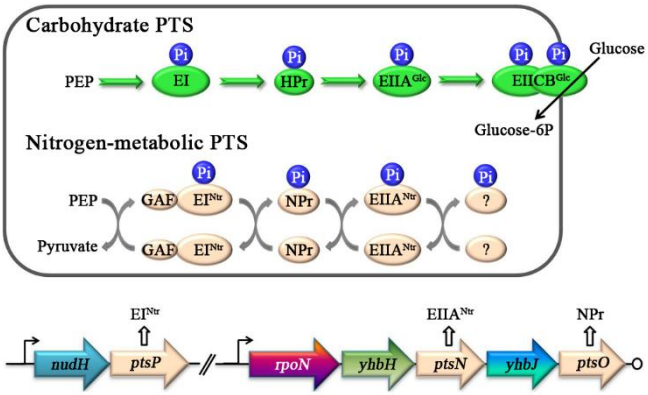

Figure III-1. Organization of the nitrogen-PTS in *Salmonella* Typhimurium. The nitrogen-PTS catalyzes a cascade of phosphoryl-transfer reactions. First, EI^{Ntr} autophosphorylates with phosphoenolpyruvate and subsquently transfers the phosphoryl group to NPr, which finally phosphorylates $EIIA^{Ntr}$. So far, final acceptor for the phosphoryl groups of $EIIA^{Ntr}$ remains unknown. NPr and $EIIA^{Ntr}$ are encoded in the *rpoN* operon. EI^{Ntr} is encoded elsewhere on the chromosome in the *nudH-ptsP* operon.

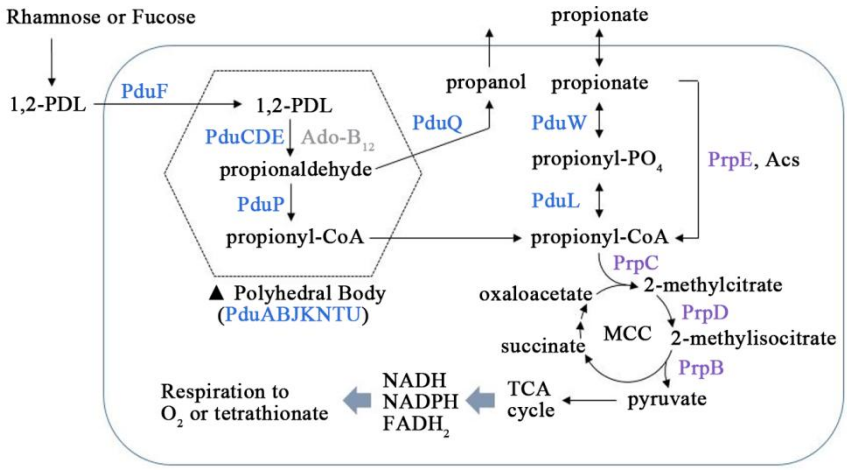

Figure III-2. Catabolism of 1,2-PDL and propionate in *Salmonella* Typhimurium. 1,2-PDL catabolism is achieved by 1,2-PDL utilization operon indicated blue. 1,2-PDL is converted into propionyl-CoA within polyhedral microcompartment. Propionate catabolism is accomplished by propionate operon indicated purple. The common intermediate propionyl-CoA provides pyruvate by 2-methycitrate cycle (MCC) which can be used as energy source. Oxygen or tetrathionate is used as an electron acceptor under aerobic or anaerobic condition, respectively.

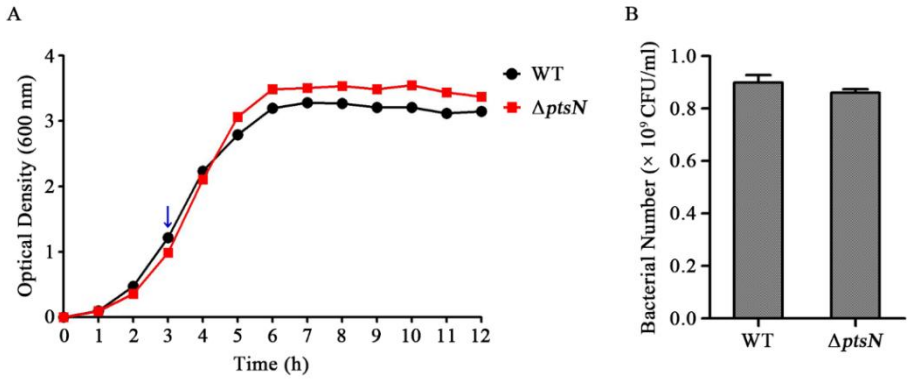

Figure III-3. No significant differences in bacterial growth rate and viability between *Salmonella* Typhimurium SL1344 wild-type and the Δ*ptsN* mutant strain. (A) Overnight cultures of *Salmonella* Typhimurium SL1344 wild-type and Δ*ptsN* mutant strain were harvested at 13,000 × g for 2 min, and the cells were resuspended in fresh LB medium and incubated at 37°C with shaking. The OD_{600} value was measured every 1 h to draw and compare the growth curve. This experiment was performed in triplicate. **(B)** To compare the bacterial cell viability between wild-type and the Δ*ptsN* mutant strain, cultures were collected at 3 h time point (blue arrow, Figure S3A), and then serially diluted in PBS approximately. Dilutions of the suspension were plated on LB agar medium to enumerate the CFU. This experiment was performed in triplicate.

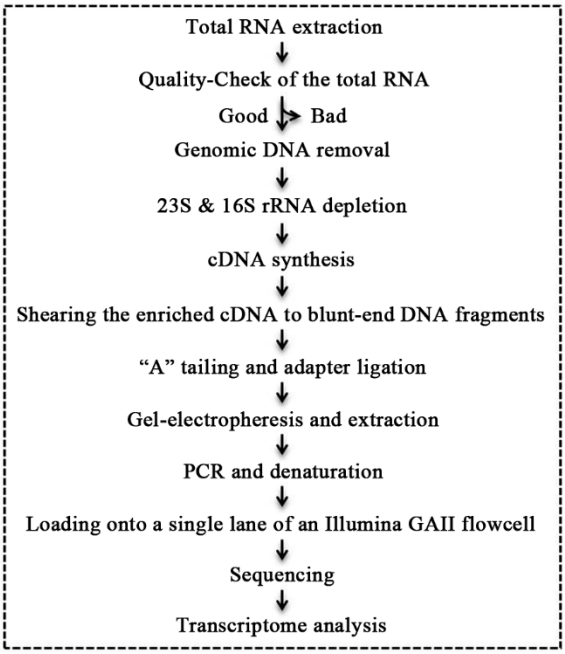

Figure III-4. The whole process of RNA sequencing. After the quality-check of total RNA, rRNA is depleted, and mRNA is converted into cDNA. The synthesized cDNA is sheared to blunt-end and ligated with adapter containing primer sites for sequencing. The adequate cDNA fragments are selected via gel-electrophoresis and then denatured to form a single strand after PCR. The completed samples are loaded onto a single lane of an Illumina GAII flowcell and sequenced. Finally, transcriptome analysis was conducted.

Table III-1. Bacterial strains and plasmids used in this study.

Strains	Description	References or source
***Salmonella enterica* serovar Typhimurium**		
SL1344	Wild type, Sm^R	(Robin & Lee, 2000)
SR7001	Δ*ptsN*	(Yoo *et al*, 2016)
Plasmids		
pKD46	Ap^R P_{BAD}-*gam-beta-exo oriR101 repA101*^{ts}	(Datsenko & Wanner, 2000)
pKD13	Ap^R FRT Km^R FRT PS1 PS4 *oriR6Kγ*	(Datsenko & Wanner, 2000)
pCP20	Ap^R Cm^R *cI*857 λP_R*flp oripSC101*^{ts}	(Datsenko & Wanner, 2000)

Table III-2. Primers used to construct the bacterial strains and plasmids.

Primers	Sequence (5' to 3')
ptsN-del-F	CTG GCC ATC AAC CTG ACA GGA CAG GTT CTT AGG TGA AAT TTG TAG GCT GGA GCT GCT TCG
ptsN-del-R	CGT TTC GCC ACC AGC GAC AGC GTG TGC AGA TGC GTT TTA ATT CCG GGG CTC CGT CGA CC

III-3. Results and Discussion

Comprehensive understanding of EIIA^{Ntr} roles in *Salmonella* using transcriptome analysis. Multifaceted regulatory roles have been imposed in EIIA^{Ntr} in diverse bacterial species including *Escherichia coli* (Lee *et al*, 2007; Lüttmann *et al*, 2009), *Pseudomonas putida* (Cases *et al*, 2001) and *Salmonella* Typhimurium (Choi *et al*, 2010). In this study, transcriptome profiling of a *Salmonella* Δ*ptsN* mutant strain was conducted to understand comprehensive roles of EIIA^{Ntr} in *Salmonella* metabolism and virulence. The Δ*ptsN* mutant strain did not show growth defects under LB broth at 37°C when compared to its parent strain *S.* Typhimurium SL1344 (Fig. III-3A and 2B). Total RNA was extracted at a mid-exponential phase of growth (OD_{600} = 1) and analyzed using RNA-seq. Statistical comparison between two strains (p value < 0.05) revealed that 2.40% (116/4837) and 1.12% (54/4837) of the total genes were up- and down-regulated, respectively, by 3-fold or more in the Δ*ptsN* mutant strain compared to the wild-type (Fig. III-5A). The differentially expressed genes (DEGs) were categorized based on their predicted functions by cluster of

orthologous groups (COG) designations (Tatusov *et al*, 1997). Genes with functions of energy production and conversion, amino acid transport and metabolism, coenzyme transport and metabolism, and secondary metabolites biosynthesis/transport/catabolism were down-regulated overall in the absence of $EIIA^{Ntr}$, while genes involved in cell wall/membrane/envelope biogenesis, inorganic ion transport and metabolism, signal transduction, intracellular trafficking/secretion/vesicular transport, and defense mechanism were generally up-regulated (Fig. III-5B). The likelihood of multiphasic cellular regulation by $EIIA^{Ntr}$ was predicted from the previously identified roles of $EIIA^{Ntr}$ in K^+ homeostasis (Lee *et al*, 2007; Lüttmann *et al*, 2009), phosphate starvation responses (Lüttmann *et al*, 2012), ppGpp synthesis/hydrolysis (Karstens *et al*, 2014), amino acid synthesis/metabolism (Lee *et al*, 2005; Lee *et al*, 2013), and carbon metabolism (Pflüger-Grau *et al*, 2011). Taken together, these results suggest that $EIIA^{Ntr}$ might affect the diverse metabolisms associated with *Salmonella* fitness.

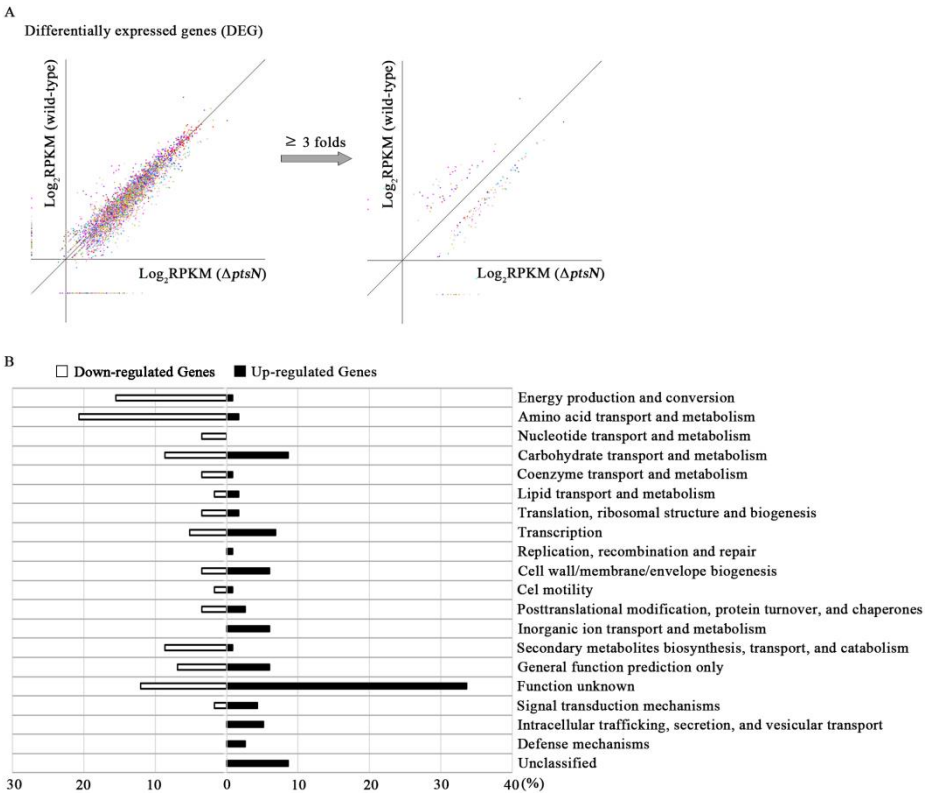

Figure III-5. Classification of differentially expressed genes (DEG) based on predicted functions. (A) Differentially expressed genes (DEG) analysis from RNA-seq data between wild-type *Salmonella* and the Δ*ptsN* mutant strain. The y-axis shows log-scaled RPKM value of wild-type, and the x-axis shows log-scaled RPKM values of the Δ*ptsN* mutant strain. Total gene expressions in the two strains (left) were filtered for sorting significantly down- or up-regulated genes (right) with criteria of p-value ≤ 0.05 and fold-change ≥ 3. **(B)** Genes up-regulated or down-regulated in the Δ*ptsN* mutant strain 3-fold or more are grouped into functional

categories. Genes are annotated based on the COGs database.

$EIIA^{Ntr}$ activated expression of genes involved in vitamin B_{12} synthesis and 1,2-PDL utilization. An effort to make sense of primary roles of $EIIA^{Ntr}$ in *Salmonella* led us to search for genes coordinately controlled as an operon by $EIIA^{Ntr}$. Genes constituting the 1,2-PDL utilization (*pdu*) operon were predominantly decreased in the Δ*ptsN* mutant strain, indicating a positive role of $EIIA^{Ntr}$ in utilizing 1,2-PDL as a carbon source (Fig. III-6, Table III-3). The *pdu* operon consists of 21 genes with *pocR* and *pduF* encoding its cognate activator and membrane transporter, respectively, in the opposite direction on the chromosome and encodes proteins for the catabolism of 1,2-PDL. *Salmonella* degrades 1,2-PDL into propionaldehyde with the aid of a cofactor adenosyl cobalamin (Ado-B_{12}) and further processes into propanol and propionate through propionyl-CoA to acquire energy in nutrient-restricted conditions (Sampson & Bobik, 2008). In accordance with a decrease in *pdu* expression, the *cob-cbi* operon encoding enzymes for the biosynthesis of Ado-B_{12} was inclined toward down-regulation by the absence of $EIIA^{Ntr}$ (Fig. III-6, Table III-3). The 1,2-PDL enables *Salmonella* to produce energy and carbon sources, and outcompete commensal microbiota in the nutrient-restricted host intestine.

Thus, the transcriptome profiling indicates that $EIIA^{Ntr}$ activates transcription of multiple genes coordinately to exploit 1,2-PDL disfavored carbon sources by bystander microbiota.

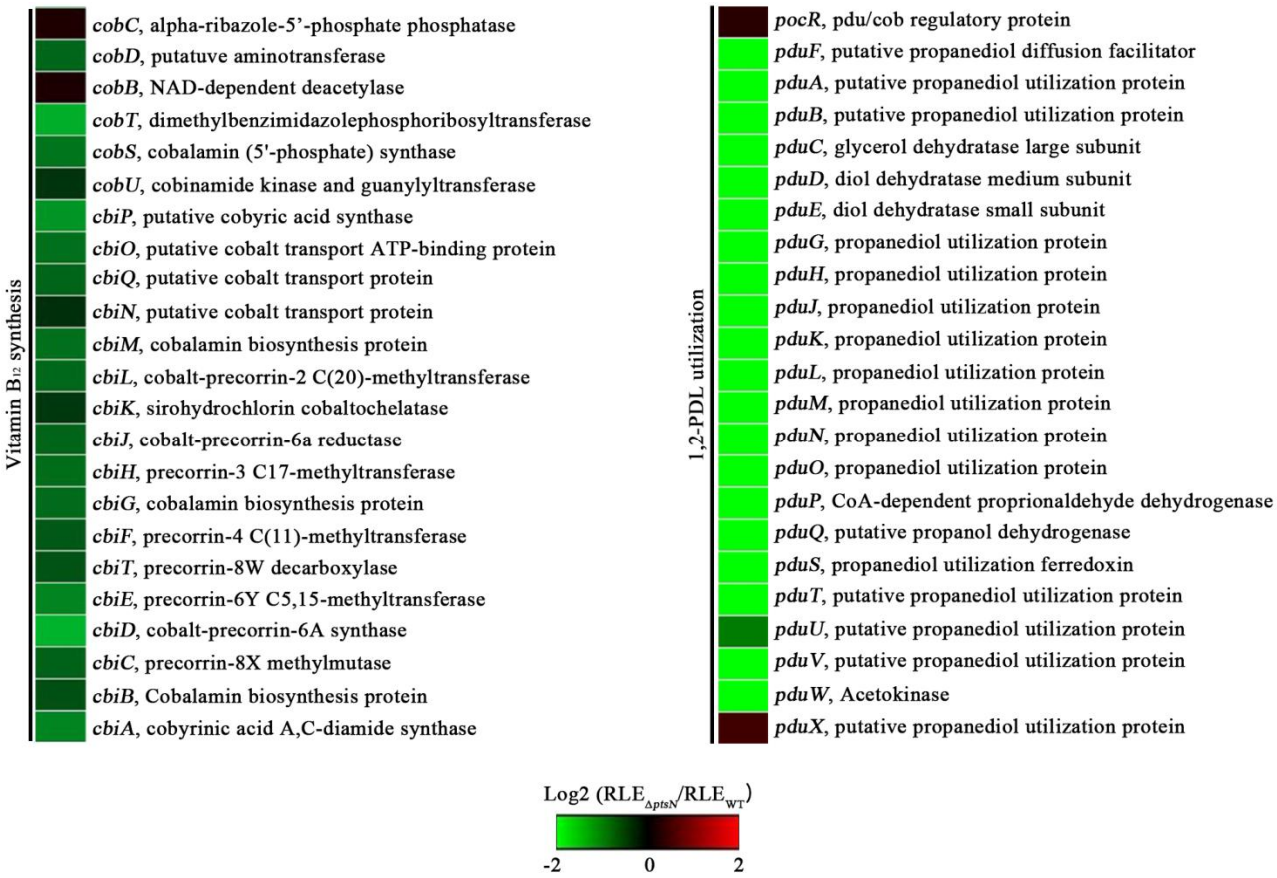
Vitamin B12 synthesis
cobC, alpha-ribazole-5'-phosphate phosphatase
cobD, putatuve aminotransferase
cobB, NAD-dependent deacetylase
cobT, dimethylbenzimidazolephosphoribosyltransferase
cobS, cobalamin (5'-phosphate) synthase
cobU, cobinamide kinase and guanylyltransferase
cbiP, putative cobyric acid synthase
cbiO, putative cobalt transport ATP-binding protein
cbiQ, putative cobalt transport protein
cbiN, putative cobalt transport protein
cbiM, cobalamin biosynthesis protein
cbiL, cobalt-precorrin-2 C(20)-methyltransferase
cbiK, sirohydrochlorin cobaltochelatase
cbiJ, cobalt-precorrin-6a reductase
cbiH, precorrin-3 C17-methyltransferase
cbiG, cobalamin biosynthesis protein
cbiF, precorrin-4 C(11)-methyltransferase
cbiT, precorrin-8W decarboxylase
cbiE, precorrin-6Y C5,15-methyltransferase
cbiD, cobalt-precorrin-6A synthase
cbiC, precorrin-8X methylmutase
cbiB, Cobalamin biosynthesis protein
cbiA, cobyrinic acid A,C-diamide synthase
1,2-PDL utilization
pocR, pdu/cob regulatory protein
pduF, putative propanediol diffusion facilitator
pduA, putative propanediol utilization protein
pduB, putative propanediol utilization protein
pduC, glycerol dehydratase large subunit
pduD, diol dehydratase medium subunit
pduE, diol dehydratase small subunit
pduG, propanediol utilization protein
pduH, propanediol utilization protein
pduJ, propanediol utilization protein
pduK, propanediol utilization protein
pduL, propanediol utilization protein
pduM, propanediol utilization protein
pduN, propanediol utilization protein
pduO, propanediol utilization protein
pduP, CoA-dependent proprionaldehyde dehydrogenase
pduQ, putative propanol dehydrogenase
pduS, propanediol utilization ferredoxin
pduT, putative propanediol utilization protein
pduU, putative propanediol utilization protein
pduV, putative propanediol utilization protein
pduW, Acetokinase
pduX, putative propanediol utilization protein
Log2 (RLE ΔptsN/RLE WT)
-2
0
2

Figure III-6. The effects of *ptsN* on the expression of genes involved in vitamin B_{12} synthesis and 1,2-PDL utilization. Heat-map analysis of expression ratios of *cob-cbi*, and *pdu* genes between the Δ*ptsN* mutant and wild-type strain ($\log_2$[Δ*ptsN* mutant/wild-type]).

EIIA^{Ntr} negatively controlled expression of SPI-1 and SPI-4 important for *Salmonella* invasion. Recently, propionyl-CoA, the intermediate of 1,2-PDL utilization pathways, was found to exert a new role as a regulatory signal. Intracellular propionyl-CoA synthesized from 1,2-PDL abundant in the host intestine attenuated the stability of HilD, the master regulator of SPI-1, which led to reduced *Salmonella* invasion into epithelial cells (Hung *et al*, 2013). In agreement with the observation, altered expression of *pdu* operons depending on the presence of EIIA^{Ntr} also influenced the expression of SPI-1 and SPI-4 (Fig. III-7, Table III-3). The Δ*ptsN* mutant strain degraded 1,2-PDL into propionyl-CoA less than wild-type *Salmonella* did. A reduction in propionyl-CoA in the Δ*ptsN* mutant strain was presumed to activate SPI-1 expression by the accumulation of HilD, which in turn stimulated SPI-4 expression via HilA. Accordantly, the capacity to utilize 1,2-PDL as carbon sources influenced *Salmonella* invasiveness into the epithelial cells. The presence of 1,2-PDL can attenuate the invasiveness of *Salmonella* wild-type strains probably due to an increase in propionyl-CoA via the 1,2-PDL utilization pathways.

Consequently, this result suggests that EIIA^{Ntr} lowers

Salmonella invasion into host cells when 1,2-PDL is abundant in the milieu and processed into propionyl-CoA.

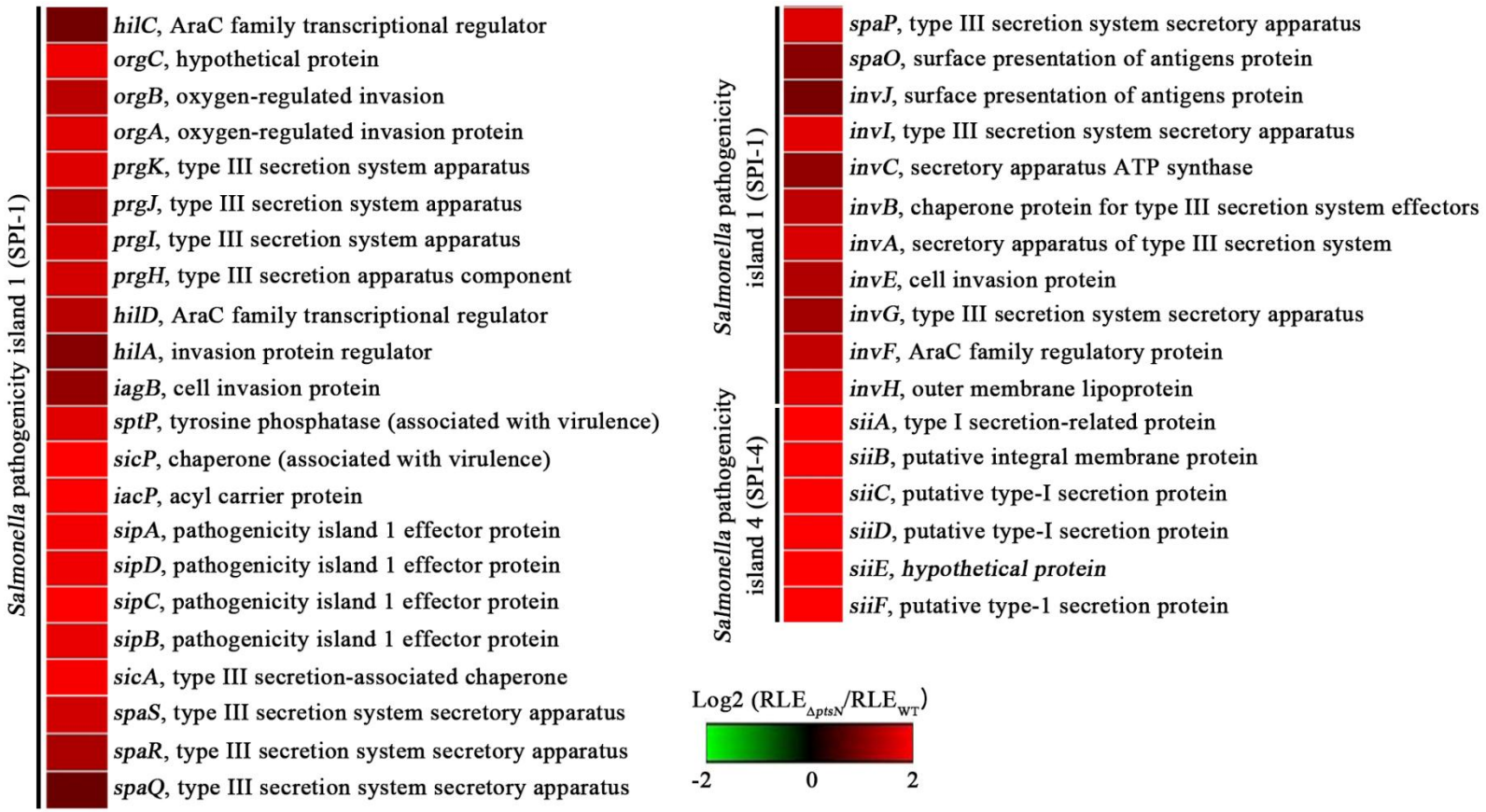
Salmonella pathogenicity island 1 (SPI-1)
hilC, AraC family transcriptional regulator
orgC, hypothetical protein
orgB, oxygen-regulated invasion
orgA, oxygen-regulated invasion protein
prgK, type III secretion system apparatus
prgJ, type III secretion system apparatus
prgI, type III secretion system apparatus
prgH, type III secretion apparatus component
hilD, AraC family transcriptional regulator
hilA, invasion protein regulator
iagB, cell invasion protein
sptP, tyrosine phosphatase (associated with virulence)
sicP, chaperone (associated with virulence)
iacP, acyl carrier protein
sipA, pathogenicity island 1 effector protein
sipD, pathogenicity island 1 effector protein
sipC, pathogenicity island 1 effector protein
sipB, pathogenicity island 1 effector protein
sicA, type III secretion-associated chaperone
spaS, type III secretion system secretory apparatus
spaR, type III secretion system secretory apparatus
spaQ, type III secretion system secretory apparatus
Salmonella pathogenicity island 1 (SPI-1)
spaP, type III secretion system secretory apparatus
spaO, surface presentation of antigens protein
invJ, surface presentation of antigens protein
invI, type III secretion system secretory apparatus
invC, secretory apparatus ATP synthase
invB, chaperone protein for type III secretion system effectors
invA, secretory apparatus of type III secretion system
invE, cell invasion protein
invG, type III secretion system secretory apparatus
invF, AraC family regulatory protein
invH, outer membrane lipoprotein
Salmonella pathogenicity island 4 (SPI-4)
siiA, type I secretion-related protein
siiB, putative integral membrane protein
siiC, putative type-I secretion protein
siiD, putative type-I secretion protein
siiE, hypothetical protein
siiF, putative type-1 secretion protein
Log2 (RLE ΔptsN/RLE WT)
-2
0
2

Figure III-7. The effects of *ptsN* on the expression of genes involved in bacterial invasiveness. Heat-maps were generated to describe the expression patterns of SPI-1 and SPI-4 genes in the Δ*ptsN* mutant strain. Gene expression ratios between the Δ*ptsN* mutant and wild-type SL1344 were shown by means of a colorimetric gradient: down-regulation in green and up-regulation in red.

Table III-3. Genes specifically regulated by *ptsN*.

Category	Gene	Fold expression	Function
Vitamin B_{12} synthesis	*cobC*	0.18	alpha-ribazole-5'-phosphate phosphatase
	cobD	-0.80	putative aminotransferase CobD
	cobB	0.16	NAD-dependent deacetylase
	cobT	-1.37	Nicotinate-nucleotide--dimethylbenzimidazolephosphoribosyltransferase
	cobS	-0.91	cobalamin (5'-phosphate) synthase
	cobU	-0.37	cobinamide kinase and guanylyltransferase
	cbiP	-1.18	putative cobyric acid synthase
	cbiO	-0.88	putative cobalt transport ATP-binding protein
	cbiQ	-0.79	putative cobalt transport protein
	cbiN	-0.34	putative cobalt transport protein CbiN
	cbiM	-0.43	cobalamin biosynthesis protein
	cbiL	-0.81	cobalt-precorrin-2 C(20)-methyltransferase
	cbiK	-0.41	sirohydrochlorin cobaltochelatase
	cbiJ	-0.78	cobalt-precorrin-6a reductase
	cbiH	-0.85	precorrin-3 C17-methyltransferase
	cbiG	-0.88	cobalamin biosynthesis protein
	cbiF	-0.84	precorrin-4 C(11)-methyltransferase
	cbiT	-0.68	precorrin-8W decarboxylase
	cbiE	-0.63	precorrin-6Y C5,15-methyltransferase
	cbiD	-1.04	cobalt-precorrin-6A synthase
	cbiC	-1.41	precorrin-8X methylmutase
	cbiB	-0.76	Cobalamin biosynthesis protein
	cbiA	-0.62	cobyrinic acid A,C-diamide synthase

Table III-3. Genes specifically regulated by *ptsN*.

Category	Gene	Fold expression	Function
1,2-PDL utilization	*pocR*	-0.25	pdu/cob regulatory protein
	pduF	-1.97	putative propanediol diffusion facilitator
	pduA	-2.43	putative propanediol utilization protein
	pduB	-3.86	putative propanediol utilization protein
	pduC	-3.57	propanediol dehydratase large subunit
	pduD	-4.03	propanediol dehydratase medium subunit
	pduE	-3.86	propanediol dehydratase small subunit
	pduG	-4.34	putative propanediol utilization
	pduH	-4.58	putative propanediol utilization
	pduJ	-3.68	putative propanediol utilization
	pduK	-3.70	putative propanediol utilization
	pduL	-4.07	putative propanediol utilization
	pduM	-3.76	putative propanediol utilization
	pduN	-5.90	putative propanediol utilization
	pduO	-5.40	propanediol utilization protein
	pduP	-3.36	putative propionaldehyde dehydrogenase
	pduQ	-4.33	putative propanediol dehydrogenase
	pduS	-3.62	propanediol utilization ferredoxin
	pduT	-3.50	putative propanediol utilization protein
	pduU	-1.00	putative propanediol utilization protein PduU
	pduV	-3.14	putative propanediol utilization protein PduV
	pduW	-2.89	acetokinase

Table III-3. Genes specifically regulated by *ptsN*.

Category	Gene	Fold expression	Function
	hilC	0.89	AraC family transcriptional regulator
	orgC	1.88	hypothetical protein
	orgB	1.46	oxygen-regulated invasion protein
	orgA	1.77	oxygen-regulated invasion protein
	prgK	1.75	type III secretion system apparatus
	prgJ	1.53	type III secretion system apparatus
	prgI	1.67	type III secretion system apparatus
	prgH	1.65	type III secretion apparatus component
	hilD	1.43	AraC family transcriptional regulator
	hilA	1.04	invasion protein regulator
	iagB	1.16	cell invasion protein
	sptP	1.76	tyrosine phosphatase (associated with virulence)
	sicP	2.11	chaperone (associated with virulence)
	iacP	2.73	acyl carrier protein
	sipA	1.92	pathogenicity island 1 effector protein
	sipD	1.88	pathogenicity island 1 effector protein
***Salmonella* pathogenicity island-1**	*sipC*	2.11	pathogenicity island 1 effector protein
	sipB	1.83	pathogenicity island 1 effector protein
	sicA	1.95	type III secretion-associated chaperon
	spaS	1.63	type III secretion system secretory apparatus
	spaR	1.33	type III secretion system secretory apparatus
	spaQ	0.83	type III secretion system secretory apparatus
	spaP	1.74	type III secretion system secretory apparatus
	spaO	1.06	surface presentation of antigens protein (associated with type III secretion and virulence)
	invJ	0.93	surface presentation of antigens protein (associated with type III secretion and virulence)
	invI	1.77	type III secretion system secretory apparatus
	invC	1.14	secretory apparatus ATP synthase (associated with virulence)
	invB	1.49	chaperone protein for type III secretion system effectors
	invA	1.69	secretory apparatus of type III secretion system
	invE	1.38	cell invasion protein
	invG	1.27	type III secretion system secretory apparatus
	invF	1.53	AraC family regulatory protein
	invH	1.80	outer membrane lipoprotein

Table III-3. Genes specifically regulated by *ptsN*.

Category	Gene	Fold expression	Function
***Salmonella* pathogenicity island-4**	*siiA*	2.29	type I secretion-related protein
	siiB	2.50	putative integral membrane protein
	siiC	3.06	putative type I secretion protein
	siiD	3.19	putative type I secretion protein
	siiE	2.50	large repetitive protein
	siiF	3.16	putative type-1 secretion protein

Chapter IV.

$EIIA^{Ntr}$ regulates *Salmonella* virulence via 1,2-propanediol utilization pathway

IV-1. Introduction

Salmonella enterica serovar Typhimurium is a bacterial pathogen that can infect a wide range of animals and cause food-borne gastroenteritis in millions of people worldwide (Haraga *et al*, 2008; Ibarra & Steele-Mortimer, 2009). In the animal intestinal tract, *Salmonella* should compete with the resident bacteria occupying colonization niches and has been evolved to harness diverse metabolic pathways to enhance its fitness during infection (Staib & Fuchs, 2014). For instance, *Salmonella* can acquire carbon and energy sources from 1,2-propanediol (1,2-PDL), an abundant fermentation product derived from plant sugars, L-rhamnose and L-fucose. 1,2-PDL serve as a carbon and energy source for *Clostridium glycolicum* and *Klebsiella pneumoniae* in a cobalamin-dependent manner under anaerobic conditions (Gaston & Stadtman, 1963; Toraya *et al*, 1979). *Salmonella* Typhimurium was able to grow with 1,2-PDL in the presence of this vitamin under aerobic conditions (Jeter, 1990). Growth of *Salmonella* Typhimurium with 1,2-PDL in the absence of oxygen, however, was observed only when tetrathionate, which serve as a terminal electron

acceptor for anaerobic respiration of 1,2-PDL, was added to the medium (Price-Carter *et al*, 2001). 1,2-PDL is the fermentation end-product of bacterial growth with L-fucose and/or L-rhamnose (Daniel *et al*, 1998). While *Escherichia coli* is unable to further metabolize 1,2-PDL when kept under anaerobic conditions, this compound vanishes from the *Salmonella* Typhimurium culture medium suggesting its further utilization by this pathogen (Obradors *et al*, 1988).

The two sugars L-fucose and L-rhalnose are frequently found in the carbohydrate moiety of mucosal glycoconjugates, herbal cell walls, and bacterial exopolysaccharides (Sampson & Bobik, 2008). L-fucose, comprising 4–14% of the oligosaccharide content of mucins, is found mainly as a terminal sugar of the oligosaccharide chains linked to the mucin protein backbone (Muraoka & Zhang, 2011). Thus, mucus is the main source of gastrointestinal L-fucose provided by the enzymatic activities of Bacteroides (Keeney & Finlay, 2013). Degradation of L-fucose monomers is not restricted to commensal bacteria such as Bacteroides. The genetic determinants for L-fucose utilization are also found in the genomes of many enteropathogens (Staib & Fuchs, 2014), although to date, experimental confirmation of fucose utilization is

largely lacking. Fermentation of L-fucose and subsequent 1,2-PDL secretion have been described for *E. coli* (Cocks *et al*, 1974), *K. pneumoniae*, and *S.* Typhimurium (Badia *et al*., 1985). More recently, proteomic and glycomic evidence has been provided that *S.* Typhimurium takes advantage of fucose metabolization while growing in the mouse gut (Deatherage Kaiser *et al*, 2013).

As I previously described, 1,2-PDL is degraded into propionaldehyde by B_{12}-dependent 1,2-propanediol dehydratase and further processed to 1-propanol and propionate through intermediate propionyl-CoA with the coordinated action of *pdu* operon products (Havemann *et al*, 2002; Sampson & Bobik, 2008) (Fig. IV-1), and propionyl-CoA can exert a role as a regulatory signal compromising the stability of HilD, the transcriptional regulator of *Salmonella* pathogenicity island-1 (SPI-1). SPI-1, a chromosomal region composed of 39 genes, encodes a type 3 secretion system (T3SS), whereby its cognate effector proteins are translocated into host cells to promote bacterial invasion. An increase in propionyl-CoA production lowers the stability of HilD, thus attenuating *Salmonella* invasion into intestinal epithelial cells (Hung *et al*, 2013). Although SPI-1 is prominently

responsible for *Salmonella* invasion into host cells, SPI-4 is also required for bacterial adhesion to polarized epithelial cells as well as for invasion (Gerlach *et al*, 2008). SPI-4 locus contains six genes, *siiABCDEF*, forming an operon. SiiE, which is secreted via SPI-4-encoded type 1 secretion system (SPI-4 T1SS), facilitates *Salmonella* adhesion to polarized host cells. Not surprisingly, the expression of SPI-4 is coordinated with SPI-1 regulation. SPI-1 employs its cognate regulators of HilD, HilC, HilA, and InvF for its systematic regulation. HilD and HilC induce the expression of HilA in combination or independently. HilA in turn directly activates the expression of *invF* and genes encoding T3SS and also indirectly induces the transcription of SPI-4. HilA antagonizes H-NS-mediated transcriptional silencing of SPI-4 (Main-Hester *et al*, 2008).

As described in the previous chapter, I compared whole transcriptome between the wild-type and a mutant strain lacking *ptsN* by RNA-seq. Genes involved in B_{12} synthesis and 1,2-PDL utilization were significantly down-regulated in the Δ*ptsN* mutant strain, while SPI-1 and SPI-4 were up-regulated. This phenomenon was complemented with the addition of glutathione (GSH) into the growth medium. Therefore I

compared the quantity of GSH between wild-type and Δ*ptsN* mutant strain, and confirmed that GSH was about 3 folds lower in Δ*ptsN* mutant strain than wild-type.

In accordance with the transcriptional differences, the Δ*ptsN* mutant strain was more competent in invasion into host cells than wild-type bacteria when they were pre-cultured with 1,2-PDL. I disclosed that $EIIA^{Ntr}$ controls *Salmonella* invasion via balancing propionyl-CoA in response to environmental carbon metabolites.

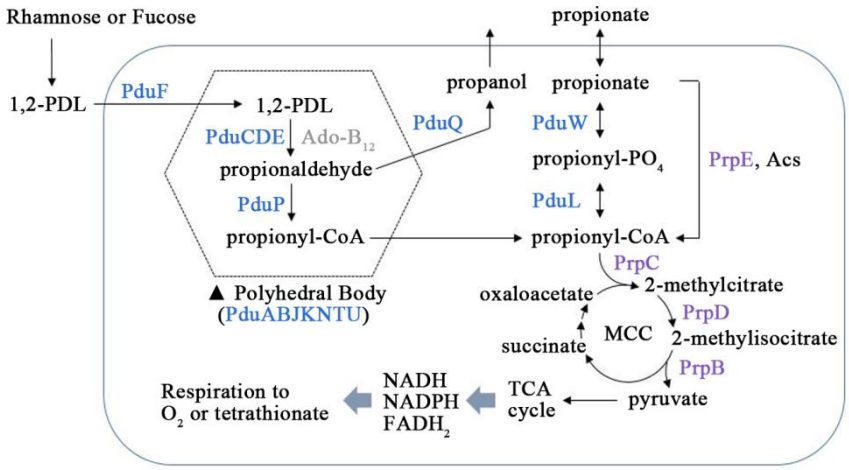

Figure IV-1. Catabolism of 1,2-PDL and propionate in *Salmonella* Typhimurium. 1,2-PDL catabolism is achieved by 1,2-PDL utilization operon indicated blue. 1,2-PDL is converted into propionyl-CoA within polyhedral microcompartment. Propionate catabolism is accomplished by propionate operon indicated purple. The common intermediate propionyl-CoA provides pyruvate by 2-methycitrate cycle (MCC) which can be used as energy source. Oxygen or tetrathionate is used as an electron acceptor under aerobic or anaerobic condition, respectively.

IV-2. Materials and Methods

Bacterial strains, media, and culture conditions. All bacterial strains were derived from *Salmonella* Typhimurium SL1344 as the parent and are listed in Table IV-1. Luria-Bertani (LB) medium containing 1% Bacto-tryptone, 0.5% yeast extract and 1% NaCl, pH 7.5 was used as the complex culture medium for the routine growth of bacteria. All *Salmonella* Typhimurium strains were grown aerobically at 37°C with antibiotics supplementation at the following concentrations: ampicillin, 50 μg/ml; kanamycin, 50 μg/ml; chloramphenicol, 25 μg/ml. As an alternative carbon source, 1,2-PDL (12.5 mM) was added when bacterial cultures reached an optical density at 600 nm (OD_{600}) of 0.5-0.6. In the case of 1,2-PDL utilization, Ado-B_{12} (20 nM) was also added as a cofactor to the LB medium.

Construction of strains and plasmids. The *ptsN* deletion mutant strain was constructed using the lambda red recombination method for in-frame gene deletion (Datsenko & Wanner, 2000). For the construction of Δ*ptsN* mutant strain, SR7001, the Km^R cassette from

pKD13 was amplified using primers ptsN-del-F and ptsN-del-R. The resulting PCR products were integrated into the *ptsN* region in the SL1344 wild-type strain containing the plasmid pKD46, followed by selection for Δ*ptsN*::kan transformants. The Km^R cassette was removed using the plasmid pCP20 (Datsenko & Wanner, 2000). The *gshB* deletion mutant strain was also constructed using the same method described above with primer sets gshB-del-F and gshB-del-R. The tagging of $EIIA^{Ntr}$ and HilD with the FLAG and HA peptide respectively at the C-terminus was also constructed using the same recombination system with each primer set; ptsN-FLAG-F/ptsN-FLAG-R and HilD-HA-F/HilD-HA-R. Plasmid pWJ04 expresses the *ptsN* gene from its own promoter. For the construction of this plasmid, the *ptsN* gene was amplified by PCR using primers ptsN-comple-F and ptsN-comple-R containing restriction sites, HindIII and SphI. The PCR product was introduced between HindIII and SphI restriction sites of pACYC184 vector. To construct pWJ25 expressing PocR under the *lac* promoter, the *pocR* gene was amplified by PCR using the pocR-over-R and pocR-over-R primers and the purified PCR product was inserted between the BamHI and HindIII sites of the pUHE21-2$lacI^q$ vector (Soncini *et al*,

1995). To construct the strain carrying a *lacZ* reporter gene, Km^R cassette from pKD13 was amplified using primer sets. The lambda red recombination method was used as mentioned above and then the *lacZ* gene was introduced using the plasmid pCE70 (Merighi *et al*, 2005). To make *lacZ* fusion in mutant strains, the integrated *lacZ* gene was transferred by bacteriophage P22 transduction (Sternberg & Maurer, 1991). The sequences of primers used in constructing *Salmonella* strains and plasmids are listed in Table VI-2.

Quantitative real-time RT-PCR. *Salmonella* strains were grown in LB medium to the log phase with the OD_{600} of 1.2-1.4 under aerobic condition at 37°C. RNAprotect bacterial reagent (Qiagen, Hilden, Germany) was treated to appropriate volume of each collected sample before total RNA extraction. Total RNA was isolated by using RNeasy mini kit (Qiagen) according to the manufacturer's instructions and residual DNA was removed with Ambion Turbo DNA-*free*™ (ThermoFisher Scientific, Braunschweig, Germany). cDNA was synthesized using RNA to cDNA EcoDry™ Premix (Random Hexamers) (Clontech). Quantification of cDNA was carried out using

2×iQ SYBR Green Supermix (Bio-Rad, CA, USA), and real-time amplification of the PCR products was performed using the iCycler iQ real-time detection system (Bio-Rad). The calculated threshold cycle (C_t) corresponding to a target gene was normalized by the C_t of the control *gyrB* gene. The topoisomerase *gyrB* gene was chosen as a control because no significant variation of *gyrB* expression. Experiments were performed in triplicate. The sequences of primers used in the quantitative reverse transcription-PCR (qRT-PCR) analysis were listed in Table IV-3.

Propanediol utilization assay. A pH indicator Neutral-Red was used to test the formation of propionate (Parsons *et al*, 2008). Its color changes from red to yellow between pH 6.8 and 8.0. When Neutral-Red was added to LB media in 0.0033% as a final concentration, the utilization of 1,2-PDL produces red-color due to the reduction in pH indicating the formation of propionate. Broth colors were examined after 8 h incubation in LB media.

β-Galactosidase assay. *Salmonella* strain containing a *lacZ*

gene was grown in LB medium with the indicated additives. β-Galactosidase assays were carried out in triplicate and the activity was determined as described previously (Miller, 1992).

Western blotting analysis. Proteins were separated on the gel depending on the molecular weights by SDS-PAGE and transferred to a polyvinylidene difluoride (PVDF) membrane. The membrane was blocked with 0.5% nonfat dry milk in 1× Tris-buffered saline-Tween 20 (TBS-T) buffer and probed with anti-FLAG antibody (1:1,000 dilution, Sigma-Aldrich, Taufkirchen, Germany), anti-HA antibody (3:2,000 dilution, Sigma-Aldrich) or anti-DnaK antibody (1:10,000 dilution, Enzo Life Science, NY, USA) as primary antibodies. Anti-mouse IgG conjugated with peroxidase (3:5,000 dilution, Santa Cruz Biotechnology, CA, USA) was used as the secondary antibody in all of the western blotting experiments. The chemiluminescent signals were developed with a West-Zol plus western blot detection system (iNtRON Biotechnology, Seongnam, Korea).

Analysis of EIIA^{Ntr} and HilD stability. The protein stability

was determined as previously described (Biran *et al*, 2000). *Salmonella* strains encoding $EIIA^{Ntr}$-FLAG or HilD-HA protein from the chromosome were grown in LB medium with the indicated additives for 4 h, and chloramphenicol was added at 0.2 mg/ml to block *de novo* protein synthesis. Aliquots of these cultures were taken at the indicated time points after the addition of chloramphenicol and were subjected to western blotting, as described above.

Gentamicin protection assay. Caco-2 cells were grown in Dulbecco modified Eagle medium (DMEM) supplemented with 10% heat-inactivated fetal bovine serum (FBS), penicillin (50 U/ml) and streptomycin (50 U/ml). At least 1 h prior bacterial infection, a monolayer of 2.5×10^5 Caco-2 cells was prepared in a 24-well tissue culture plate and was incubated in DMEM-10% FBS without antibiotics at 37°C under 5% CO_2. Bacteria were subcultured from an overnight culture (1:100) in fresh LB medium containing the indicated additives and grown for 4 h at 37°C with aeration. Bacteria were applied to the cell monolayer at a multiplicity of infection (MOI) of 10. After 30 min of incubation at 37°C under 5% CO_2, non-invaded bacteria were

removed by washing three times with pre-warmed phosphate-buffered saline (PBS) and were then incubated for 1 h with the pre-warmed medium supplemented with 100 μg/ml of gentamicin to kill extracellular bacteria. Afterward, the wells were washed three times with pre-warmed PBS, lysed in 1% Triton X-100 in PBS for 30 min at 37°C, and then diluted in PBS. A dilution of the suspension was plated on LB agar medium to enumerate the CFU.

Glutathione (GSH) assay. *Salmonella* strains were grown in LB medium to the log phase with the OD_{600} of 0.5 under aerobic condition at 37°C. 1,2-PDL was added into the bacterial culture medium and further incubated for 2 h. *Salmonella* cells were harvested by centrifugation. The next steps of GSH assay were following the manufacturer's instructions of Glutathione Assay Kit (Sigma CS0260, St. Louis, MO, USA).

Table IV-1. Bacterial strains and plasmids used in this study.

Strains	Description	References or source
***Salmonella enterica* serovar Typhimurium**		
SL1344	Wild type, Sm^R	(Lucas & Lee, 2000)
SR7001	Δ*ptsN*	(Yoo *et al*, 2016)
SR7021	$EIIA^{Ntr}$-FLAG	(Yoo *et al*, 2016)
SR7024	HilD-HA	This study
SR7025	HilD-HA, Δ*ptsN*	This study
SR7026	P*ptsN-lacZ*	This study
SR7030	P*pduA-lacZ*	This study
SR7031	P*pduA-lacZ,* Δ*ptsN*	This study
SR7041	Δ*gshB*	This study
Escherichia coli		
DH5α	*gyrA96 recA1 relA1 endA1 thi-1 hsdR17 glnV44 deoR Δ(lacZYA-argF)U169*[Φ80d Δ(*lacZ*)*M15*]	(Woodcock *et al.*, 1989)
Plasmids		
pKD46	Ap^R P_{BAD}-*gam-beta-exo oriR101 repA101*^{ts}	(Datsenko & Wanner, 2000)
pKD13	Ap^R FRT Km^R FRT PS1 PS4 *oriR6Kγ*	(Datsenko & Wanner, 2000)
pCP20	Ap^R Cm^R *cI*857 λP_R*flp oripSC101*^{ts}	(Datsenko & Wanner, 2000)
pCP70	Km^R FRT *tnpR lacZY*$^+$ *oriR6Kγ*	(Merighi *et al*, 2005)
pACYC184	Tet^R Cm^R p15A *ori*	(Chang & Cohen, 1978)
pUHE21-2*lacI*^{q}	$rep_{pMB1}Ap^R$*lacI*^{q}	(Soncini *et al*, 1995)
pWJ04	pACYC184::*ptsN*	(Yoo *et al*, 2016)
pWJ25	pUHE21-2*lacI*^{q}-*pocR*	(Yoo *et al*, 2016)

Table VI-2. Primers used to construct the bacterial strains and plasmids.

Primers	Sequence (5' to 3')
ptsN-del-F	CTG GCC ATC AAC CTG ACA GGA CAG GTT CTT AGG TGA AAT TTG TAG GCT GGA GCT GCT TCG
ptsN-del-R	CGT TTC GCC ACC AGC GAC AGC GTG TGC AGA TGC GTT TTA ATT CCG GGG CTC CGT CGA CC
ptsN-comple-F	AAA AAG CTT ACG CAC ATC TCG GAT GCG AC
ptsN-comple-R	AAA GCA TGC CCG CTG ACG ATC ATC AGT AC
hilD-HA-F	TAA AAC TAC GCC ATC GAC ATT CAT AAA AAT GGC GAA CCA TTA TCC GTA TGA TGT TCC TGA TTA TGC TAG CCT CTA ATG TAG GCT GGA GCT GCT TCG
hilD-HA-R	TTA ATA AAA ATC TTT ACT TAA GTG ACA GAT ACA AAA AAT GAT TCC GGG GAT CCG TCG ACC
ptsN-FLAG-F	TCA AAT CAT TAC TGA CAC CGA AGG TGA GCA GAA TGA GGC AGG CAG CGG CGA CTA CAA AGA CGA TGA CGA CAA GTA ATG TAG GCT GGA GCT GCT TCG
ptsN-FLAG-R	GTT TCT CCT CAC AAC GAC AGA AAT AAA TGC CAT TGA GTT GAT TCC GGG GAT CCG TCG ACC
ptsN-lacZ-F	AAT CAT TAC TGA CAC CGA AGG TGA GCA GAA TGA GGC ATA ATG TAG GCT GGA GCT GCT TCG
ptsN-lacZ-R	ACC ATG TAC CGT TTC TCC TCA CAA CGA CAG AAA TAA ATG CAT TCC GGG GAT CCG TCG ACC
pduA-lacZ-F	CGA TGT AGA AAA AAT CTT ACC GAA GGG AAT TAG CCA ATG ATG TAG GCT GGA GCT GCT TCG
pduA-lacZ-R	CAC ACG GGC AAT CAC CTG CGC CAT GAT CTG TTC CAC CAG CAT TCC GGG GAT CCG TCG ACC
pocR-over-F	AAA GGA TCC TTT CAC GCC GTT TTG TCA GT
pocR-over-R	AAA AAG CTT ACT ATC AAA AAT CGG CAA TAG C
gshB-del-F	GGA GAT TAA ACT CGC CGA TCT GGA CGT CAT TTT GAT GCG CTG TAG GCT GGA GCT GCT TCG
gshB-del-R	AGA TCG GGT ATT CCG CTT CAA TTT CAC GCA CGC AGG TTG GAT TCC GGG GAT CCG TCG ACC

Table VI-3. Primers used in qRT-PCR analysis.

Primers	Sequence (5' to 3')
qRT-cobT-F1	TCT GAT CCC GTC GCA CTT TT
qRT-copT-R1	CCT CCG GCA GGA CAA TAT TAC T
qRT-cbiA-F1	CCC ACT ATC AGC TCC TCA AA
qRT-cbiA-R1	CAC ATC CAC TGT TTG TTC CA
qRT-pocR-F1	TTT CAC GCC GTT TTG TCA GTT
qRT-pocR-R1	GAA CCT GCC CGC ATA AAA CA
qRT-pduF-F1	GCG GTA GCG TCG AAA GTT TG
qRT-pduF-R1	AAC GGC AAC CAG TAT CCC AAT
qRT-pduA-F1	GGA ATG GTA GAA ACC AAA GGC TTA
qRT-pduA-R1	GCC AAT CTT TTC ATA GCC CAC TA
qRT-pduC-F1	GTT CGC CCA GGA AAT CAT CA
qRT-pduC-R1	ATA ATG GCG GAG GTG TGC AA
qRT-pduP-F1	AAC CCG ACG GAA ACC ATC AT
qRT-pduP-R1	ATC TGC TGG GTC GCT TCG AA
qRT-pduW-F1	GGC TGA TTG AGC GTA TCG GTA T
qRT-pduW-R1	CGT TCG ATT TGC GCT AAC G
qRT-ptsN-F1	AGC GGC GTT CAT TGT CAG A
qRT-ptsN-R1	GGA GGT AAA CTG AGC TGT TTT GC

Table VI-3. Primers used in qRT-PCR analysis.

Primers	Sequence (5' to 3')
qRT-hilD-F1	CAA CGA CTT GGC GCT CTC TAT
qRT-hilD-R1	ACA GGA GAA CGC CGT TTT CA
qRT-hilA-F1	CTG CCG GTG ACC ATT ACG A
qRT-hilA-R1	GCG GGT TGG TGT TCT ATC AAC T
qRT-invF-F1	GGG TTT TGC TGA GTC CTG AGT T
qRT-invF-R1	TTC TCC CAG CAT TCT CAT CGT
qRT-spaS-F1	CCG CTA AAA AAG GCC AGT CA
qRT-spaS-R1	AAA TGA GCC ATA CGA CAC CAG AT
qRT-sopE2-F1	CCA CCC AGC ACT ACA GAA TCC
qRT-sopE2-R1	GAT GCA GGC TAA AAC GAT CTG A
qRT-sipA-F1	CCA ACG CTT CAT CCG AAA GT
qRT-sipA-R1	AAG CGG CTT CAC ATT CAC AAT
qRT-siiA-F1	ATG GCA GGC TGA GAA GCT TTT
qRT-siiA-R1	CCC GTT CAT ATC CCA GTC GTA
qRT-siiE-F1	TGG TTG CCA GCG TTG ATG T
qRT-siiE-R1	GCT CAA TCG TCG GCT TTT CT
qRT-gyrB-F1	ATA ACG CCA CGC AGA AAA TGA
qRT-gyrB-R1	TGG CTG ATA CAC CAG CTC TTT G

IV-3. Results

EIIA^{Ntr} positively regulates the expression of genes involved in Ado-B$_{12}$ synthesis and 1,2-PDL utilization. According to the previous results, the transcriptome profiling revealed that genes constituting the vitamin B_{12} synthesis and 1,2-PDL utilization (*pdu*) operons were predominantly decreased in the Δ*ptsN* mutant strain, indicating a positive role of EIIA^{Ntr} in utilizing 1,2-PDL as a carbon and energy sources. In order to confirm the EIIA^{Ntr} effect on 1,2-PDL utilization gene expression, first I constructed P*pduA-lacZ* fusion strain to measure the expression level of *pdu* operon by β-Galactosidase assay in the presence or absence of 1,2-PDL. As a result of β-Galactosidase assay, *pduA* expression level was not induced in the absence of 1,2-PDL in wild-type. The expression level of *pduA*, however, was significantly decreased in Δ*ptsN* mutant strain compared with wild-type in the LB medium supplemented with 1,2-PDL (Fig. IV-2). The levels of mRNAs relevant to vitamin B_{12} synthesis (*cobT* and *cbiA*), and 1,2-PDL utilization (*pocR*, *pduF, pduA, pduC, pduP* and *pduW*) were measured using qRT-PCR to verify the RNA-Seq results. When *Salmonella* strains

were supplemented with Ado-B_{12} and 1,2-PDL, genes of *cob-cbi*, and *pdu* operons were less transcribed in the Δ*ptsN* mutant strain than in wild-type in accordance with the transcriptome analysis, and the decreases were complemented with *trans*-encoded $EIIA^{Ntr}$ by pWJ04 plasmid (Fig.IV-3A).

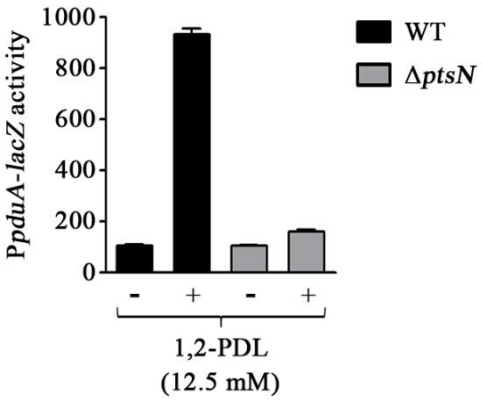

Figure IV-2. The effects of *ptsN* on the expression of *pduA* in the presence of 1,2-PDL. Effects of *ptsN* mutation on the *pduA* gene was measured by β-Galactosidase assay using P*pduA-lacZ* reporter in wild-type and the Δ*ptsN* mutant strain. These strains were cultivated in LB medium in the presence or absence of either 1,2-PDL.

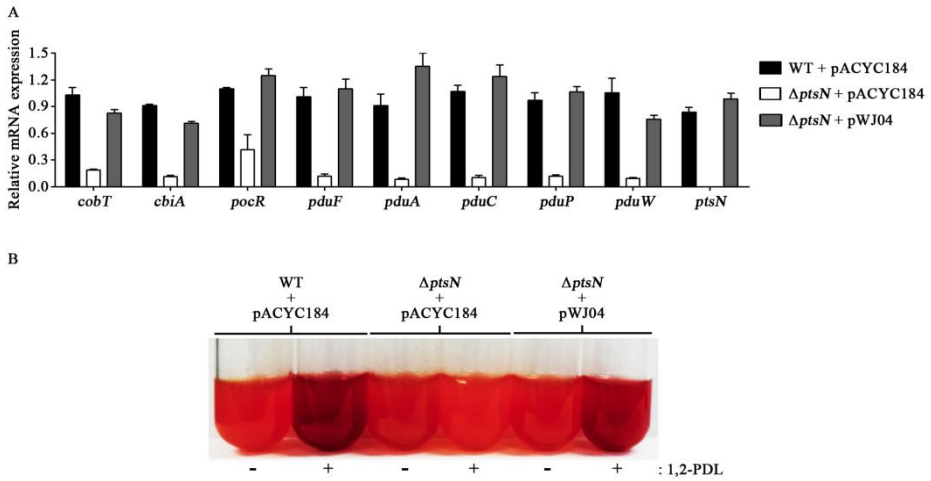

Figure IV-3. The effects of *ptsN* on the expression of genes involved in vitamin B_{12} synthesis and 1,2-PDL utilization. (A) Evaluation of mRNA levels of *cob-cbi* and *pdu* genes in strains of wild-type, Δ*ptsN*, and Δ*ptsN* containing pWJ04 has been normalized to the mRNA level of *ptsN* in wild-type containing pACYC184 which was set at 1.0. The pWJ04 plasmid has *ptsN* and its putative promoter sequences on the backbone of pACYC184. Ado-B_{12} (20 nM) and 1,2-PDL (12.5 mM) were added in the culture to stimulate *prp* operon under aerobic conditions. **(B)** Intracellular pH was assayed to compare the activity of 1,2-PDL catabolism in wild-type SL1344 containing pACYC184 and the Δ*ptsN* mutant strain harboring pWJ04 or pACYC184. Neutral-Red (0.0033%) was added in the culture as a pH indicator and changed its color to dark red in proportion to the levels of propionate, a byproduct of 1,2-PDL

pathway. All cultures were supplemented with Ado-B_{12} (20 nM) and 1,2-PDL (12.5 mM) was added as a substrate for 1,2-PDL pathway. The result shown is a representative of three independent tests.

Dissecting EIIA^{Ntr} roles in transcriptional regulation of *pdu* operon and SPI-1 and -4.

Recently, propionyl-CoA, the intermediate of 1,2-PDL, was found to play a new role as a regulatory signal. Intracellular propionyl-CoA synthesized from 1,2-PDL abundant in the host intestine attenuated the stability of HilD, the master regulator of SPI-1, which led to reduced *Salmonella* invasion into epithelial cells (Hung *et al*, 2013). The expression levels of *cob-cbi* and *pdu* operon were significantly decreased in Δ*ptsN* mutant strain, I guessed that degraded 1,2-PDL into propionate was less than wild-type *Salmonella* did. As expected, I observed Neutral-Red, an acidic pH indicator, in Δ*ptsN* mutant strain turned into light red while wild-type strain turned it dark red in the propionate production assay (Fig. 3B).

Propionyl-CoA is known to reduce *Salmonella* SPI-1 expression by destabilizing HilD (Hung *et al*, 2013), I checked the expression level of SPI-1 and SPI-4 genes between wild-type and Δ*ptsN* mutant strain in the presence or absence of 1,2-PDL by qRT-PCR indicating that *Salmonella* invasion genes (SPI-1 and SPI-4) were about 3-folds higher in Δ*ptsN* mutant strain compared to wild-type (Fig. IV-

4A). SPI-1 expression is tightly controlled by a multitude of regulators including HilD, HilC, RtsA, HilA, and InvF, while HilD rules the regulatory circuit predominantly (Mills *et al*, 1995; Ellermeier & Slauch, 2003). SPI-4, which is activated by HilA, is coupled with SPI-1 in the context of transcriptional regulation and cellular function and stimulates *Salmonella* invasion into host cells in concert with SPI-1 (Main-Hester *et al*, 2008). Therefore, the increased expression of SPI-1 and SPI-4 in the Δ*ptsN* mutant strain was likely attributable to HilD accumulated at low propionyl-CoA levels. In order to examine this possibility, the HilD protein stability was compared between wild-type and the Δ*ptsN* mutant strains in the presence of 1,2-PDL as a precursor for propionyl-CoA. The Δ*ptsN* mutant strain maintained HilD continually for 90 min at least after chloramphenicol addition, whereas wild-type *Salmonella* degraded HilD gradually (Fig IV-4B). Furthermore, the negative role of $EIIA^{Ntr}$ in SPI-1 and SPI-4 expression was reversible by the overexpression of PocR, the cognate activator for *pdu* operon. (Fig. IV-5). These results suggest that $EIIA^{Ntr}$ affects the expression of SPI-1 and SPI-4 indirectly by modulating HilD stability via the 1,2-PDL catabolic pathways.

Accordantly, the capacity to utilize 1,2-PDL as carbon sources influenced *Salmonella* invasiveness into the epithelial cells (Fig. IV-6). The presence of 1,2-PDL attenuated the invasiveness of *Salmonella* wild-type strains probably due to an increase in propionyl-CoA via the 1,2-PDL catabolic pathways, whereas the differential invasion ability in response to 1,2-PDL was abolished in the absence of $EIIA^{Ntr}$. Complementing the Δ*ptsN* mutant strain with pWJ04 producing $EIIA^{Ntr}$ in *trans* restored the ability to control invasiveness depending on 1,2-PDL. Consequently, this result suggests that $EIIA^{Ntr}$ lowers *Salmonella* invasion into host cells when 1,2-pronanediol is abundant in the milieu and processed into propionyl-CoA.

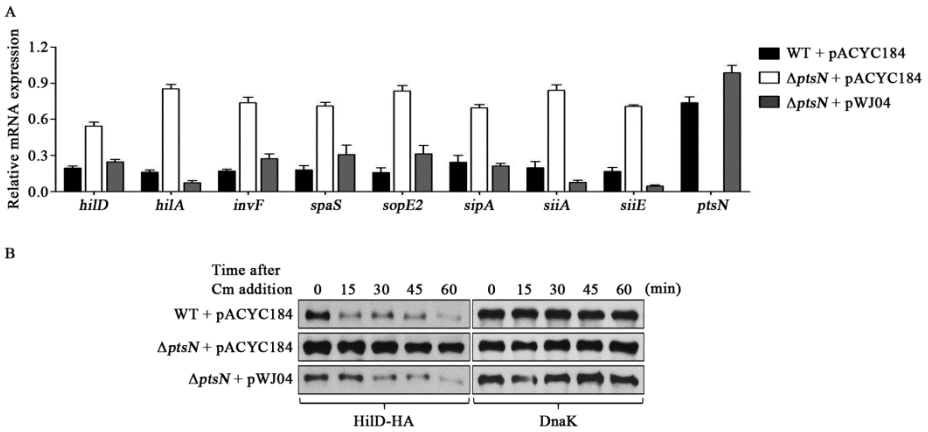

Figure IV-4. The effects of *ptsN* on the expression of genes involved in bacterial invasiveness. (A) The relative mRNA levels of genes involved in SPI-1 and SPI-4 were measured by qRT-PCR. Tested genes include SPI-1 regulator genes (*hilD*, *hilA*, and *invF*), SPI-1 genes (*spaS*, *sopE2*, and *sipA*) and SPI-4 genes (*siiA* and *siiE*) and their expression levels relative to *gyrB* were compared among wild-type strain contacting pACYC184 and Δ*ptsN* mutant strains with either pACYC184 or pWJ04. As alternative carbon sources Ado-B_{12} (20 nM) and 1,2-PDL (12.5 mM) were added in the culture. The relative mRNA levels have been normalized to the mRNA level of *ptsN* in wild-type containing pACYC184 which was set at 1.0. All experiments were performed in triplicate and the averaged values were depicted in graphs. **(B)** The stability of HilD-HA protein was compared under the identical conditions used in **(A)**. Three strains of wild-type with pACYC184, and Δ*ptsN*

mutant strains with either pACYC184 or pWJ04 were cultivated in the presence of 1,2-PDL. *De novo* protein synthesis was quenched by the addition of chloramphenicol (0.2 mg/ml) at 4 h post inoculation. Total proteins were harvested every 15 min, and equivalent amounts were subjected to SDS-PAGE analysis. The stability of HilD-HA was assessed using anti-HA antibody. The levels of DnaK as controls were comparable between lanes.

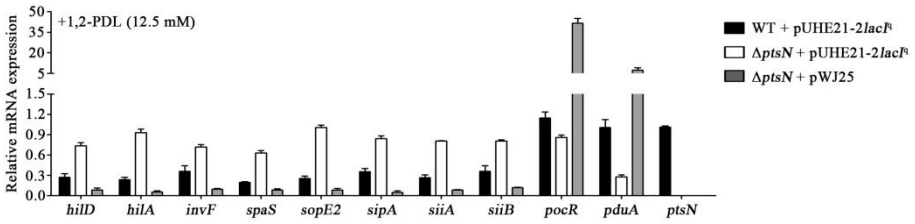

Figure IV-5. The effect of PocR overexpression on SPI-1 and SPI-4 in Δ*ptsN* mutant strain in the presence of 1,2-PDL. The relative mRNA expression of genes involved in SPI-1 and SPI-4 was determined by qRT-PCR in wild-type containing pUHE21-2*lacI*^{q} and Δ*ptsN* mutant strains harboring either pUHE21-2*lacI*^{q} or pWJ25. *pocR* encoding the transcriptional activator of *pdu* operon was induced by the addition of 1 mM IPTG from pWJ25. Strains were grown in LB medium containing 1,2-PDL (12.5 mM) as an additional carbon source. All experiments were conducted in triplicate and the gene expression relative to *gyrB* expression was shown in a base-2 logarithm scale.

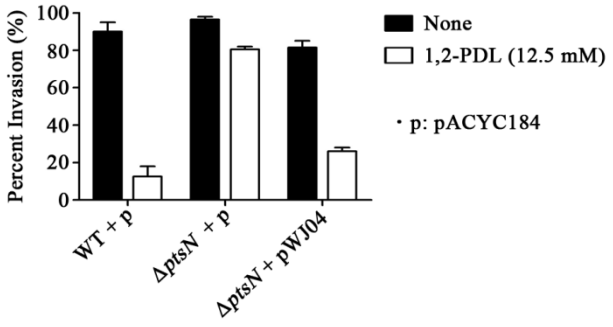

Figure IV-6. Invasion of epithelial cells by *Salmonella* in the presence of 1,2-PDL. Three *S.* Typhimurium strains including wild-type, the Δ*ptsN* mutant, and the Δ*ptsN* mutant containing pWJ04 were pre-cultured with Ado-B_{12} (20 nM) and 1,2-PDL (12.5 mM) or not prior to infection and added into monolayers of Caco-2 cells at MOI of 10. At 1.5 h post infection, cells were lysed and intracellular bacteria were enumerated by plating. Values represent the relative amount of internalized bacteria and have been normalized to the level of internalization of wild-type containing the empty vector, which was set at 100%. Invasion testes were carried out at least three times independently and the averaged values were demonstrated with standard deviations.

Translational levels of $EIIA^{Ntr}$ is up-regulated in response to 1,2-PDL.

The *ptsN* is a component of the *rpoN* operon, which is co-transcribed with *rpoN* from a single promoter upstream of *rpoN*. Since *rpoN*-encoded sigma 54 (σ^{54}) controls the transcription of a plethora of genes involved in nitrogen assimilation and stress responses, PTS^{Ntr} has been considered as a regulatory system associated with nitrogen metabolism (Peterkofsky *et al*, 2006; Pflüger-Grau & Görke, 2010). However, it still remains unclear which stimuli trigger the activation of PTS^{Ntr}. Intracellular balance between nitrogen and carbon was found to modulate the phosphorylation status of $EIIA^{Ntr}$, the output regulator of PTS^{Ntr} (Doucette *et al*., 2011). Besides, the availability of amino sugar was recently revealed to control the degradation rate of $EIIA^{Ntr}$ (Yoo *et al*, 2016). The fact that the positive role of $EIIA^{Ntr}$ in *pdu* expression was remarkable only in the presence of 1,2-PDL prompted us to test whether the expression or activity of $EIIA^{Ntr}$ could be enhanced in response to 1,2-PDL. The expression level of *ptsN* was measured in two different manners: β-Gal assay using *lacZ* fusion to the promoter of *ptsN* and *ptsN* mRNA quantification using qRT-PCR. The expression of *ptsN* was not

affected by 1,2-PDL (**Fig. IV-7A**). However, the protein level of $EIIA^{Ntr}$ was significantly higher in the presence of 1,2-PDL (**Fig. IV-7B**). In order to rule out the possibility that the different $EIIA^{Ntr}$ levels were caused by accelerated degradation of $EIIA^{Ntr}$ in the absence of 1,2-PDL, the stability of $EIIA^{Ntr}$ was compared after quenching protein synthesis using chloramphenicol. Degradation rates of $EIIA^{Ntr}$ were not influenced by the presence of 1,2-PDL, showing comparable protein levels for 90 min (**Fig. IV-7B**). These results suggest that *ptsN* mRNA might be translated into $EIIA^{Ntr}$ with different efficiency in response to the abundance of 1,2-PDL.

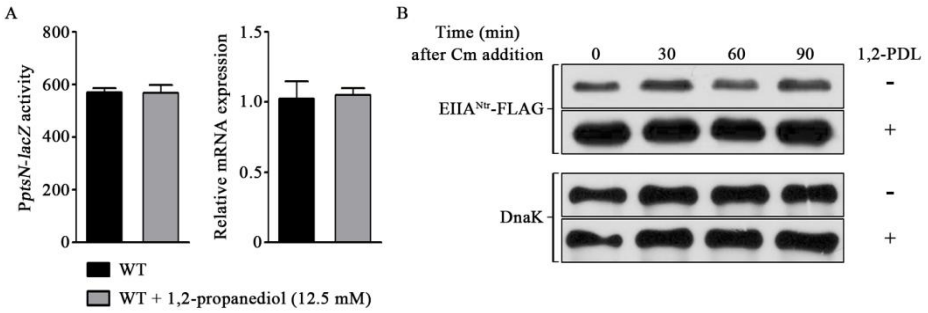

Figure IV-7. EIIA^{Ntr} production was increased in response to 1,2-PDL. (A) The transcriptional expression of *ptsN* was measured with or without 1,2-PDL. β-Galactosidase activity from P*ptsN*::*lacZ* was measured in Miller unit (left) and the relative *ptsN* mRNA expression was determined using qRT-PCR (right). Each bar represents the average value of three independent experiments. **(B)** The stability of EIIA^{Ntr}-FLAG was evaluated by western blot analysis with or without 1,2-PDL (12.5 mM). At 5 h post inoculation, mRNA translation was halted by chloramphenicol (0.2 mg/ml) addition, which was set at time 0 min. Total proteins were harvested every 30 min, and equivalent amounts were subjected to SDS-PAGE analysis. The stability of EIIA^{Ntr}-FLAG was assessed using anti-FLAG antibody. The levels of DnaK were used as controls.

EIIA^{Ntr} positively regulates the expression of genes involved in 1,2-PDL utilization pathway by controlling glutathione (GSH) production.

A pathway for 1,2-PDL degradation by *Salmonella* Typhimurium begins with the conversion of 1,2-PDL to propionaldehyde by Ado-B_{12}-dependent diol dehydratase (Abeles & Lee, 1961). Next, the aldehyde is converted to 1-propanol and propionic acid by propanol dehydrogenase, coenzyme A-dependent propionaldehyde dehydrogenase, phosphotransacylase, and propionate kinase (Leal *et al*, 2003; Liu *et al*, 2007). This process supports growth by providing ATP, an electron sink, and a three-carbon intermediate (propionyl-coenzyme A) that is degraded to pyruvate and succinate via the methylcitrate pathway.

Bacterial microcompartments (MCPs) are primitive organelles that function in carbon fixation (carboxysomes) and various catabolic processes (enterosomes, metabolosomes, and polyhedral organelles), including B_{12}-dependent 1,2-PDL and ethanolamine degradation in *S.* enterica (Bobik, 2006; 2007). MCPs involved in B_{12}-dependent 1,2-PDL degradation include at least 14 different polypeptides

(PduABB'CDEGHJKOPTU), and function to mitigate aldehyde toxicity. It has been reported that glutathione (GSH) is required for maximal transcription of the *cob/pdu* expression in *Salmonella* Typhimurium LT2 (Rondon *et al*, 1995). Glutathione is a tripeptide and an important antioxidant in plant, animals, fungi, and some bacteria. Glutathione is capable of preventing damage of cellular components caused by reactive oxygen species (ROS) or aldehyde (Pompella *et al*, 2003). Therefore I guessed that reduced amount of GHS in Δ*ptsN* mutant strain blocked the induction of the gene expression of *pdu* operon. As a result of β-Galactosidase assay, decreased expression level of *pduA* gene in Δ*ptsN* mutant strain was recovered to the similar to that of wild-type by the addition of GSH (Fig. IV-8A). I also found that this phenomenon was caused by the different amount of GSH produced from *Salmonella* strains wild-type and Δ*ptsN* mutant (Fig. IV-8B).

The exact mechanism of how GSH affects the maximal transcription of *pdu* operon remains unknown, but I suggest that $EIIA^{Ntr}$ regulated GSH production to maintain the balance of carbon and/or nitrogen source in bacterial cytosol, and 1,2-PDL utilization pathway was inhibited under GSH-limited condition to avoid the toxic effect of

propionaldehyde generated from 1,2-PDL utilization pathway.

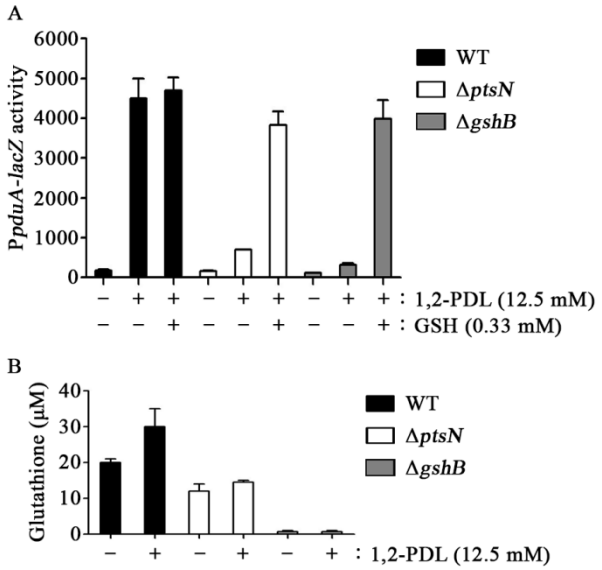

Figure IV-8. EIIA^{Ntr} positively affects the gene expression of 1,2-PDL utilization via glutathione (GSH) synthesis. (A) Effect of glutathione (GSH) on the *pduA* gene expression was measured by β-Galactosidase assay using P*pduA-lacZ* reporter in wild-type, Δ*ptsN* and Δ*gshB* mutant strain. These strains were cultivated in LB medium in the presence or absence of either 1,2-PDL or GSH. **(B)** Glutathione (GSH) was measured in wild-type, Δ*ptsN* and Δ*gshB* mutant strain. These strains were cultivated in LB medium in the presence or absence of 1,2-PDL.

IV-4. Discussion

In this study, I found out that *ptsN*-encoded $EIIA^{Ntr}$, a component of the nitrogen-metabolic PTS, is a key factor controlling vitamin B_{12} synthesis, 1,2-PDL utilization and virulence in *Salmonella* Typhimurium. Transcriptome analysis using RNA-seq revealed that the lack of $EIIA^{Ntr}$ decreased the expression of genes required for vitamin B_{12} synthesis and 1,2-PDL utilization and this observation was validated by qRT-PCR using total RNA extracted from cultures grown in the presence of 1,2-PDL. I also found that decreased expression level of *cob-cbi* and *pdu* operon was caused by the decreased amount of GSH produced in *Salmonella* strains wild-type and Δ*ptsN* mutant suggesting that $EIIA^{Ntr}$ prevents bacteria from propionaldehyde-mediated-cellular damage by producing GSH in response to the cellular carbon and/or nitrogen ratio.

In accordance with the previous report about the negative regulation of *Salmonella* pathogenicity island-1 (SPI-1) by propionyl-CoA (Hung *et al*, 2013), the down-regulation of the 1,2-PDL utilization pathways in the Δ*ptsN* mutant strain alleviated the rapid degradation of

HilD, a dominant SPI-1 activator, and consequently led to an increase in *Salmonella* virulence.

Salmonella Typhimurium causes non-typhoidal gastroenteritis in humans and typhoid-like disease in mice (Tsolis *et al*, 1999; Zhang *et al*, 2003). During the infection of host, *Salmonella* invades intestinal epithelial cells and replicates inside macrophages (Galán *et al*, 1996; Ochman *et al*, 1996). The ability to acquire nutrients during the infection process is crucial for enteric pathogens to survive and proliferate in the host, because they have to compete against commensal microbiota for limited nutrients (Staib & Fuchs, 2014). With regard to bacterial competition for restricted carbon sources, *S.* Typhimurium outcompetes commensal bacteria by the 1,2-PDL utilization pathway. Plant sugars such as L-rhamnose and L-fucose abundant in digested food molecules are degraded into 1,2-PDL by gut microbiota. L-fucose also constitutes the mucosal glycoconjugates as a terminal sugar of the oligosaccharide chains linked to the mucin protein backbone and is easily accessible to enteric bacteria in the intestinal lumen (Sampson & Bobik, 2008; Muraoka & Zhang, 2011). However, only enteropathogenic *Enterobacteriaceae* including *S.* Typhimurium can utilize 1,2-PDL as

carbon sources to generate energy (Rivera-Chàvez & Bäumler, 2015). *S.* Typhimurium harnesses the 1,2-PDL utilization pathways to convert the less-favored carbon sources into pyruvate and eventually to ATP.

When *Salmonella* resides in oxygen-abundant milieu, propionyl-CoA is integrated into the 2-methylcitrate cycle (MCC) coupled with the citric acid cycle and processed to release energy via an electron-transport chain using oxygen as the final electron acceptor. Meanwhile, in anaerobic conditions like the distal gut, *Salmonella* exploits the *cob-cbi* and *pdu* operons in concert with *ttr* operon for anaerobic respiration using tetrathionate as the final electron acceptor instead (Jakobson & Tullman-Ercek, 2016). The *cob-cbi* operon encodes factors required for vitamin B_{12} synthesis only under anaerobic conditions (Roth *et al*, 1996). Ado-B_{12} is then used as a cofactor in the 1,2-PDL pathway, which catabolizes 1,2-PDL to propionyl-CoA in combination with propanol and propionate. Propionyl-CoA is further processed via the MCC and the citric acid cycle as in the case of aerobic condition, whereas the metabolic byproducts such as NADH and its equivalents are oxidized sequentially with the electron acceptor being tetrathionate. Tetrathionate, usually known to be present in humid soils,

has been recently found to be produced naturally during the inflammation response to enteropathogen infection. Hydrogen sulfide (H_2S), produced by colonic bacteria, is detoxified to thiosulfate ($S_2O_3^{2-}$) and further oxidized to tetrathionate ($S_4O_6^{2-}$) by nitric oxide radicals and reactive oxygen species generated in the intestinal lumen (Winter *et al*, 2010). In contrast to coliforms inactivated by tetrathionate, *S.* Typhimurium possesses the *ttr* operon composed of *ttrABCRS*, which enables this gastrointestinal pathovar to exploit tetrathionate as an electron acceptor in respiratory chain. This process gives *S.* Typhimurium a competitive edge over the gut microbiota, which allows *Salmonella* to outgrow commensal bacteria and ultimately to achieve transmission to new recipients (Stecher *et al*, 2007; Lawley *et al*, 2008).

Considering the opposite roles of $EIIA^{Ntr}$ between the *cob-cbi* and *pdu* operons and SPI-1 and SPI-4 regulation, *S.* Typhimurium in the intestinal lumen enriched with 1,2-PDL seems to produce propionyl-CoA inevitably and thus lower the expression of SPI-1 and SPI-4, which are critical for *Salmonella* to invade the epithelial cells. A negative role of $EIIA^{Ntr}$ in *Salmonella* virulence was also reported in the regulation of SPI-2, a *Salmonella* pathogenicity island essential for the proliferation of

Salmonella in macrophages (Hensel, 2000). *ssrA*/*ssrB* encoding the two-component regulatory system of SPI-2 are expressed ectopically within phagosomes in response to intracellular cues. $EIIA^{Ntr}$ directly interacts with SsrB and inhibits SsrB from activating the transcription of SPI-2 genes (Choi *et al*, 2010). The opposite roles of $EIIA^{Ntr}$, which provides a growth benefit for *S.* Typhimurium over the competing microbiota but dampens the virulence activity in the intestinal lumen, may be a sophisticated strategy programmed for bacterial fitness inside host. *S.* Typhimurium is a gastrointestinal pathovar, which causes inflammation in general in human intestine and is hardly disseminated into deeper tissues leading to systemic infection. However, invasive typhoidal *Salmonella* serovars such as *S.* Typhi are prone to disrupt intestinal epithelial barrier and spread over the whole body. Interestingly, the invasive *Salmonella* serovars evolutionally adapted for extraintestinal lifestyles are defective in anaerobic metabolic networks (Nuccio & Bäumler, 2014). Bacterial functions attributable to the *cob*, *pdu*, and *ttr* operons have been sequentially compromised during evolution away from an intestinal lifestyle. *S.* Typhimurium adapted for the intestinal lifestyle may employ $EIIA^{Ntr}$ as a regulatory switch balancing between

bacterial intestinal colonization and internalization into host cells in response to environmental nutrient repertoire.

Finally, I conclude that $EIIA^{Ntr}$ is a key player of physiological and functional linkage between *Salmonella* fitness and virulence during the host infection.

References

Abeles RH, HA Lee (1961) Intramolecular oxidation-reduction requiring a cobamide coenzyme. *J Biol Chem* **236:** 2347–2350

Alekshun MN (2001) Beyond comparison-antibiotics form genome data. *Nat Biotechnol* **19:** 1124-1125

Alekshun S, Boyd EF, Choy C, Cheng P, Florea L, Proctor E, McClelland M (2004) Chracterization of *Salmonella enterica* subspecies I genovars by use of microarray. *J Bacteriol* **186:** 5883-5898

Alpuchearanda CM, Racoosin EL, Swanson JA, Miller SI (1994) *Salmonella* stimulate macrophage macropinocytosis and persist within spacious phagosomes. *J Exp Med* **179:** 601-608

Bader MW, Navarre WW, Shiau W, Nikaido H, Frye JG, McClelland M, Fang FC, Miller SI (2003) Regulation of *Salmonella typhimurium* virulence gene expression by cationic antimicrobial peptides. *Mol Microbiol* **50:** 219-230

Badia J, Ros J, Aguilar J (1985). Fermentation mechanism of fucose and rhamnose in *Salmonella typhimurium* and *Klebsiella pneumoniae*.

J Bacteriol **161:** 435–437

Bajaj V, Hwang C, Lee CA (1995) HilA is a novel OmpR/ToxR family member that activates the expression of *Salmonella* typhimurium invasion genes. *Mol Microbiol* **18:** 715–727

Bailly-Bechet M, Benecke A, Hardt WD, Lanza V, Sturm A, Zecchina R (2011) An externally modulated, noise-driven switch for the regulation of SPI1 in *Salmonella enterica* serovar Typhimurium. *J Math Biol* **63:** 637–662

Biran D, Gur E, Gollan L, Ron EZ (2000) Control of methionine biosynthesis in *Escherichia coli* by proteolysis. *Mol Microbiol* **37:** 1436-1443

Blaser MJ, Newman LS (1982) A review of human salmonellosis: I. Infective dose. *Rev Infect Dis* **4:** 1096-1106.

Bobik TA, Xu Y, Jeter RM, Otto KE, Roth JR (1997) Propanediol utilization genes (*pdu*) of *Salmonella typhimurium*: Three genes for the propanediol dehydratase. *J Bacteriol* **179:** 6633-6639

Boël G, Mijakovic I, Mazè A, Poncet S, Taha MK, Larribe M, Darbon E, Khemiri A, Galinier A, Deutscher J (2003) Transcription regulators protentially controlled by HPr kinase-

phosphorylase in gram-negative bacteria. *J Mol Microbiol Biotechnol* **5:** 206-215

Boronat A, Aguilar J (1981) Metabolism of L-fucose and L-rhamnose in *Escherichia coli:* Differences in induction of Propanediol Oxidoreductase. *J Bacteriol* **147:** 181-185

Brenner FW, Villar RG, Angulo FJ, Tauxe R, Swaminathan B (2000) *Salmonella* nomenclature. *J. Clin. Microbiol* **38:** 2465-2467

Brumell JH, Goosney DL, Finlay BB (2002) SifA, a type III secreted effector of *Salmonella typhimurium*, directs *Salmonella*-induced filament (Sif) formation along microtubules. *Traffic* **3:** 407-415

Brumell JH, Grinstein S (2004) *Salmonella* redirecrts phagosomal maturation. *Curr Opin Microbiol* **7:** 78-84

Brumell JH, Tang P, Mills SD, Finlay BB (2001) Characterization of *Salmonella*-induced filament (Sifs) reveals a delayed interaction between *Salmonella*-containing vacuoles and late endocytic compartments. *Traffic* **2:** 642-653

Buchwald DS, Blaser MJ (1984) A review of human salmonellosis: II. Duration of excretion following infection with nontyphi Salmonella. *Rev Infect Dis* **6:** 345-356

Bumann D (2009) System-level analysis of *Salmonella* metabolism during infection. *Curr Opin Microbiol* **12:** 559-567

Cases I, Lopez JA, Albar JP, Lorenzo VD (2001) Evidence of multiple regulatory functions for the PtsN (IIA^{Ntr}) protein of *Pseudomonas putida*. *J Bacteriol* **183**: 1032-1037

Chalker RB, Blaser MJ (1988) A review of human salmonellosis: III. Magnitude of *Salmonella* infection in the United States. *Rev Infect Dis* **10:** 111-124

Chan RK, Botstein D, Watanabe T, Ogata Y (1972) Specialized transduction of tetracycline resistance by phage P22 in *Salmonella typhimurium*. *Virol* **50:** 883-898

Chang ACY, Cohen SN (1978) Construction and characterization of amplifiable multicopy DNA cloning vehicles derived from the P15A cryptic miniplasmid. *J Bacteriol* **134:** 1141-1156

Chavarría M, Kleijn RJ, Sauer U, Pflüger-Grau K, Lorenzo V (2012) Regulatory tasks of the phosphoenolpyruvate-phosphotransferase system of *Pseudomonas putida* in central carbon matabolism. *mBio* **3:** 00028-12

Chen P, Andersson DI, Roth JR (1994) The control region of the

pdu/cob regulon in *Salmonella typhimurium*. *J Bacteriol* **176:** 5474-5482

Choi J, Shin D, Yoon H, Kim J, Lee CR, Kim M, Seok YJ, Ryu S (2010) *Salmonella* pathogenicity island 2 expression negatively controlled by $EIIA^{Ntr}$-SsrB interaction is required for *Salmonella* virulence. *Proc Natl Acad Sci USA* **107:** 20506-20511

Cocks GT, Aguilar T, Lin EC (1974). Evolution of L-1,2-propanediol catabolism in *Escherichia coli* by recruitment of enzymes for L-fucose and L-lactate metabolism. *J Bacteriol* **118:** 83–88

Collins JA, Irnov I, Baker S, Winkler WC (2007) Mechanism of mRNA destabilization by the *glmS* ribozyme. *Genes Dev* **21:** 3356-3368

Comas I, González-Candelas F, Zúñiga M (2008) Unraveling the evolutionary history of the phosphoryl-transfer chain of the phosphoenolpyruvate:phosphotransferase system through phylogenetic analyses and genome context. *BMC Evol Biol* **8:** 147

C**rouch ML, Becker AL, Bang IS, Tanabe H, Ouellette AJ, Fang FC** (2005) The alternative sigma factor σ^E is required for resistance of *Salmonella enterica* serovar Typhimurium to anti-microbial peptides.

Mol Microbiol **56:** 789-799

Daniel R, Bobik TA, Gottschalk G (1998) Biochemistry of coenzyme B_{12}-dependent glycerol and diol dehydratases and organization of the encoding genes. *FEMS Microbiol Rev* **22:** 553–566

Datsenko KA, Wanner BL (2000) One-step inactivation of chromosomal genes in *Escherichia coli* K-12 using PCR products. *Proc Natl Acad Sci USA* **97:** 6640-6645

Deatherage Kaiser BL, Li J, Sanford J A, Kim YM, Kronewitter SR, Jones MB (2013). A multi-omic view of host-pathogen-commensal interplay in -mediated intestinal infection. *PLoS ONE* **8:**e67155

Deutscher J, Akè FMD, Derkaoui M, Zèbrè AC, Cao TN, Bouraoui H, Kentache T, Mokhtari A, Milohanic E, Joyet P (2014) The bacterial phosphoenolpyruvate:carbohydrate phosphotransferase system: regulation by protein phosphorylation and phosphorylation-dependent protein-protein interactions. *Microbiol Mol Biol Rev* **78:** 231-256

Deutscher J, Francke C, Postma PW (2006) How phosphotransferase system-related protein phosphorylation regulates carbohydrate metabolism in bacteria. *Microbiol Mol Biol Rev* **70:** 939-1031

Dozot M, Poncet S, Nicolas C, Copin R, Bouraoui H, Mazè A, Deutscher J, Bolle XD, Letesson J (2010) Functional characterization of the incomplete phosphotransferase system (PTS) of the intracellular pathogen *Brucella melitensis*. *PLoS One* **5:** e12679

Doucette CD, Schwab DJ, Wingreen NS, Rabinowitz JD (2011) alpha-ketoglutarate coordinates carbon and nitrogen utilization via enzyme I inhibition. *Nat Chem Biol* **7:** 894-901

Drecktrah DL, Knodler LA, Ireland R, Steele-Mortimer O (2006) The mechanism of *Salmonella* entry determines the vacuolar environment and intracellular gene expression. *Traffic* **7:** 39-51

Durand P, Golinelli-Pimpaneau B, Mouilleron S, Badet B, Badet-Denisot MA (2008) Highlights of glucosamine-6P synthase catalysis. *Arch Biochem Biophys* **474:** 302-317

Durant JA, Lowry VK, Nisbet DJ, Stanker LH, Corrier DE, Ricke SC (1999) Short-chain fatty acids affect cell-association and invasion of HEp-2 cells by *Salmonella* Typhimurium. *J Environ Science & Health Part B* **34:** 1083-1099

Eichelberg K, Galán JE (1999) Differential regulation of *Salmonella typhimurium* type III secreted proteins by pathogenicity island 1 (SPI-

1)-encoded transcriptional activators InvF and HilA. *Infect Immun* **67:** 4099–4105

Ellermeier CD, Janakiraman A, Slauch JM (2002) Construction of targeted single copy *lac* fusions using λ RED and FLP-mediated site-specific recombination in bacteria. *Gene* **290:** 153-161

Ellermeier CD, Slauch JM (2003) RtsA and RtsB coordinately regulate expression of the invasion and flagellar genes in *Salmonella enterica* serovar Typhimurium. *J Bacteriol* **185:** 5096–5108

Escalante A, Cervantes AS, Gosset G, Bolivar F (2012) Current knowledge of the *Escherichia coli* phosphoenolpyruvate-carbohydrate phosphotransferase system: peculiarities of regulation and impact on growth and product formation. *Appl Microbiol Biotechnol* **94:** 1483-1494

Ezaki T, Kawamura Y, Yabuuchi E (2000) Recognition of nomenclatural standing of *Salmonella typhi* (Approved Lists 1980), *Salmonella enteritidis* (Approved Lists 1980) and *Salmonella typhimurium* (Approved Lists 1980), and conservation of the specific epithets *enteritidis* and *typhimurium*. Request for an opinion. *Int. J. Syst. Evol. Microbiol* **2:** 945-947

Fábrega A, Vila J (2013) *Salmonella enterica* serovar Typhimurium skills to succeed in the host: virulence and regulation. *Clin Microbiol Rev* **26:** 308-341

Feucht BU, Saier, Jr. MH (1980) Fine control of adenylate cyclase by the phosphoenolpyruvate:sugar phosphotransferase systems in *Escherichia coli* and *Salmonella typhimurium*. *J Bacteriol* **141:** 603-610

Figueira R, Holden DW (2012) Functions of the *Salmonella* pathogenicity island 2 (SPI-2) type III secretion system effectors. *Microbiol* **158:** 1147-1161

Fisher MA, Grimm D, Henion AK, Elias AF, Stewart PE, Rosa PA, Gherardini FC (2005) *Borrelia burgdorferi* σ^{54} is required for mammalian infection and vector transmission but not for tick colonization. *Proc Natl Acad Sci USA* **102:** 5162-5167

Flannagan RS, Cosio G, Grinstein S (2009) Antimicrobial mechanisms of phagocytes and bacterial evasion strategies. *Nat Rev Microbiol* **7:** 355-366

Francis CL, Starnbach MN, Falkow S (1992) Morphological and cytoskeletal changes in epithelial-cells occur immediately upon

interaction with *Salmonella*-Typhimurium grown under low-oxygen conditions. *Mol Microboil* **6:** 3077-3087

Francke C, Kormelink TG, Hagemeijer Y, Overmars L, Sluijter V, Moezelaar R, Siezen R (2011) Comparative analyses imply that the enigmatic sigma factor 54 is a central controller of the bacterial exterior. *BMC Genomics* **12:** 385

Galán JE (1996) Molecular genetics bases of *Salmonella* entry into host cells. *Mol Microbiol* **20:** 263-271

Galán JE (2001) *Salmonella* interactions with host cells: type III secretion at work. *Annu Rev Cell Dev Biol* **17:** 53-86

G**arcia-del P, Foster JW, Finlay BB** (1993) Role of acid tolerance response genes in Salmonella typhimurium virulence. *Infect Immun* **61:** 4489-4492

Garmendia J, Beuzon CR, Ruiz-Albert J, Holden DW (2003) The roles of SsrA-SsrB and OmpR-EnvZ in the regulation of genes encoding the *Salmonella typhimurium* SPI-2 type III secretion system. *Microbiol* **149:** 2385-2396

Gaston LW, Stadtman ER (1963) Fermentation of ethylene glycol by *Clostridium glycolicum*, sp. n. *J Bacteriol* **85:** 356–362

Gerlach RG, Cláudio N, Rohde M, Jäckel D, Wagner C, Hensel M (2008) Cooperation of *Salmonella* pathogenicity islands 1 and 4 is required to breach epithelial barriers. *Cell Microbiol* **10:** 2364-2376

Golubeva YA, Sadik AY, Ellermeier JR, Slauch JM (2012) Integrating global regulatory input into the *Salmonella* pathogenicity island 1 type III secretion system. *Genetics* **190:** 79-90

Göpel Y, Khan MA, Görke B (2014) Post-transcriptional control of the key enzyme for cell envelope synthesis by a base-pairing small RNA, an RNase adaptor protein, and a small RNA mimic. *RNA Biol* **11:** 433-442

Göpel Y, Papenfort K, Reichenbach B, Vogel J, Görke B (2013) Targeted decay of a regulatory small RNA by an adaptor protein for RNase E and counteraction by an anti-adaptor RNA. *Genes Dev* **27:** 552-564

Görke B, Stülke J (2008) Carbon catabolite repression in bacteria: many ways to make the most out of nutrients. *Nat Rev Microbiol* **6:** 613-624

Görke B, Vogel J (2008) Noncoding RNA control of the making and breaking of sugars. *Genes Dev* **22:** 2914-2925

Groisman EA, Ochman H (1997) How *Salmonella* became a pathogen.

Trends Microbiol **5:** 343-349

Gutnick, Calvo JM, Klopotowski T, Ames BN (1969) Compounds which serve as the sole source of carbon or nitrogen for *Salmonella typhimurium* LT-2. *J Bacteriol* **100:** 215-219

Hammelman TA, O'Toole GA, Trzebiatowski JR, Tsang AW, Rank D, Escalante-Semerena JC (1996) Identification of a new *prp* locus required for propionate catabolism in *Salmonella typhimurium* LT2. *FEMS Microbiology Letter* **137:** 233-239

Hansen-Wester I, Hensel M (2001) *Salmonella* pathogenicity islands encoding type III secretion systems. *Microbes Infect* **3:** 549-559

Haraga A, Ohlson MB, Miller SI (2008) Salmonellae interplay with host cells. *Nat Rev Microbiol* **6:** 53-66

Harwood JP, Gazdar C, Prasad C, Peterkofsky A (1976) Involvement of the glucose enzymes II of the sugar phosphotransferase system in the regulation of adenylate cyclase by glucose in *Escherichia coli*. *J Biol Chem* **251:** 2462-2468

Havemann GD, Sampson EM, Bobik TA (2002) PduA is a shell protein of polyhedral organelles involved in coenzyme B_{12}-dependent degradation of 1, 2-propanediol in *Salmonella enterica* serovar

Typhimurium LT2. *J Bacteriol* **184:** 1253-1261

Hensel M (2000) *Salmonella* Pathogenicity Island 2. *Mol Microbiol* **36:** 1015-1023

Higa F, Edelstein PH (2001) Potential virulence role of the *Legionella pneumophila ptsP* ortholog. *Infect Immun* **69:** 4782-4789

Horswill AR, Escalante-Semerena JC (1997) Propionate catabolism in *Salmonella* Typhimurium LT2: two divergently transcribed units comprise the *prp* locus at 8.5 centisomes, *prpR* encodes a member of the sigma-54 family of activators, and the *prpBCDE* genes constitute an operon. *J Bacteriol* **179:** 928-940

Humphreys S, Stevenson A, Bacon A, Weinhardt AB, Roberts M (1999) The alternative sigma factor, σ^E, is critically important for the virulence of *Salmonella typhimurium*. *Infect Immun* **67:** 1560-1568

Hung CC, Garner CD, Slauch JM, Dwyer ZW, Lawhon SD, Frye JG, McClelland M, Ahmer BMM, Altier C (2013) The intestinal fatty acid propionate inhibits *Salmonella* invasion through the post-translational control of HilD. *Mol Microbiol* **87:** 1045-1060

Ibarra JA, Steele-Mortimer O (2009) *Salmonella*–the ultimate insider. *Salmonella* virulence factors that modulate intracellular

survival. *Cellular Microbiol* **11:** 1579-1586

Jahn S, Rijsewijk BH, Sauer U, Bettenbrock Katja (2013) A role for $EIIA^{Ntr}$ in controlling fluxes in the central metabolism of *E. coli* K12. *Biochimica et Biophysica Acta* **1833:** 2879-2889

Jakobsonm CM, Tullman-Ercek D (2016) Dumpster diving in the gut: Bacterial microcompartments as part of a host-associated lifestyle. *PLoS Pathog* **12:** e1005558

Jeong JY, Kim YJ, Cho N, Shin D, Nam TW, Ryu S, Seok YJ (2004) Expression of *ptsG* encoding the major glucose transporter is regulated by ArcA in *Escherichia coli*. *J Biol Chem* **279:** 38513-38518

Jeter RM (1990). Cobalamin-dependent 1,2-propanediol utilization by *Salmonella typhimurium*. *J Gen Microbiol* **136:** 887–896

Jones BD, Ghori N, Falkow S (1994) *Salmonella* Typhimurium initiates murine infection by penetrating and destroying the specialized epithelial M-cells of the Peyers-patches. *J Exp Med* **180:** 15-23

Kalamorz F, Reichenbach B, März W, Rak B, Görke B (2007) Feedback control of glucosamine-6-phosphate synthase GlmS

expression depends on the small RNA GlmZ and involves the novel protein YhbJ in *Escherichia coli*. *Mol Microbiol* **65:** 1518-1533

Karimova G, Pidoux J, Ullmann A, Ladant D (1998) A bacterial two-hybrid system based on a reconstituted signal transduction pathway. *Proc Natl Acad Sci USA* **95:** 5752-5756

Karimova G, Ullmann A, Ladant D (2000) A bacterial two-hybrid system that exploits a cAMP signaling cascade in *Escherichia coli*. *Methods Enzymol* **328:** 59-73

Karimova G, Ullmann A, Ladant D (2001) Protein-protein interaction between *Bacillus stearothermophilus* tyrosyl-tRNA synthetase subdomains revealed by a bacterial two-hybrid system. *J Mol Microbiol Biotechnol* **3:** 73-82

Karstens K, Zschiedrich CP, Bowien O, Stülke J, Görke B (2014) Phosphotransferase protein $EIIA^{Ntr}$ interacts with SpoT, a key enzyme of the stringent response in *Ralstonia eutropha* H16. *Microbiol* **160:** 711-722

Kawada-Matsuo M, Mazda Y, Oogai Y, Kajiya M, Kawai T, Yamada S, Miyawaki S, Oho T, Komatsuzawa H (2012) GlmS and NagB regulate amino sugar metabolism in opposing directions and

affect *Streptococcus mutans* virulence. *PLoS One* **7:** e33382

Keeney KM, Finlay B B (2013). Microbiology: EHEC downregulates virulence in response to intestinal fucose. *Curr Biol* **23:** R108–R110

Kim HJ, Lee CR, Kim M, Peterkofsky A, Seok YJ (2011) Dephosphorylated NPr of the nitrogen PTS regulates lipid A biosynthesis by direct interaction with LpxD. *Biochem Biophys Res Commun* **409:** 556-561

Kim K, Jeong JH, Lim D, Hong Y, Yun M, Min JJ, Kwak SJ, Choy HE (2013) A novel balanced-lethal host-vector system based on *glmS*. *PLoS One* **8:** e60511

Kingsley RA, Humphries AD, Weening EH, De Zoete MR, Winter S, Papaconstantinopoulou A, Dougan G, Baumler AJ (2003) Molerular and phenotypic analysis of the CS54 island of *Salmonella enterica* serotype *typhimurium*: identification of intestinal colonization and persistence determinants. *Infect Immun* **71:** 629-640

Klumpp J, Fuchs TM (2007) Identification of novel genes in genomic islands that contribute to *Salmonella typhimurium* replication in macrophages. *Microbiol* **153:** 1207-1220

Kuhle V, Hensel M (2004) Cellular microbiology of intracellular

Salmonella enterica: functions of the type III secretion system encoded by *Salmonella* pathogenicity island 2. *Cell Mol Life Sci* **61:** 2812-2826

Kukanich KS (2011) Update on *Salmonella* spp. contamination of pet food, treats, and nutritional products and safe feeding recommendations. *J Am Vet Med Assoc* **239:** 1430-1434

Lawhon SD, Maurer R, Suyemoto M, Altier C (2002) Intestinal short-chain fatty acids alter *Salmonella* Typhimurium invasion gene expression and virulence through BarA/SirA. *Mol Microbiol* **46:** 1451-1464

Lawley TD, Bouley DM, Hoy YE, Gerke C, Relman DA, Monack DM (2008) Host transmission of *Salmonella enterica* serovar Typhimurium is controlled by virulence factors and indigenous intestinal microbiota. *Infect Immun* **76:** 403-416

Leal NA, GD Havemann, TA Bobik (2003) PduP is a coenzyme A-acylating propionaldehyde dehydrogenase associated with the polyhedral bodies involved in B_{12}-dependent 1,2-propanediol degradation by *Salmonella enterica* serovar Typhimurium LT2. *Arch Microbiol* **180:** 353–361

Lee AK, Detweiler CS, Falkow S (2000) OmpR regulates the two-component system SsrA-SsrB in *Salmonella* pathogenicity island 2. *J Bacteriol* **182:** 771-781

Lee CR, Cho SH, Yoon MJ, Peterkofsky A, Seok YJ (2007) *Escherichia coli* enzyme IIA^{Ntr} regulates the K^+ transporter TrkA. *Proc Natl Acad Sci USA* **104:** 4124-4129

Lee CR, Cho SH, Kim HJ, Kim M, Peterkofsky A, Seok YJ (2010) Potassium mediates *Escherichia coli* enzyme IIA^{Ntr}-dependent regulation of sigma factor selectivity. *Mol Microbiol* **78:** 1468-1483

Lee CR, Koo BM, Cho SH, Kim YJ, Yoon MJ, Peterkofsky A, Seok YJ (2005) Requirement of the dephospho-form of enzyme IIA^{Ntr} for derepression of *Escherichia coli* K-12 *ilvBN* expression. *Mol Microbiol* **58:** 334-344

Lee CR, Park YH, Kim YR, Peterkofsky A, Seok YJ (2013a) Phosphorylation-dependent mobility shift of proteins on SDS-PAGE is due to decreased binding of SDS. *Bull Korean Chem Soc* **34:** 2063-2066

Lee CR, Park YH, Kim M, Kim YR, Park S, Peterkofsky A, Seok YJ (2013b) Reciprocal regulation of the autophosphorylation of

enzyme I^{Ntr} by glutamine and alpha-ketoglutarate in *Escherichia coli*. *Mol Microbiol* **88:** 473-485

Lengeler JW, Jahreis K (2009) Bacterial PEP-dependent carbohydrate: phosphotransferase systems couple sensing and global control mechanisms. *Contrib Microbiol* **16:** 65-87

Li Y, Lopez P, Durand P, Ouazzani J, Badet B, Badet-Denisot MA (2007) An enzyme-coupled assay for amidotransferase activity of glucosamine-6-phosphate synthase. *Anal Biochem* **370:** 142-146

Little R, Dixon R (2003) The amino-terminal GAF domain of *Azotobacter vinelandii* NifA binds 2-oxoglutarate to resist inhibition by NifL under nitrogen-limiting conditions *J Biol Chem* **278:** 28711-28718

Liu Y, NA Leal, EM Sampson, CL Johnson, GD Havemann, TA Bobik (2007) PduL is an evolutionarily distinct phosphotransacylase involved in B_{12}-dependent 1,2-propanediol degradation by *Salmonella enterica* serovar Typhimurium LT2. *J Bacteriol* **189:** 1589–1596

Lostroh CP, Lee CA (2001) The HilA box and sequences outside it determine the magnitude of HilA-dependent activation of P(*prgH*) from *Salmonella* pathogenicity island 1. *J Bacteriol* **183:** 4876–4885

Lucas RL, Lee CA (2000) Unravelling the mysteries of virulence gene regulation in *Salmonella typhimurium*. *Mol Microbiol* **36:** 1024-1033

Lüttmann D, Göpel Y, Görke B (2012) The phosphotransferase protein $EIIA^{Ntr}$ modulates the phosphate starvation response through interaction with histidine kinase PhoR in *Escherichia coli*. *Mol Microbiol* **86:** 96-110

Lüttmann D, Heermann R, Zimmer B, Hillmann A, Rampp IS, Jung K, Görke B (2009) Stimulation of the potassium sensor KdpD kinase activity by interaction with the phosphotransferase protein IIA^{Ntr} in *Escherichia coli*. *Mol Microbiol* **72:** 978-994

Macfarlane G, Gibson G, Cummings J (1992). Comparison of fermentation reactions in different regions of the human colon. *Journal of Applied Bacteriology* **72:** 57-64

Magasanik B (1993) The regulation of nitrogen utilization in enteric bacteria. *J Cell Biochem* **51:** 34-40

Main-Hester KL, Colpitts KM, Thomas GA, Fang FC, Libby SJ (2008) Coordinate regulation of *Salmonella* pathogenicity island 1 (SPI1) and SPI4 in *Salmonella enterica* serovar Typhimurium. *Infect Immun* **76:** 1024-1035

Maurizi MR (1992) Proteases and protein degradation in *Escherichia coli*. *Experientia* **48:** 178-201

Mengin-Lecreulx D, Van Heijenoort J (1993) Identification of the *glmU* gene encoding *N*-acetylglucosamine-1-phosphate uridyltransferase in *Escherichia coli*. *J Bacteriol* **175:** 6150-6157

Mengin-Lecreulx D, Van Heijenoort J (1994) Copurification of glucosamine-1-phosphate acetyltransferase and *N*-acetylglucosamine-1-phosphate uridyltransferase activities of *Escherichia coli*: Characterization of the *glmU* gene product as a bifunctional enzyme catalyzing two subsequent steps in the pathway for UDP-*N*-acetylglucosamine synthesis. *J Bacteriol* **176:** 5788-5795

Mengin-Lecreulx D, Van Heijenoort J (1996) Characterization of the essential gene *glmM* encoding phosphoglucosamine mutase in *Escherichia coli*. *J Biol Chem* **271:** 32-39

Merighi M, Ellermeier CD, Slauch JM, Gunn JS (2005) Resolvase-in vivo expression technology analysis of the *Salmonella enterica* serovar Typhimurium PhoP and PmrA regulons in BALB/c mice. *J Bacteriol* **187:** 7407-7416

Merrick MJ, Coppard JR (1989) Mutations in genes downstream of the

rpoN gene (encoding σ^{54}) of *Klebsiella pneumoniae* affect expression from σ^{54}-dependent promoters. *Mol Microbiol* **3:** 1765-1775

Merrick MJ, Taylor M, Saier MH, Jr., Reizer J (1995) The role of genes downstream of the σ^{N} structural gene *rpoN* in *Klebsiella pneumoniae*. *Nitrogen Fixation: Fundamentals and Applications* **27:** 189-194

Miao EA, Freeman JA, Miller SI (2002) Transcription of the SsrAB regulon is repressed by alkaline pH and is independent of PhoPQ and magnesium concentration. *J bacteriol* **184:** 1493-1497

Michetti PM, Mahan MJ, Slauch JM, Mekalanos JJ, Neutra MR (1992) Monoclonal secretory immunoglobulin A protects mice against oral challenge with the invasive pathogen *Salmonella typhimurium*. *Infect Immun* **60:** 1786-1792

Miller JH (1972) Experiments in Molecular Genetics (Cold Spring Harbor Laboratory Press, Plainview, NY)

Miller JH (1992) A short course in bacterial genetics: a laboratory manual and handbook for *Escherichia coli* and related bacteria. Cold Spring Harbor, NY: Cold Spring Harbor Laboratory

Miller SI, Kukral AM, Mekalanos JJ (1989) A two components

regulatory system (*phoP phoQ*) controls *Salmonella typhimurium* virulence. *Proc Natl Acad Sci USA* **86:** 5054-5058

Mills DM, Bajaj V, Lee CA (1995) A 40-kb chromosomal fragment encoding *Salmonella typhimurium* invasion genes is absent from the corresponding region of the *Escherichia coli* K-12 chromosome. *Mol Microbiol* **15:** 749–759

Mouilleron S, Badet-Denisot MA, Pecqueur L, Madiona K, Assrir N, Badet B, Golinelli-Pimpaneau G (2012) Structural basis for morpheein-type allosteric regulation of *Escherichia coli* glucosamine-6-phosphate synthase: equilibrium between inactive hexamer and active dimer. *J Biol Chem* **287:** 34533-34546

Muraoka WT, Zhang Q (2011) Phenotypic and genotypic evidence for L-fucose utilization by *Campylobacter jejuni*. *J Bacteriol* **193:** 1065-1075

Nam TW, Cho SH, Shin D, Kim JH, Jeong JY, Lee JH, Roe JH, Peterkofsky A, Kang SO, Ryu S, Seok YJ (2001) The *Escherichia coli* glucose transporter enzyme $IICB^{Glc}$ recruits the global repressor Mlc. *EMBO J* **20:** 491-498

Ninfa AJ, Atkinson MR (2000) PII signal transduction proteins. *Trends*

Microbiol **8:** 172-179

Nuccio SP, Bäumler AJ (2014). Comparative analysis of *Salmonella* genomes identifies a metabolic network for escalating growth in the inflamed gut. *MBio* **5:** e00929-00914

Obradors N, Badía J, Baldomà L, Aguilar J (1988) Anaerobic metabolism of the L-rhamnose fermentation product 1,2-propanediol in *Salmonella typhimurium*. *J Bacteriol* **170:** 2159-2162

Ochman HF, Soncini FC, Solomon F, Groisman EA (1996) Identification of a pathogenicity island required for *Salmonella* survival in host cells. *Proc Natl Acad Sci USA* **93:** 7800-7804

Palacios S, Starai VJ, Escalante-Semerena JC (2003) Propionyl coenzyme A is a common intermediate in the 1, 2-propanediol and propionate catabolic pathways needed for expression of the *prpBCDE* operon during growth of *Salmonella enterica* on 1, 2-propanediol. *J Bacteriol* **185:** 2802-2810

Parsons JB, Dinesh SD, Deery E, Leech HK, Brindley AA, Heldt D, Frank S, Smales CM, Lünsdorf H, Rambach A (2008) Biochemical and structural insights into bacterial organelle form and biogenesis. *J Biol Chem* **283:** 14366-14375

Passerat J, Got P, Dukan S, Monfort P (2009) Respective roles of culturable and viable-but-nonculturable cells in the heterogeneity of *Salmonella enterica* serovar Typhimurium invasiveness. *Appl Environ Microbiol* **75:** 5179–5185

Peterkofsky A, Wang G, Seok YJ (2006) Parallel PTS systems. *Arch Biochem Biophys* **453:** 101-107

Pflüger-Grau K, Chavarría M, Lorenzo V (2011) The interplay of the $EIIA^{Ntr}$ component of the nitrogen-related phosphotransferase system (PTS^{Ntr}) of *Pseudomonas putida* with pyruvate dehydrogenase. *BioChim Biophys Acta* **1810:** 995-1005

Pflüger-Grau K, Görke B (2010) Regulatory roles of the bacterial nitrogen-related phosphotransferase system. *Trends Microbiol* **18:** 205-214

Pflüger-Grau K, Lorenzo V (2007) Growth-dependent phosphorylation of the PtsN (EII^{Ntr}) protein of *Pseudomonas putida*. *J Biol Chem* **282:** 18206-18211

Pflüger-Grau K, Lorenzo V (2008) Evidence of in vivo cross talk between the nitrogen-related and fructose-related branches of the carbohydrate phosphotransferase system of *Pseudomonas putida*. *J*

Bacteriol **190:** 3374-3380

Plumbridge J (1995) Co-ordinated regulation of amino sugar biosynthesis and degradation: the NagC repressor acts as both an activator and a repressor for the transcription of the *glmUS* operon and requires two separated NagC binding sites. *EMBO J* **14:** 3958-3965

Plumbridge JA, Cochet O, Souza JM, Altamirano MM, Calcahno ML, Badet B (1993) Coordinated regulation of amino sugar-synthesizing and -degrading enzymes in *Escherichia coli* K-12. *J Bacteriol* **175:** 4951-4956

Pompella A, Visvikis A, Paolicchi A, Tata V, Casini AF (2003) The changing faces of glutathione, a cellular protagonist. *Biochem Pharmacol* **66:** 1499–1503

Poncet S, Milohanic E, Mazè A, Abdallah JA, Akè F, Larribe M, Deghmane AE, Taha MK, Dozot M, Bolle XD, Letesson JJ, Deutscher J (2009) Correlation between carbon metabolism and virulence in bacteria. *Bacterial Sensing and Signaling* **16:** 88-102

Postma PW, Lengeler JW, Jacobson GR (1993) Phosphoenolpyruvate:carbohydrate phosphotransferase systems of bacteria. *Microbiol Rev* **57:** 543-594

Powell BS, Court DL, Inada T, Nakamura Y, Michotey V, Cui X, Reizer A, Saier MH, Jr., Reizer J (1995) Novel proteins of the phosphotransferase system encoded within the *rpoN* operon of *Escherichia coli*. *J Biol Chem* **270:** 4822-4839

Price-Carter M, Tingey J, Bobik TA, Roth JR (2001) The alternative electron acceptor tetrathionate supports B_{12}-dependent anaerobic growth of *Salmonella enterica* serovar Typhimurium on ethanolamine or 1,2-propanediol. *J Bacteriol* **183:** 2463-2475

Rabus R, Reizer J, Paulsen I, Saier MH, Jr. (1999) Enzyme I^{Ntr} from *Escherichia coli*. A novel enzyme of the phosphoenolpyruvate-dependent phosphotransferase system exhibiting strict specificity for its phosphoryl acceptor, NPr. *J Biol Chem* **274:** 26185-26191

Ramsden AE, Mota LJ, Munter S, Shorte SL, Holden DW (2007) The SPI-2 type III secretion system restricts motility of *Salmonella*-containing vacuoles. *Cell Microbiol* **9:** 2517-2529

Reichardt N, Duncan SH, Young P, Belenguer A, McWilliam Leitch C, Scott KP (2014) Phylogenetic distribution of three pathways for propionate production within the human gut microbiota. *Isme J* **8:** 1323-1335

Reitzer L, Schneider BL (2001) Metabolic context and possible physiological themes of σ^{54}-dependent genes in *Escherichia coli*. *Microbiol Mol Biol Rev* **65:** 422-444

Reizer J, Reizer A, Merrick MJ, Plunkett III G, Rose DJ, Saier MH, Jr. (1996) Novel phosphotransferase-encoding genes revealed by analysis of the *Escherichia coli* genome: a chimeric gene encoding an Enzyme I homologue that possesses a putative sensory transduction domain. *Gene* **181:** 103-108

Rhodius VA, Suh WC, Nonaka G, West J, Gross CA (2006) Conserved and variable functions of the σ^{E} stress response in related genomes. *PLoS Biol* **4:** e2

Rivera-Chàvez F, Bäumler AJ (2015) The pyromaniac inside you: *Salmonella* metabolism in the host gut. *Annu Rev Microbiol* **69:** 31-48

Robin L. Lucas, Lee CA (2000) Unravelling the mysteries of virulence gene regulation in *Salmonella typhimurium*. *Mol Microbiol* **36:** 1024-1033

Rondon MR, Kazmierczak R, Escalante-semerena JC (1995) Glutathione is required for maximal transcription of cobalamin biosynthsis and 1,2-propanediol utiization (*cob/pdu*) regulon and for

the catabolism of ethaholamine, 1,2-propanediol and propionate in *Salmonella typhimurium* LT2. *J Bacteriol* **177:** 5434-5439

Ronneau S, Petit K, Bolle XD, Hallez R (2016) Phosphotransferase-dependent accumulation of (p)ppGpp in response to glutamine deprivation in *Caulobacter crescentus*. *Nat Commun* **7:** 11423.

Roth JR, Lawrence JG, Bobik TA (1996) Cobalamin (Coenzyme B_{12}): Synthesis and biological significance. *Microbiol* **50:** 137-181

Saini S, Ellermeier JR, Slauch JM, Rao CV (2010) The role of coupled positive feedback in the expression of the SPI1 type three secretion system in *Salmonella*. *PLoS Pathog* **6:** e1001025

Sampson EM, Bobik TA (2008) Microcompartments for B_{12}-dependent 1,2-propanediol degradation provide protection from DNA and cellular damage by a reactive metabolic intermediate. *J Bacteriol* **190:** 2966-2971

Sanchez-Vargas FM, Abu-El-Haija MA, Gomez-Duartre OG (2011) *Salmonella* infections: an update on epidemiology, management, and prevention. *Travel Med Infect Dis* **9:** 263-277

Sarvas M (1971) Mutant of *Escherichia coli* K-12 defective in D-

glucosamine biosynthesis. *J Bacteriol* **105:** 467-471

Schlumberger MC, Hardt WD (2006) *Salmonella* type III secretion effectors: pulling the host cell's strings. *Curr Opin Microbiol* **9:** 46-54

Selsted ME, Miller SI, Henschen AH, Ouellette AJ (1992) Enteric defensins: antibiotics peptide components of intestinal host defense. *J Cell Biol* **118:** 929-936

Soncini FC, Vèscovi EG, Groisman EA (1995) Transcriptional autoregulation of the *Salmonella typhimurium phoPQ* operon. *J Bacteriol* **177:** 4364-4371

Song M, Kim HJ, Kim EY, Shin M, Lee HC, Hong Y, Rhee JH, Yoon H, Ryu S, Lim S, Choy HE (2004) ppGpp-dependent stationary phase induction of genes on *Salmonella* pathogenicity island 1. *J Biol Chem* **279:** 34183–34190

Staib L, Fuchs TM (2014) From food to cell: nutrient exploitation strategies of enteropathogens. *Microbiol* **160:** 1020-1039

Staib L, Fuchs TM (2015) Regulation of fucose and 1, 2-propanediol utilization by *Salmonella enterica* serovar Typhimurium. *Frontiers in microbiology* **6:** 1116

Stecher B, Robbiani R, Walker AW, Westendorf AM, Barthel M,

Kremer M, Chaffron S, Macpherson AJ, Buer J, Parkhill J, Dougan G, Mering C, Hardt WD (2007) *Salmonella enterica* serovar Typhimurium exploits inflammation to compete with the intestinal microbiota. *PLoS Biol* **5:** 2177-2189

Sternberg NL, Maurer R (1991) Bacteriophage-mediated generalized transduction in *Escherichia coli* and *Salmonella* Typhimurium. *Methods in enzymology* **204:** 18-43

Studier FW, Moffattf BA (1986) Use of bacteriophage T7 RNA polymerase to direct selective high-level expression of cloned genes. *J Mol Biol* **189:** 113-130

Tatusov RL, Koonin EV, Lipman DJ (1997) A genomic perspective on protein families. *Sci* **278:** 631-637

Testerman TL, Vazquez-Torres A, Xu Y, Jones-Carson J, Libby SJ, Fang FC (2002) The alternative sigma factor σ^E controls antioxidant defences required for *Salmonella* virulence and stationary-phase survival. *Mol Microbiol* **43:** 771-782

Tomljenovic-Berube AM, Mulder DT, Whiteside MD, Brinkman FS, Coombes BK (2010) Identification of the regulatory logic controlling *Salmonella* pathoadaptation by the SsrA-SsrB two-component system.

PLoS Genet **6:** e1000875

Toraya T, Honda S, Fukui S (1979) Fermentation of 1,2-propanediol and 1,2-ethanediol by some genera of *Enterobacteriaceae*, involving coenzyme B_{12}- dependent diol dehydratase. *J Bacteriol* **139:** 39-47

Tsolis RM, Adams LG, Ficht TA, Bäumler AJ (1999) Contribution of *Salmonella typhimurium* virulence factors to diarrheal disease in calves. *Infect Immun* **67:** 4879-4885

Valdez Y, Ferreira RB, Finlay BB (2009) Molecular mechanisms of *Salmoenella* virulence and host resistance. *Curr Top Microbiol Immunol* **337:** 93-127

Vazquez-Torres A, Xu Y, Jones-Carson J, Holden DW, Lucia SM, Dinauer MC, Mastroeni P, Fang FC (2000) *Salmonella* pathogenicity island 2-dependent evasion of the phagocyte NADPH oxidase. *Science* **287:** 1655-1658

Walter D, Ailion M, Roth J (1997) Genetic characterization of the *pdu* operon: Use of 1,2-propanedoil in *Salmonella typhimurium*. *J Bacteriol* **179:** 1013-1022

Weber CJ (2009) Update on *Salmonella* infection. Urologic nursing **29:** 129-131

Weisberger AS (1967) Inhibition of protein synthesis by chloramphenicol. *Annu Rev of medicine* **18:** 483-494

Winter SE, Thiennimitr P, Winter MG, Butler BP, Huseby DL, Crawford RW, Russell JM, Bevins CL, Adams LG, Tsolis RM (2010) Gut inflammation provides a respiratory electron acceptor for *Salmonella*. *Nature* **467:** 426-429

Woodcock DM, Crowther PJ, Doherty J, Jefferson S, DeCruz E, Noyer-Weidner M, Smith SS, Michael MZ, Grahaml MW (1989) Quantitative evaluation of *Escherichia coli* host strains for tolerance to cytosine methylation in plasmid and phage recombinants. *Nucleic Acids Res* **17:** 3469-3478

Yoo W, Yoon H, Seok Y J, Lee C R, Lee H H, Ryu S (2016) Fine-tuning of amino sugar homeostasis by $EIIA^{Ntr}$ in *Salmonella* Typhimurium. *Sci Rep* **6**: 33055

Yoon HJ, McDermott JE, Porwollik S, McClelland M, Heffron F (2009) Coordinated regulation of virulence during systemic infection of *Salmonella enterica* serovar Typhimurium. *PLoS Pathog* **5:** e1000306

Zhang S, Chen Y, Potvin E, Sanschagrin F, Levesque RC, McCormack FX, Lau GW (2005) Comparative signature-tagged

mutagenesis identifies *Pseudomonas* factors conferring resistance to the pulmonary collectin SP-A. *PLoS Path* **1:** 259-268

Zhang S, Kingsley RA, Santos RL, Andrews-Polymenis H, Raffatellu M, Figueiredo J, Nunes J, Tsolis RM, Adams LG, Bäumler AJ (2003) Molecular pathogenesis of *Salmonella enterica* serotype Typhimurium-induced diarrhea. *Infect Immun* **71:** 1-12

Zimmer B, Hillmann A, Görke B (2008) Requirements for the phosphorylation of the *Escherichia coli* $EIIA^{Ntr}$ protein *in vivo*. *FEMS Microbiol Lett* **286:** 96-102

국문 초록

Salmonella Typhimurium은 그람 음성, 간균으로서, 운동성을 보이며, 산소가 없는 환경에서도 살 수 있는 통성혐기성균이다. *Salmonella* Typhimurium은 가벼운 설사부터 장티푸스와 같은 질환에 이르기 까지 다양한 병을 일으키는 대표적인 식중독 원인 균으로서, 동물에서 사람까지 다양한 숙주를 대상으로 감염시킨다. 현재까지 다양한 독성인자와 그들의 조절 기작들이 알려져 있지만, 아직도 여전히 세부적인 기능과 숙주의 표적에 관한 연구가 더욱 더 필요한 실정이다.

Phosphotransferase system (PTS)는 phosphoenolpyruvate (PEP)로 부터 인산을 공급받아 다음 구성요소로 순차적으로 전달하는 인산전달 시스템이다. 일반적으로, 두 종류의 PTS가 존재하는데, 하나는 당을 인산화 시켜 이를 세포 내로 흡수하는 당-PTS이고, 또 다른 하나는 조절 기능으로서의 역할이 많이 알려져 있는 질소대사-PTS이다.

많은 *Proteobacteria*는 EI^{Ntr}, NPr, 그리고 $EIIA^{Ntr}$로 이루어진 질소대사-PTS를 가지고 있는데, NPr과 $EIIA^{Ntr}$을 coding하는 유전자가 질소동화와 관련된 sigma factor인 *rpoN*과 같은 operon

이기 때문에 이 시스템은 질소대사-PTS라고 여겨지고 있다. 하지만 질소대사-PTS에 의해 전달되는 기질이 아직 알려지지 않고 있기 때문에, 이 시스템은 현재까지 알려진 바를 바탕으로 했을 때 주로 조절기작을 담당하고 있다고 여겨지고 있다.

Salmonella Typhimurium에서 질소대사-PTS의 주된 역할에 대해 알아보기 위해 질소대사-PTS의 마지막 구성요소 $EIIA^{Ntr}$을 bait로 하여 Ligand-fishing을 수행하였고, 그 결과 D-glucosamine-6-phosphate (GlcN6P)를 생합성 하는 효소인 GlmS와 단백질 상호작용을 한다는 것을 찾아내었다. GlmS는 glutamine 가수분해를 통해 D-fructose-6-phosphate (Fru6P)를 D-glucosamine-6-phosphate (GlcN6P)로 전환시켜 주어 amino sugar를 만들어 내는 효소이다. Amino sugar는 세균의 peptidoglycan과 LPS를 생합성 하는데 필요한 중요 구성 물질이다. 본 연구에서 $EIIA^{Ntr}$이 GlmS와 이종 삼합체를 형성하여 그 활성을 저해하고, 이는 인산화 의존적인 방식으로 진행됨을 확인 할 수 있었다. $EIIA^{Ntr}$은 질소원이 초과된 환경에서는 일반적으로 탈 인산화 되고, amino sugar가 고갈된 환경에서는 인산화 되며 이는 Lon protease에 의해 급격히 분해된다. GlmS 효소는 $EIIA^{Ntr}$과의 단백질 상호작용으로 인해 그 활성이 조절되며, 또한 *ptsN* 유전자의 downstream

에 존재하는 *rapZ*유전자의 생산물인 RapZ단백질에 의해 translational 수준에서 조절된다. 이를 통해 *rpoN* operon을 구성하는 유전자들이 세균의 세포질 내의 질소원 및 amino sugar농도에 반응하여 amino sugar 항상성을 조절하는 역할을 수행한다는 것을 알 수 있었다.

또한 질소대사-PTS의 역할을 조금 더 이해하기 위해, wild-type과 *ptsN* 유전자가 결여된 돌연변이 균주를 이용하여 RNA-sequencing (RNA-seq)을 통한 전사체 분석을 수행하였다. 전사체 분석을 통해 약 3.5%의 유전자의 발현이 *ptsN*에 의해 3배 이상 증가 또는 감소됨을 확인하였고, 이들 유전자는 크게 탄수화물 수송 및 대사, 아미노산 수송 및 대사, 에너지 생산 및 전환, 전사, 그리고 세모막 및 세포벽 합성 등으로 그룹화 될 수 있다. 이들 중 1,2-propanediol (1,2-PDL) 대사 관련 유전자와 Ado-B_{12} 합성 관련 유전자들의 발현이 *ptsN* 유전자가 결여된 돌연변이 균주에서 wild-type과 비교하여, 큰 폭으로 감소하였음이 발견되었고, 이는 *ptsN* 돌연변이 균주에서 glutathione (GSH)의 합성량이 wild-type에 비해 적어서 생기는 현상임을 알 수 있었다. 1,2-PDL은 대사과정 중에 propionaldehyde를 만들어 내는데 이는 세포독성을 띄고 있다고 많이 알려져 있다. GSH는

세포독성을 약화시키는 역할을 하게 되는데 $EIIA^{Ntr}$ 단백질이 GSH의 합성량을 조절하면서 1,2-PDL의 대사 시기를 조절하는 역할을 수행한다는 사실을 알 수 있었고, 또한 GSH이 3개의 아미노산으로 구성되어 있다는 것을 감안 하였을 때 세포 내 탄소와 질소량을 질소대사-PTS가 감지하여 $EIIA^{Ntr}$을 통해 탄소와 질소의 유용성을 유지한다는 측면 또한 알 수 있었다. 결과적으로 이는 곧 *ptsN* 돌연변이 균주는 1,2-PDL이 존재하는 환경에서 1,2-PDL 대사의 최종산물인 propionate를 적게 만들어 낸다는 의미이다.

흥미롭게도 *Salmonella*의 장 상피세포 침투능력이 1,2-PDL이 존재할 때 wild-type에 비하여 *ptsN*이 결여된 돌연변이 균주에서 약 5배이상 증가하였다. 장내에서 높은 농도로 존재하는 1,2-PDL은 일반적으로 식물성당인 L-rhamnose와 L-fucose의 발효에 의해서 생성되며, L-fucose는 또한 병원균과 숙주의 상호작용이 일어나는 장소인 장 상피세포의 glycoconjugates에서 많이 발견된다. 그리고 1,2-PDL 대사의 중간 산물인 propionyl-CoA가 *Salmonella* pathogenicity island-1 (SPI-1)의 조절인자인 HilD의 안정성을 떨어뜨려 *Salmonella*의 병원성을 조절한다는 보고가 있으며, $EIIA^{Ntr}$의 단백질 발현량이 1,2-PDL이 존재하는

환경에서 약 3배 정도 증가함을 보면 $EIIA^{Ntr}$이 1,2-PDL대사를 통해 *Salmonella*의 생장과 병원성을 조절한다는 중요한 요인 이라는 것을 예측해 볼 수 있다.

결론적으로 본 연구에서 *Salmonella* Typhimurium의 질소 대사 PTS의 구성요소인 $EIIA^{Ntr}$이 1,2-PDL대사와 amino sugar 항상성조절에 대한 새로운 조절자로서의 역할을 수행한다는 것을 밝혀냈다. 1,2-PDL은 *Salmonella*가 장내 미생물총과 경쟁하기 위해 이용하는 주요 탄소원 및 에너지원이고, GlmS는 peptidoglycan과 LPS를 생합성 하기 위해 이용하는 유일한 효소이다. 본 연구에서는 $EIIA^{Ntr}$이 주변환경적 신호인 1,2-PDL과 amino sugar에 반응하여 transcriptional 수준 또는 post-translational 수준에서 *cob-pdu* operon의 발현과 GlmS의 효소 활성을 조절한다는 것을 밝혀냈다. 그리고 $EIIA^{Ntr}$은 같은 환경적 신호에 반응하여 translational 수준 또는 post-translational 수준에서 그 발현이 조절된다. 이는 $EIIA^{Ntr}$이 *Salmonella*가 숙주와의 상호작용을 통해 그 생장과 병원성을 유지하는 데에 필요한 중요 요소라는 것임을 증명하며, $EIIA^{Ntr}$의 발현과 활성을 조절하여 *Salmonella* 관련 질병을 저감화 시킬 수 있을 것이라는 새로운 가능성 또한 제시할 수 있다.

주제어: 1,2-propanediol utilization (*pdu*), Glucosamine-6-phosphate 생합성 효소 (GlmS), 질소대사-PTS (PTS^{Ntr}), RNA 시컨싱, *Salmonella* pathogenicity island-1 (SPI-1), *Salmonella* pathogenicity island-4 (SPI-4), *Salmonella* Typhimurium

학 번: 2011 - 21304